Rock Slope Stability Analysis along a Selected Slope Section of a Rhyolite Quarry in Adama, Central Ethiopia

Fikeru Kefyalew Deresso

A Thesis Submitted To the Department of Applied Geology

School of Applied Natural Science

Presented in Partial Fulfilment of the Requirement for the Degree of Master's In Engineering Geology

Office of Graduate Studies

Adama Science and Technology University

November, 2024

Adama, Ethiopia

Rock Slope Stability Analysis along a Selected Slope Section of a Rhyolite Quarry in Adama, Central Ethiopia

Fikeru Kefyalew Deresso

Advisor

Melesse Alemayehu (PhD)

Co-Advisor

Tola Garo (MSc.)

A Thesis Submitted To the Department of Applied Geology
School of Applied Natural Science
Presented in Partial Fulfilment of the Requirement for the Degree of Master's In Engineering Geology

Office of Graduate Studies
Adama Science and Technology University

November, 2024
Adama, Ethiopia

DECLARATION

I hereby declare that this Master Thesis entitled **"Rock Slope Stability Analysis along a Selected Slope Section of a Rhyolite Quarry in Adama, Central Ethiopia"** is my original work. That is, it has not been submitted for the award of any academic degree, diploma or certificate in any other university. All sources of materials that are used for this thesis have been duly acknowledged through citation

Fikeru Kefyalew	________________________	________________________
Name of student	Signature	Date

RECOMMENDATION OF ADVISORS

We, the advisors of this thesis, hereby certify that we have read the revised version of the thesis entitled "**Rock Slope Stability Analysis along a Selected Slope Section of a Rhyolite Quarry in Adama, Central Ethiopia**" prepared under our guidance by Fikeru Kefyalew submitted in partial fulfilment of the requirements for the degree of Mater's of Science in Engineering Geology. Therefore, we recommend the submission of revised version of the thesis to the department following the applicable procedures

Major Advisor	Signature	Date
Co-advisor	Signature	Date

APPROVAL PAGE

We, the advisors of the thesis entitled **"Rock Slope Stability Analysis along a Selected Slope Section of a Rhyolite Quarry in Adama, Central Ethiopia"** and developed by Fikeru Kefyalew hereby certify that the recommendation and suggestions made by the board of examiners are appropriately incorporated into the final version of the thesis.

____________________	__________________	________________
Major Advisor	Signature	Date
____________________	__________________	________________
Co-advisor	Signature	Date

We, the undersigned, members of the Board of Examiners of the thesis by Fikeru Kefyalew have read and evaluated the thesis entitled "**Rock Slope Stability Analysis along a Selected Slope Section of a Rhyolite Quarry in Adama, Central Ethiopia"** and examined the candidate during open defense. This is, therefore, to certify that the thesis is accepted for partial fulfilment of the requirement of the degree of Master of Science in Engineering Geology

____________________	__________________	________________
Chairperson	Signature	Date
____________________	__________________	________________
Internal Examiner	Signature	Date
____________________	__________________	________________
External Examiner	Signature	Date

Finally, approval and acceptance of the thesis is contingent upon submission of its final copy to the Office of Postgraduate Studies (OPGS) through the Department Graduate Council (DGC) and School Graduate Committee (SGC)

____________________	__________________	________________
Department Head	Signature	Date
____________________	__________________	________________
School Dean	Signature	Date
____________________	__________________	________________
Office of Postgraduate Studies, Dean	Signature	Date

ACKNOWLEDGEMENT

I am writing to express my sincere gratitude and acknowledgement to the individuals and organizations who have supported and contributed to the development of this research work.

First, I humbly acknowledge and appreciate the Almighty God for His continual blessings, guidance, and unwavering support throughout my life, as well as the successful completion of my research work. I am forever grateful for His presence on my journey.

Next, I would like to express my deepest appreciation to my advisor, Melesse Alemayehu (PhD), and co-advisor, Tola Garo (MSc.), for their guidance and unwavering support throughout my research work. Their valuable insights, constructive feedback, and dedication to my academic growth have been invaluable throughout this process.

I would also like to thank the Engineering Corporation of Oromia for the laboratory support they provided for me to accomplish this research work.

Finally, I extend my appreciation to the colleagues, friends, and family members who have provided support and encouragement throughout this research work.

ABSTRACT

Slope instability at the rhyolite quarry site in Adama is one of the most frequent and common problems and issues in quarrying activity. The stability of the quarry slope depends on several factors, including a combination of both internal and external factors. This study aims to assess and evaluate the slope stability of the rhyolite quarry site in Adama, central Ethiopia, by using kinematic analysis, limit equilibrium, and finite element methods. Input parameters were determined through field surveys, such as the orientation of discontinuities and slope geometry, and a buoyancy technique were used in the laboratory to determine the unit weight of rocks. The strength of the intact rock was determined using a point-load laboratory test and the Schmidt hammer in the field. Rocscience software was utilized to determine the shear strength parameters along the failure plane, such as cohesion and friction angle. The kinematic analysis was used to determine the mode of failure, whereas limit equilibrium and finite element methods were used to determine factors of safety for critical slope sections of the quarry that were identified during the field survey. According to kinematic analysis, results QSS_1, QSS_3, show wedge failure, while QSS_2 and QSS_3 show planer failure. Moreover, deterministic analysis was conducted under a variety of circumstances: static dry, static saturated, dynamic dry, and dynamic saturated. According to the results, both quarry slope sections are unstable in static saturated and dynamic saturated conditions and stable in other conditions, and wedge failures at QSS_1 and QSS_3 under dynamic saturated conditions FOS are 0.95 and 0.248, respectively. For non-structurally controlled slope sections, Slide 6.0 and Phase 2 were used to determine the factor of safety of QSS_4 and QSS_5. Based on the findings, both slope sections are unstable under static and dynamic load conditions. From the analysis result, the combined effect of quarry operation by removal of rock material through excavation, steep slope cuts, and discontinuity orientation with respect to the slope face, rainfall, and seismic activity are factors that significantly affect slope stability in the quarry site. Based on the findings, the study recommends increasing the benching by multi-benched excavation systems with bench width and height of 8 m and 12 m, respectively, and reducing the slope angle to 65^0 of each bench with an overall slope angle of 46^0 as the most important aspects of stabilizing the critical slope sections of the quarry site.

***Key words**: kinematic analysis, planar failure, wedge failure, deterministic, factor of safety, limit equilibrium, and finite element method.*

TABLE OF CONTENTS

Contents **Pages**

LIST OF FIGURES

Figures **Pages**

LIST OF TABLES

LIST OF ACRONYMS AND ABBREVIATIONS

ASTM	American Society for Testing Materials Standard
ASTU	Adama Science and Technology University
D	Dip amount
DD	Dip direction
FEM	Finite element method
FOS	Factors of safety
GIS	Geographic information system
GSI	Geological strength index
ISRM	International society of rock mechanics
JS	Joint set
JV	Volumetric Joint Count
LEM	Limit equilibrium method
SMR	Slope Mass Rating
SRF	Stress reduction factor
SSR	Shear Strength Reduction
RMR	Rock Mass Rating
RRS	Rhyolite rock sample
RQD	Rock Quality Designation
TRS	Vitric tuff rock sample
UCS	Uniaxial Compressive Strength

CHAPTER ONE

1. INTRODUCTION

1.1. Background

Slope instability is one of the geological hazards that most commonly occur globally and cause infrastructure, including roads, dams, and open-pit mines, to fail (Abramson et al., 2001; Hoek & Bray, 1989; Pantelidis, 2009). As a result, slope instability issues have received more attention for a long time. Engineering geologists and geotechnical engineers have carried out numerous investigations on slope stability evaluations. Problems with slope instability are caused by a combination of internal and external factors, such as hydraulic conditions, geological structure characteristics, slope geometry, material strength, and mining excavation disturbance (Du et al., 2022; Raghuvanshi, 2017). These factors can decrease the shear strength or increase the shear stress of a slope material (Abramson et al. 2002). The slope failures are natural occurrences that commonly occur along cut slopes of roads built in hilly areas of the world, causing the loss of life, injury, and significant property damage each year (Cao et al., 2016). The most important aspect of any mining or quarrying operation is the stability of the pit slope (Abramson et al., 2001). Slope stability calculations are required to evaluate the stability of open pit slopes and the economic viability of mining operations; it is necessary to create safe, practical, and excavated slopes (Obregon & Mitri, 2019). In open-pit mines, slope failures can result in long-term production ceases, safety risks in transportation, and the destruction of equipment and lives(Sjöberg, 1996). To avoid this, effective analysis is crucial to avoiding the adverse consequences of slope instability.

In Ethiopia, most of the north, south, and western regions of the Ethiopian plateau face a record of slope instability in both superficial materials and bedrocks due to the cutting of hills and roadsides(Ayalew, 1999). The majority of these slope failures have been rainfall related (Raghuvanshi et al., 2017), resulting in fatalities, engineering structure failures, damage to agricultural lands, and negative impacts on the environment (Abebe et al., 2010; Woldearegay, 2013). Rock slope instability occurs mostly in the form of planar, wedge, and toppling modes of failure (Wyllie & Mah, 2004) with respect to the hard rock; the failure commonly occurs along the discontinuity planes.

In order to evaluate and study the stability of the slope, these techniques fall into four main categories: numerical modelling, kinematic analysis, limit equilibrium, and empirical methods, which are the most commonly employed (Hoek & Bray, 1981; Wyllie & Mah, 2004). According to Duran and Douglas (2000), rock mass categorization systems and empirical approaches are valuable instruments frequently employed for initial evaluation of the engineering behaviours of the rock mass. There are two steps that can be taken when carrying out rock slope stability evaluations (Leshchinsky, 1990). The process begins with analysing kinematic analysis to identify the mode of rock slope failure. Next, the factor of safety is often determined using limit equilibrium techniques (LEM). The kinematic method deals with the failure mode of the rock slope without reference to the forces that cause it to move (Goodman 1989; Hudson and Harrison 1997). whereas the limit equilibrium approach, which is frequently used to assess slope structural stability, analyses the strengths of the driving and resisting forces that act along the sliding planes to estimate the factor of safety (Coggan et al., 1998). In addition to providing insight into the impact of stress distribution in the slope and displacements on its behaviour, numerical modelling is applied in more complex slope geometries and failure processes (Wyllie and Mah, 2004). Among them, the earliest and most basic conventional analytical techniques for determining out the slope's stability in terms of the safety factor are limit equilibrium approaches. Therefore, the best way to assess slope with homogenous geologic materials and uniform geometry is using limit equilibrium methods (Raghuvanshi 2017). LEM models continue to be widely used because of their ease of use and simple parameterization (Mebrahtu et al. 2022). Furthermore, by taking into account the influence of stress and strain on the slope, the numerical technique is an appropriate over-limit equilibrium method to investigate instability problems of the slope with complicated geometry (Duncan, 2000). The study area methods of quarry excavation have resulted in the face of the quarry having dangerously steep slopes. To assure the safety of the quarry face, stability analysis is required (Abramson et al., 2001). Since the quarry is still in use, it is crucial to evaluate slope stability to ensure the security of the workers and the surrounding area. Therefore, this study aimed to evaluate the stability of the rhyolite quarry site using the kinematic method to identify the mode of rock slope failure, limit equilibrium, and the finite element method to determine the stability of the slope in terms of FOS and SRF, respectively.

1.2. Statement of the problem

Ethiopia is currently involved in massive infrastructural development and various excavation works. However, excavation activities face a huge risk of slope failure and damage from landslides and other slope instabilities. The rhyolite quarry site in Adama is facing potential slope stability issues, which pose significant risks to the safety of personnel, equipment, and nearby infrastructure. The existing slopes in the quarry may be prone to various forms of instability, including planer and wedge failures. The lack of a comprehensive slope stability assessment and the absence of appropriate mitigation measures increase the risk of accidents and failures within the quarry site, which can result in injuries, damage to equipment, and disruption of operations. Therefore, a slope's optimal design was essential to achieving both the safety and economic goals of a quarry mine. Thus, to minimize the damage caused by slope failures using a variety of techniques, including kinematic, limit equilibrium, and finite element methods, the study aimed to determine and analyse the slope stability issues at the selected slope section of quarry site. Therefore, it is crucial to assess the slope stability conditions of the rhyolite quarry site in Adama, Central Ethiopia to develop effective mitigation strategies along the failure slope sections of the quarry site.

1.3. Objectives of the study

1.3.1. General objective of the study

The general objective of this study was to assess and evaluate the slope stability of the rhyolite quarry in Adama, Central Ethiopia.

1.3.2. Specific objectives of the study

The specific objectives included in this study are as follows.

- Determine the geological and geotechnical characteristics of rock at the quarry site.
- To identify the different types of slope failure.
- To determine the safety factor for the critical slope section of the quarry site.
- To identify the factors that trigger slope instability in quarries.
- To determine the quarry's safe cut slope design.

1.4. Significance of the study

The stability of rock slopes is considered crucial to public safety on bench passing through rock cuts, as well as to personnel and equipment safety in quarry mines. Quarry slopes are prone to instability and slope failures, which can result in severe consequences such as injuries, fatalities, and property damage. Assessing the stability of rhyolite quarry in Adama helps to identify stability condition of slope, and implement appropriate mitigation measures. It is crucial for ensuring the safety of workers, nearby residents, and infrastructure in the vicinity. Assessing slope stability in quarries contributes to the development of sustainable mining practices. By understanding the geological and geotechnical factors influencing slope stability, quarry operators can implement better planning, design, and operational strategies. This can help minimize slope failures, reduce downtime due to slope stabilization efforts, and optimize resource extraction. Moreover, conducting a study on quarry slope stability in Adama contributes to the broader field of geotechnical engineering and earth sciences. It adds to the existing body of knowledge and helps refine methodologies, models, and predictive tools for slope stability analysis. The findings of such studies can be used as a reference for future research, aiding in the development of safer and more reliable slope stability assessment techniques.

CHAPTER TWO

2. LITERATURE REVIEW

2.1. Introduction

Slope instability is one of the most frequent and common problems and issues in mining and civil engineering structures including highways, tunnels, and dams around the world (Abramson et al., 2001; Hoek and Bray 1981; Pantelidis 2009: Wyllie & Mah, 2004:). According to Abramson et al., (2001) slope instability problems are brought on by both natural and manmade disruptions to the sensitive slopes of soil and rock. Slope failure is caused by one or more combinations of causes, including the slope's material strength, slope geometry, hydrological condition, structural discontinuity, weathering, the presence of weak zones, lithological disturbance, and excessive rainfall (Bushira et al., 2018). Additionally, this is brought on by a confluence of internal and exterior elements that reduce the shear strength or raise the shear stress of a slope material(Duncan, Wright, & Brandon, 2014; Raghuvanshi, 2019).

Instabilities in rock slopes provide a serious risk to human activity and frequently result in financial losses, property damage, and maintenance expenses in addition to injury or death. Therefore, for the purpose of planning and assessing the rock's slope stability and quarry or mine site safety, the slope stability analysis of rocks is essential. In addition to improving slope stability and safety, a well-designed slope also lowers expenses, increases mine life, and lowers the stripping ratio (Bye and Bell, 2001, Naghadehi et al., 2011).

2.2. Slope stability study in Ethiopia

Slope instability is a widespread issue in Ethiopia, particularly on the roadways that cross the country's mountainous regions. Several studies conducted on rock slope stability in Ethiopia have been carried out in a number of locations, including the highlands, rift escarpments, and along the road cut (Abebe et al., 2010; Asmare & Hailemariam, 2021; Ayele et al., 2014; Gebreyohannes et al., 2024; Kassa & Meten, 2023; Lamessa & Meten, 2021; Mebrahtu et al., 2022; Tesfaye et al., 2024). These studies aim to identify the underlying cause and suggest potential mitigation measures. These studies involve detailed field investigations, laboratory tests on geological and geotechnical properties, and numerical modelling to assess slope stability under different conditions like seismic events and saturation. The determination of critical slope sections for study and the creation of susceptibility maps for planning and mitigation actions are the results of factors influencing the stability of rock slopes, such as discontinuity, lithology, slope angle, land use, gully erosion, seismicity and rainfall-induced slope instability. For the purpose of identifying variables of safety and suggesting slope stabilization solutions, they use frequently include techniques such as kinematic analysis, limit equilibrium, finite element, and three-dimensional finite element analysis.

Furthermore, many studies have been carried out in Ethiopia to evaluate the stability of quarry slopes. For instance, research in Dangote Cement, analysed slope stability parameters, such as geological features, seismic loads, and rock mass stability probability, using techniques like fieldwork, laboratory testing, numerical modelling, and geophysical testing (Dadi & Chala, 2022). These investigations underscored the significance of variables like as variations in the groundwater table, seismic activity, and properties of the rock mass, method of excavations influencing slope stability. Researchers sought to improve the understanding of quarry slope stability for safer excavation procedures and infrastructure development. They did this by utilizing approaches such as finite element analysis, slope stability probability classification, and geomechanical process analysis. Also rock slope stability analysis of a limestone quarry in a case study of a National Cement Factory in Eastern Ethiopia (Bezie et al., 2024) using Kinematic analysis and Numerical modelling methods to analyse the stability of existing quarry cut slopes and recommended for optimal stability.

2.3. Factor govern slope stability

For the analysis of the stability of rock slopes, it is essential to understand the impact of these governing forces. Numerous causes can contribute to slope instability and failures, including unfavourable slope geometries, geological discontinuities, weak or weathered slope materials, and extreme weather. External loads such as strong precipitation and seismic activity may significantly influence slope stability. These components belong into two categories internal and external factor determine stability condition of slope (Hoek & Bray, 1981). According to Pantelidis (2009) and Raghuvanshi (2019) the slope's geometry, the features of a potential failure plane, surface drainage, and groundwater conditions are the primary internal governing factors. While rainfall, seismic activity, and human-made activities are considered, external factors cause failure either by reducing shear strength of slope materials or by increasing the shear stress on the slope. The combination of both internal and external factors determines the overall stability condition of the slope.

2.3.1. Internal factor

2.3.1.1. Geological structure

Depending on their orientations and the degree of corresponding tectonic damage, structural features like bedding plane, joints, and the intersection of joints, faults, and shear zones are the most significant geological features that affect slope stability to stabilize or destabilize rock slopes (Stead & Wolter, 2015). According to Stead & Wolter (2015) and Wyllie & Mah (2004), geological formations on a slope determine the kind or mode of failure, such as planar, wedge, circular, and toppling failure.

2.3.1.2. Gravity

The gravitational force is the main factor affecting shear stress. The two components of gravity's forces one acting perpendicularly to the slope and the other tangentially to the slope can be separated into two categories. On a steeper slope, the shear stress or tangential component of gravity increases and the perpendicular component of gravity decreases(Iverson & Reid, 1992). Therefore, the down-slope movement of a material is affected by steep slope angles, which increase the shear stress and reduce shear strength. Undercutting, mining operations, tectonic tilting, and removal of lateral support can all increase a material's shear stress. Shear strength is governed by inherent factors of rock such as; angle of internal friction, cohesion and binding action of plant roots between particles(Hoek & Bray, 1981).

2.3.1.3. Slope materials factor

The principal geotechnical factors that influence slope stability include porosity, cohesion, angle of internal friction, plastic limit, void ratio, plasticity index, liquid limit, in-situ water content, saturated unit weight, and dry density (Yalcin, 2011). On slopes, the strength of the rock varies substantially. The type of rock or its chemical composition determines its strength. The internal angle of friction serves as a gauge of a rock slope's capacity to withstand shear force. A higher factor of safety and reduced slope stress, strain, and displacement are produced by increasing the internal angle of frictions (Duncan & Norman, 1996). Lower slope stress, strain, and deformation are produced by higher cohesion values, which also increase the safety factor. Cohesion is a characteristic property of rock or soil that measures the resistance of the rock or soil to be deformed or broken by forces such as gravity. The slope that is less cohesion tends to be weaker in nature.

2.3.1.4. Slope geometry

The bench's height and width are governed by a number of variables, including the capacity of the loading machine's bucket, the bucket's cutting height, production parameters, the stability of the pit slope(Kumar & Raj Kumar, 2022). The essential objective of a slope design process is to make it possible to create a mine bench, ramp, or overall slope that is both secure and economically feasible(Steffen et al., 2008). A mine's slope design that becomes deeper and bigger inherently entails a higher danger of failure and its effect. The height, overall slope angle, and failure area are the three key variables in geometric slope design. Steeper slope will be more susceptible for instability (Raghuvanshi 2019). The chance of any failure occurring towards the back of the crests may also grow as the overall slope angle increases this should be taken into account so that local ground deformation in the mine is surrounding area can be prevented. A slope becomes more unstable the steeper the angle.

2.3.2. External factor

2.3.2.1. Seismicity

Explosions, earthquakes or volcanic eruptions can increase shear stress and trigger slope failure(Bommer et al., 2002). The vibration released during earthquakes can cause failure of slopes which were previously stable through the influence of increased vertical acceleration(Bommer et al., 2002). According to Hack et al. (2007) and Raghuvanshi (2019), rock slopes subjected to seismic stress undergo accelerations that cause instability in the rock slope.

2.3.2.2. Rainfall

In rock slopes, rainfall is the main factor that causes instability(Raghuvanshi et al., 2014). Rainfall has a significant impact on slope stability because it can alter the pore-water pressure, shear strength, and mechanical properties of the soil and rock mass(Pan et al., 2020). The stability of the slope can be affected differently by various rainfall patterns, including intensity, length, and frequency. Since the safety factor of the slope initially declines and then stabilizes during rainfall, which is defined as the effective rainfall days, rainfall intensity and its pattern have a significant impact on slope stability (Pan et al., 2020).

2.3.2.3. Man-made activities

Slope instability can be greatly increased by human activity like quarry activities, which can also have a negative impact on slope stability. According to Wyllie and Mah (2004), block failures along discontinuities are among the threats that might arise from man-made activities like quarrying, which have a substantial impact on slope stability and endanger human lives and property which influenced by factors such as the excavation depths, quarrying operation, and the geometry and strength of discontinuities in the rock mass. To reduce hazards and guarantee safety of communities and infrastructure in hilly areas, it is therefore critical to comprehend how human activity affects slope stability(Tang et al., 2017).

2.4. Mode of slope failure

The desired orientation of structural discontinuities, the cohesiveness and angle of internal friction of the discontinuities, the conditions of water saturation, geometry of the slope, slope height, slope angle, the preferred orientation of structural discontinuities, and other factors all affect these mode of failure (Bieniawski, 1989; Wyllie & Mah, 2004). Rock slope failure modes are divided into four kinds, according to Hoek & Bray, (1981) and Wyllie & Mah, (2004) these include planer failure, toppling, circular and wedge.

2.4.1. Planer Failure

When a plane of structural discontinuity, such as a bedding plane, fault plane, or the preferred orientation of a joint set, dips or daylights towards a valley or excavation at an angle that is greater than the friction angle of the discontinuity surface but smaller than the slope angle, the failure of the plane occurs (Raghuvanshi, 2019). In order to prevent a planar slide from happening, planar failure can be restricted to benches, pit regions with unfavorable geometry, or structures that strike perpendicular to the slope face (Wyllie & Mah, 2004). The presence of groundwater, which results in the stability of the slope deteriorating when there is temporary groundwater pressure, especially after heavy rainfall, is one of the main causes of planar failure (Pantelidis, 2009).

The four necessary structural conditions for planar failures according to Goodman, (1989); Hoek & Bray, (1981)and Norrish & Wyllie, (1996)

- The strikes of both the sliding plane and the slope face are parallel (±20°) to each other.
- The dip of the discontinuity must be less than the dip of the slope, and the failure plane must daylight on the slope face.
- The dip of the planar discontinuity must be greater than the angle of friction of the surface.

- The upper end of the sliding surface must intersect the upper slope or terminate in a tension crack

2.4.2. Wedge failure

In wedge failures, the line of intersection of the failure mass is inclined outward from the slope face and is marked by two discontinuities (Duncan & Norman, 1996)

According to Hoek & Bray, (1981) and Wyllie & Mah, (2004), the following structural requirements must exist for wedge failure:

- The dip of the slope must be a steeper angle than the dip of the line of intersection of the two discontinuities.
- The line of intersection must daylight on the slope face and the dip of the line of intersection must be greater than the angle of friction of the surface.
- The upper end of the line of intersection either intersects the upper slope or terminates in a tension crack.

2.4.3. Toppling

According to Wyllie & Mah, (2004), the toppling mode of a rock slope is caused by the overturning of rock strata or discontinuities that are sinking sharply into the slope face. Favorable toppling failure conditions include joined rock masses that are closely spaced and steeply dipping discontinuity sets that dip away from the slope surface(Norrish & Wyllie, 1996).

2.4.4. Circular failure

According to Wyllie & Mah, (2004), the circular mode of slope failure occurs in weak materials like extensively weathered or densely fractured rock and soils, where the collapse occurs along a surface with a roughly round shape**.**

2.4.5. Rockfall

According to Selby (1982), a rockfall is a small landslide that individually occurs when rocks separate from bedrock slopes in different modes of motion. The gradient's mean slope has a significant influence on these motion modes. The three major modes of motion are rolling over the slope surface, bouncing on the slope surface if the mean slope gradient is less than roughly 45°, and freefalling through the air, which happens on very steep slopes. Studies at different quarry sites, including the Carian quarry in Tetouan(Dellero & El Kharim, 2013), the Authume quarry in France(Garcia et al., 2022), and the Kinta Valley in Malaysia(Simon et al., 2015), has shown the value of geological assessments, rock slope stability analyses, kinematic evaluations, and rockfall trajectory models for understanding and mitigating the risk of rockfall.

An analysis of rockfall slope stability is a procedure used to determine whether a slope is stable enough to determine whether there is a risk of rockfall it can be caused by a number of factors, including geological conditions, rock cracks, and unstable slopes (Budetta, 2004). Also human activities Selby (1982) states that undercutting slopes during quarrying or infrastructure excavation can result in significant instability.

2.5. Soil and rock mass failure criteria

2.5.1. Mohr-Coulomb Failure Criterion

The Mohr-Coulomb failure criterion is a set of linear equations in principal stress space that describes the circumstances under which an isotropic material will fail, while neglecting any impact from the intermediate principal stress(Labuz & Zang, 2014). Mohr-Coulomb failure can be expressed as a function of either the major and minor principal stresses or the normal and shear stresses on the failure plane (Labuz & Zang, 2012) . It provides a failure criterion for soil and rock materials by considering the critical combination of normal and shear stresses by utilizing the cohesiveness and internal friction angle, the mechanical characteristics and stress state of rocks are naturally related.

2.5.2. Hoek-Brown Failure Criterion

The Hoek-Brown criterion was developed to help in underground excavations in rock. The criterion currently takes into account both intact rock and discontinuities, like joints, that are identified by the geological strength index (GSI), and includes both into a system intended to assess the mechanical behaviour of typical rock masses seen in tunnels, slopes, and foundations(Hoek & Brown, 2019). In preliminary design calculations for slopes and underground excavations in jointed rocks, the Hoek and Brown criterion utilized approximate relationships between rock type, rock mass quality, and the rock mass strength parameters m and s values(Hoek & Brown, 2019).

2.5.3. Barton – Bandis Criteria

The Barton-Bandis strength model can be used to model the shear strength of a joint. This criterion provides three simple items of input data; the joint-surface roughness, the joint-wall compressive strength and an empirically-derived estimate of the residual friction angle and can be expressed using an equation (Barton & Choubey, 1977)

2.6. Laboratory test

The determination of material strength parameters in slope stability analysis is usually done in a lab (Broch, 2016; ISRM, 1985). Determining the index and engineering characteristics of rocks and soil was a goal of this test. To ascertain the strength parameters of rocks and soils, a variety of laboratory tests are carried out (Ullah et al., 2020a). Dry and saturated densities were investigated for rock point load. This laboratory test, which included a unit weight and point load test, was performed on a rock sample.

2.6.1. Point load test

The point-load test is utilized for practical applications engineering geological applications(Bieniawski, 1975). The International Society for Rock Mechanics (ISRM, 1973) has taken steps to standardize the testing techniques after Broch and Franklin's (1972) thorough examination demonstrated the method's potential in rock mechanics and engineering geology.

A popular indirect technique for accurately estimating a rock material's uniaxial compressive strength with portable, easier-to-use equipment is the point load test (Broch, 2016). In the field, the Schmidt Hammer Rebound test is another method used to calculate UCS (ISRM, 1985). It is extensively employed in the engineering and construction sectors to evaluate the quality and appropriateness of materials for a range of uses. There may be a correlation between the point-load index and both the compressive and tensile strengths of rock(Bieniawski, 1975). The link between the point-load index and the uniaxial compressive strength has received the greatest attention due to the prevalence of compressive stress in rock mechanics problems (Broch and Franklin, 1972).

2.6.2. Unit weight test

The unit weight of rocks is a crucial factor in rock mechanics and geotechnical engineering for a number of analyses, such as determining the stability of rock slopes and creating appropriate engineering solutions (Pantelidis, 2009). A substance's unit weight, which is commonly stated in the amounts like kN/m^3, is the weight of a unit volume of the material. The unit weight of rocks is one of the metrics used for the stability analysis of rock slopes. According to ISRM (1978), a buoyancy technique was used to calculate the unit weight of rocks. As a result, the rocks' dry and saturated unit weights were calculated.

2.7. Slope stability analysis approach

2.7.1. Discontinuity survey

Discontinuity surveying is a technique for identifying and describing the orientation, spacing, persistence, roughness, and filling material of discontinuities in rock masses(He et al., 2021). According to Stead et al. (2015), discontinuity analysis may handle both static and dynamic conditions for the movement of intact rock blocks contained within discontinuities as well as the deformation of intact rock. This technique is very useful for simulating discontinuity behaviours and evaluating the stability of rock slopes under specific conditions.

2.7.2. Rock Mass Classification

Systems for classifying rock masses are utilized in a variety of engineering design and stability analysis processes. These are based on empirical relationships between engineering applications, such as tunnels, slopes, foundations, and excavatability, and rock mass characteristics(Bieniawski, 1989). Different rock mass classification system has been established until now by different researcher. After that various classification systems such as Rock Load Strength(Terzaghi, 1946); Rock Quality Designation(Deere, 1989); Rock Mass Rating(Bieniawski, 1989); Rock Mass Quality (Q) (Barton et al., 1974), Geological Strength Index (GSI) (Hoek & Brown, 1997)were developed.

2.7.3. Rock quality designation (RQD)

The Rock Quality Designation index (RQD) was developed by Deere to provide a quantitative estimate of rock mass quality from drill core logs. According to equation 1 RQD is defined as the percentage of intact core pieces longer than 100 mm (4 inches) in the total length of core(Deere & Deere, 1989).

$$\mathrm{RQD} = \frac{\sum(\text{Core Length} > 10\text{cm})}{\text{Total Core Run}}\ \mathrm{x}100 \qquad 1$$

Palmstrom (1982) proposed that the RQD might be approximated from the volumetric count technique (the number of discontinuities per unit volume) in cases when no core is available but discontinuity traces are visible in surface exposures. Accordingly, equation 2 suggested theoretical relationship for the rock masses is:

$$\mathrm{RQD} = 115 - 3.3 * \mathrm{Jv} \qquad 2$$

Where, Jv is the total number of discontinuities in a 1 x 1 m exposed rock face that are longer than 10 cm (Volumetric count).

Volumetric count from the number of discontinuities per unit volume or the number of joints intersecting a volume of one m^3. Where joints occurs as joint set, Jv is determined using equation 3:

$$Jv = \frac{1}{S_1} + \frac{1}{S_2} + \frac{1}{S_3} + \cdots \frac{1}{Sn} \qquad 3$$

Where S_1, S_2 and S_3 are the average spacing for the joint sets.

2.7.4. Uniaxial Compressive Strength (UCS) of Intact rock

The uniaxial compressive strength (UCS) of the intact rock is determined from Schmidt hammer strength test in the field (Barton & Choubey, 1977). The surface rebound hardness, which is related to compressive strength, is measured using the Schmidt hammer test. Tests were carried out in accordance with the ASTM D5873 (2001) test procedure. Two trials with ten readings each were conducted at each sample location. Every trial test had readings taken with a 20mm gap between the two impact test locations. After listing the rebound values in ascending order, the UCS was calculated using the average rebound value (R).

The uniaxial compressive strength of rocks along the slope sections was finally determined using the empirical equation 4 as follows (Barton & Choubey, 1977).

$$\log10(UCS) = 0.00088 * \gamma * R + 1.01 \qquad 4$$

Where UCS is the uniaxial compressive strength of rocks in MPa, γ is the dry rock density in kN/m3, and R is the average Schmidt hammer rebound value.

2.7.5. Rock Mass Rating (RMR)

The RMR has been widely utilized in a variety of engineering sectors involving rocks, including as mining and civil tunnelling, hill terrain, road construction, bridges, dams, and hydropower projects. The RMRb system and its associated geomechanics categorization were described in detail by (Bienawski, 1976). Although the modified RMRb is used to categorize the rock mass based on five factors rock strength, RQD, spacing of discontinuities, condition of discontinuities, and groundwater conditions(Bieniawski, 1989). A value of RMR is obtained by adding the ratings for all of these parameters, which is an algebraic sum of the ratings for each parameter.

2.7.6. Slope mass rating (SMR)

Slope Mass Rating (SMR; Romana, 1985) is calculated using four correction factors of basic RMR (Bieniawski, 1989). These factors depend on the existing relationship between discontinuities affecting the rock mass and the slope, and the slope excavation method. It is obtained using expression 5 (Romana et al., 2015).

$$SMR = RMR_{basic} + (F_1 * F_2 * F_3) + F_4 \qquad 5$$

Where:

- RMR$_b$ is the RMR index resulting from Bieniawski's Rock Mass Classification without any correction.
- F_1 depends on the parallelism between discontinuity, α_j (or the intersection line, α_i, in the case of wedge failure) and slope dip direction.
- F_2 depends on the discontinuity dip (β_j) in the case of planar failure and the plunge, β_i of the intersection line in wedge failure. As regards toppling failure, this parameter takes the value 1.0. This parameter is related to the probability of discontinuity shear strength.
- F_3 depends on the relationship between slope (β_s) and discontinuity (β_j) dips (toppling or planar failure cases) or the immersion line dip (β_i) (wedge failure case). This parameter retains the Bieniawski adjustment factors that vary from 0 to −60 points and express the probability of discontinuity outcropping on the slope face for planar and wedge failure.
- F_4 is a correction factor that depends on the excavation method used.

2.7.7. Geological strength index (GSI)

The GSI was first presented by Hoek & Brown (1997) for both hard and weak rock masses. Experienced field engineers and geologists typically favour a simple classification that is based on a visual examination of geological conditions and is quick and accurate. Once the geological strength index and mi have been estimated, various correlations Hoek & Brown (2019) are presented below that can be utilized to determine the rock mass strength parameters that are used to define its characteristics.

2.7.8. Kinematic Analysis

The kinematic method deals with identifying the mode of rock slope failure without reference to the forces that cause them to move (Goodman 1989; Hudson and Harrison 1997). Kinematic analysis was performed using dips software to evaluate the different failure mechanisms, such as planar, wedge, and toppling failures (Khanna & Dubey, 2021). According to Admassu & Shakoor (2013) kinematic analysis is a method used to examine the possibility for different types of structurally controlled rock slope failure brought on by the presence of discontinuities with an unfavourable orientation.

Dips Software's input parameters include slope orientations, dip and dip directions for main joint sets, and friction angle, were measured at critical rock slope sections in the field. Whereas the shear strength parameters of the discontinuity (cohesion and angle of internal friction) were obtained from RocData 3 software (Bye & Bell, 2001; Khanna & Dubey, 2021; Raghuvanshi, 2019a).

2.7.9. Limit Equilibrium Method (LEM)

The limit equilibrium method (LEM) is widely used by researchers and engineers conducting slope stability analysis. Limit equilibrium methods are relatively simple in its application, as compared to the numerical methods. The most widely used approaches for achieving limit equilibrium are slice methods, including the Bishop simplified, Spencer, Morgenstern-Price, and standard method of slices(Wyllie & Mah, 2004). Assuming a distribution of internal pressures allows one to solve the slices technique, which is known to be a statically indeterminate problem. As a result, depending on the many assumptions made, different approaches may produce different results.

Using Rocscience slide software, LEM was used to examine the stability of rock slope failures(Liu et al., 2015). By comparing the shear strength next to the sliding surface and the necessary force to maintain the slope in equilibrium, the limit equilibrium approach derives safety factor. According to Sharma et al. (1995) and Hoek and Bray (1981), the factor of safety (FOS) is defined as the ratio of resisting forces to driving forces at equilibrium. This way of evaluating forces that drive the rock mass and resisting forces is known as the limit equilibrium method. A slope is said to be stable if the FOS value is greater than 1, unstable if it is less than 1, and in a critical condition of equilibrium if it is equal to 1 (Hossain, 2011). Multiple governing parameters, including the slope geometry, failure plane characteristics, water forces, and external triggers, will influence the FOS.

2.7.10. Numerical methods

The rock slopes in general, demonstrates variability in its geometry, heterogeneity in geological formation, non-linearity in the potential failure plane, uneven distribution of the water forces in the slope with induced surcharge and the seismic loading conditions (Alzo'ubi, 2016). In order to simulate such complexities, numerical methods are required as they consider the stress and strain of the slope (Duncan 2000).

FEM slope stability modelling uses a shear strength reduction technique (Griffiths & P.A.Lane, 2013). The slope stability conditions for particular critical slope sections are determined by this study using the Phase2 software(Kanungo et al., 2013) . The phase 2 software's data preparation process includes calculating the unit weight of rocks that have undergone laboratory testing as well as the UCS of intact rocks. Field measurements were made to determine the slope height and geological strength index (GSI). The RocData software's standard table was used to obtain the material constant for intact rock and the shear strength parameters along the failure plane of rocks were calculated(Hoek et al., 2002). The Wyllie & Mah (2004) guidelines, which were based on how much the rock mass had been disturbed, were used to determine the disturbance factor.

2.8. Software used for slope stability analysis

Software used for analysing slope stability is commonly referred to as slope stability analysis software. These software programs simulate how rock and soil materials will behave in different circumstances, including variations in water content, loads, slope geometry and seismic activity. Software to slope stability analysis comes in a variety of forms, including as kinematic, finite element, and limit equilibrium approaches (Wyllie & Mah, 2004). The most commonly used applications for slope stability analysis are Dip.6, RocData 3.0, RocPlane 2.0, Swedge V. 4.0, Slide 6.0, and Phase 2 (Rocscience, 2004). The choice of software often depends on the specific requirements of the project, the complexity of the slope geometry and failure mechanisms (Raghuvanshi, 2019a). Geotechnical engineers and geologists use slope stability analysis software to evaluate the stability of slopes and embankments and to create suitable stabilization solutions to guarantee public safety and prevent property damage.

2.8.1. Dip.6 software

A kinematic analysis is the first step in evaluating rock slope stability were performed in Dips 6.0 software to identify the possible mode of failure (Rocscience, 2004). Dip 6 allows users to input data related to the orientation of discontinuities and slope face within the rock mass. This data entered from field measurements Rocscience (2004a). Based on data obtained from filed and RocData Dip 6 performs a kinematic analysis to assess the potential for different failure modes failure. By combining the kinematic analysis with limit equilibrium methods, Dip 6 provides a comprehensive approach to evaluating the stability of rock slopes, making it a valuable tool for geotechnical engineers and geologists working on rock slope stability projects.

2.8.2. RocData 3.0 software

The shear strength of discontinuities and failure planes in this investigation were computed using RocData 3.0 software in compliance with the non-linear failure criteria of Barton and Bandis (1990). Rocscience created the software application RocData to manage and analyse rock mass and rock engineering data statistically (Rocscience, 2004). The program facilitates the direct transfer of data and analysis results across other Rocscience software, including Rocplane, Swedge, Slide 6, and Phase 2 (Rocscience, 2004). Comprehensive slope stability studies and geotechnical design tasks are made easier by this combination. Overall, RocData is a strong tool that makes managing, analysing, and interpreting rock engineering data easier for geologists and geotechnical engineers (RocData, 2004).

2.8.3. RocPlane 2.0 software

RocPlane is a Rocscience software for analysing the stability of planar failure in rock slopes. It can handle complex slope geometries and failure surfaces. Planar failure is a common mode of failure in rock slopes, where the slope fails along a single discontinuity plane, such as a joint Rocscience (2004c). Rocplane allows users to input data related to the discontinuities in the rock mass, including the orientation (dip direction and dip amount), friction angle, and cohesion of the discontinuity plane (Rocscience, 2004). The software also allows the user to specify the slope geometry, including the slope angle and the slope height. Rocplane uses the limit equilibrium method to analyse the stability of the rock slope against planar failure. By taking into account the self-weight of the rock block, the cohesive and frictional forces along the discontinuity plane, and any external forces like water pressure or earthquakes, the software determines the factor of safety (FS) for the probable planar failure surface(Rocscience, 2004). Because of this, it is a useful tool for geologists and geotechnical engineers who examine the stability of rock slopes, especially in mining, transportation, and building projects.

2.8.4. Swedge V. 4.0 software

Swedge is a Rocscience software specifically designed for analysing the stability of rock wedges failure in rock slopes (Rocscience, 2004). It uses 3D analysis to assess the potential for wedge failure. Wedge failure occurs when two intersecting discontinuities create a wedge-shaped block that can slide out of the slope. Swedge allows users to input data related to the two discontinuities that form the wedge, including their orientation (dip direction and dip amount), friction angle, and cohesion Rocscience (2004d). Swedge uses the limit equilibrium method to analyse the stability of the rock slope. The software calculates the factor of safety (FS) for the potential wedge failure. Swedge can assist in the design of reinforcement measures, such as rock bolts or anchors, to improve the stability of the rock slope against wedge failure (Rocscience, 2004). The software can calculate the required reinforcement force or spacing to achieve a target factor of safety.

2.8.5. Slide 6.0 software

Slope stability study of both soil and rock slopes can be done with the help of the powerful computer-based program Slide, which was first proposed by Rocscience Inc. in Toronto, Canada (Rocscience, 2004b). It is capable of assessing the stability for both circular and non-circular failure surfaces and uses a 2D limit equilibrium approach (Rocscience, 2004). It can be used to analyse the stability of soil and rock slopes using various methods like Bishop, Janbu, Spencer, and others (Slide 6.0 rocscience, 2004). Overall, Slide provides a comprehensive set of limit equilibrium method for assessing the stability of rock and soil slopes, making it a widely adopted software in geotechnical engineering practice.

2.8.6. Phase2 software

Phase2 is a 2D finite element analysis software developed by Rocscience, which can be used for advanced slope stability analysis, including for rock slopes (Rocscience, 2004). Phase2 uses the strength reduction technique to evaluate the factor of safety for slope stability (Phase V 2.0 rocscience, 2004). This involves systematically reducing the soil/rock strength parameters until the slope becomes unstable. In addition to stability analysis, Phase2 can also perform deformation analysis, providing insights into the slope's behaviour under various loading conditions. Compared to the limit equilibrium-based approach in SLIDE, the finite element-based analysis in Phase2 provides a more comprehensive and accurate representation of the slope's behaviour, particularly for complex slope geometries and loading conditions (Rocscience, 2004). This makes Phase2 a valuable tool for advanced slope stability analysis in geotechnical engineering projects.

2.9. Remedial measure

Slope stabilization is a crucial aspect of civil and mining engineering projects that involve heavy demolition and excavation activities. The stability of excavated rock slopes must be maintained until the end of the design life for the successful delivery of a project(Hoek et al., 2000). The experts divided the stabilization techniques into five categories: surface protection (reinforcements), ground improvement (grouting, cement stabilization, chemicals), column supported embankments (retaining walls, beams, shotcrete, pile walls, bolts), and increase resisting force (change geometry, lower groundwater, increase shear strength of slope mass, drainages). Each category was taken into consideration for different types of slope (Abramson et al., 2001). To protect the slope against them in the future, these successful solutions aim to prevent failure in the installation of structures and slope modifications.

2.9.1. Modification of Slope Geometry

Slope geometry has a significant impact on slope stability. Bench height, overall slope angle, and surface area make up the basic geometrical slope design factors(Chaulya & Prasad, 2016). Gibson et al. (2006) claim that a variety of bench height, bench face angle, and berm width configurations can be used in the slope design to achieve a bench stack angle that meets the stability criterion. The proper bench face angle and berm width geometries must be selected in order to satisfy the bench stack angle and provide a berm large enough to collect the volume of failed wedge material from the bench faces above. By maximizing bench width, mining companies can maintain stable, increase operational effectiveness, cut costs, and increase worker safety. This process is important to every mining practice and contributes to the safe and long term success of mining operations(Karacan et al., 2011). In certain mining circumstances, the multi-bench slope technique can be utilized to change the slope. The technique is a vital part of contemporary open-pit mining since it makes natural resources extraction affordable, effective, and safe(Bye & Bell, 2001)

2.9.2. Drainage system

In open pit mining, a variety of drainage maintenance tasks are crucial and are actually influenced by seasonal change. In order to properly construct cut slopes Sophocleous (2002) state that it is crucial to consider both the natural drainage patterns of the surrounding area and how the new slope would affect them. It is necessary to evaluate two situations: surface water flowing down the slope's face and surface water seeping into or entering the cut's head. The shear strength of slope material decreases because of slope material disintegrating when surface water seeps into or penetrates the cut's head. In order to control it, rapid drainage must be maintained.

2.10. Quarry site design

The safe, effective, and long-term functioning of a quarry depends significantly on the design of the quarry site. A well-designed slope not only increases slope stability and safety, but it also lowers expenses, increases mine life, and lowers the stripping ratio (Bye and Bell, 2001; Naghadehi et al., 2011). As shown on figure 2.1 benchmark design methodology is one popular strategy for safe quarry cut design(Alejano et al., 2007). Bench heights and width depends on depending on the equipment that is available and the properties of the rock mass to ensure safe access and operation (Bar & Barton, 2017). Quarry operators may reduce the possibility of slope failures, improve operating safety, and guarantee the quarry's long-term sustainability by using this bench design technique to create a safe and stable layout (Kolapo et al., 2022).

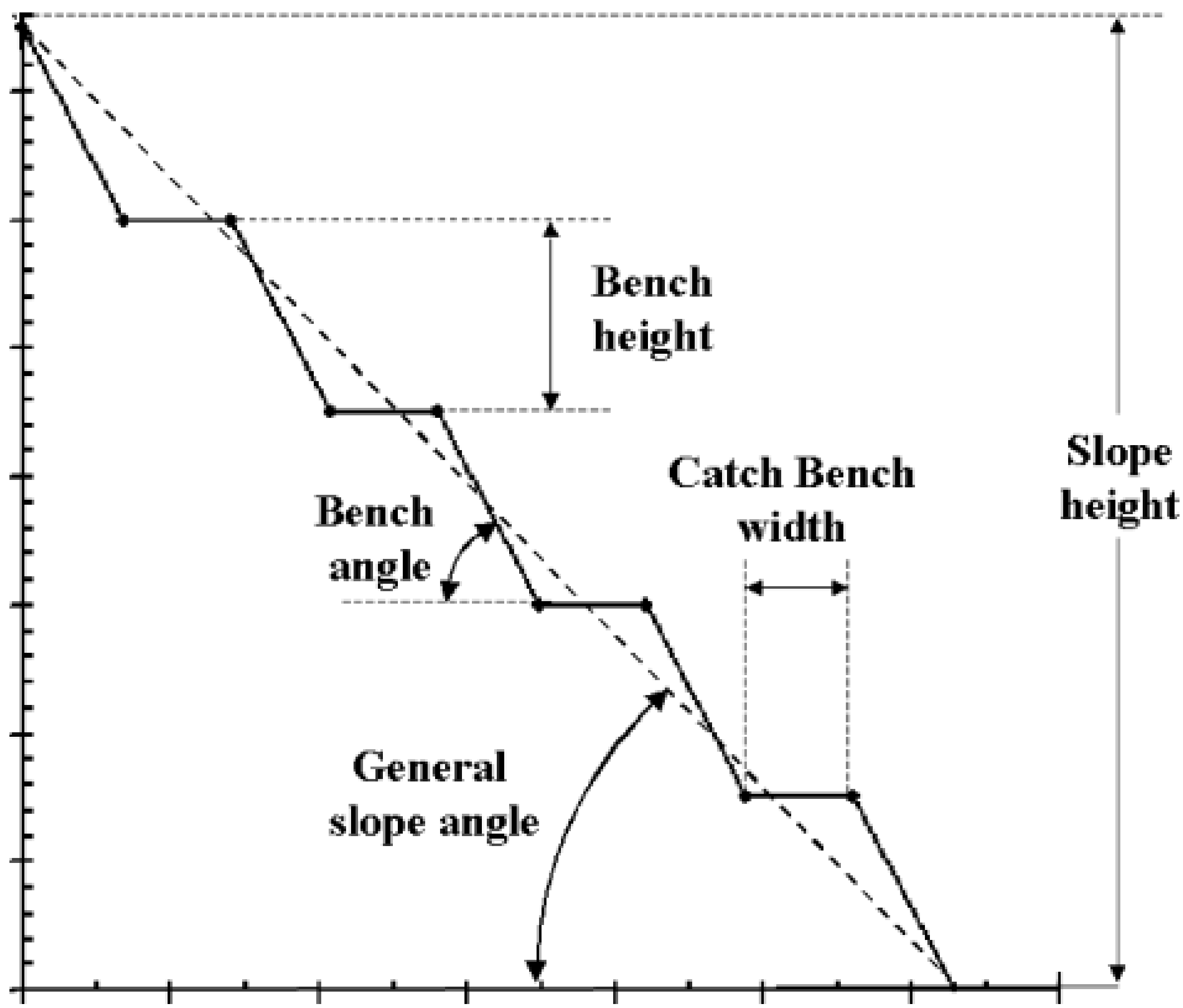

Figure 2.1: Geometrical descriptions of quarry slopes (Alejano et al., 2007; Wyllie & Mah, 2004)

CHAPTER THREE

3. MATERIALS AND METHODS

3.1. Materials

The following tools was utilized to complete this research work these included topographic map, geological hammer, GPS, compass, calliper, meter, Schmidt hammer, and software were used in this study to collect , process data and analysis. This study was conducted using Rocscience software, which is required to process data, analyse failure zones, and compute FOS and SRF of critical slope section of quarry site.

3.2. Method

The research methodology for this study was involved the integrated methodology and approach used in this study consists of several parts, including a desk study, detailed field investigation, rock sampling, laboratory testing, and data processing methods to evaluate the stability conditions of the quarry slopes. The general approaches used in research activity are desk study, detail field and laboratory work, as well as data processing and analysis.

3.2.1. Desk study

This stage involved conducting literature reviews and study field research thorough assessment of past studies, books, as well as published and unpublished reports, done in order to appreciate the geological and geotechnical conditions in the study area and to compile the field data for this study. We gathered a variety of data significant to determining the stability of the slope, including meteorological data from NASA for 12years rainfall data, geological and topographic maps, and reports on the surrounding regional geology from past research works of the study area from Ethiopian Geological Survey map of Nazret-Dera area, 1:50,000 scale. Finally, a conceptual framework and a general methodology flow chart for quarry stability study were constructed using the information gathered from the literature review.

3.2.2. Detail field survey

In the research region, the geotechnical parameters of the exposed rock mass was examined by a combination of laboratory testing and field observations and measurements. In order to determine the instability condition of the slope, as well as its critical location and the most critical slope sections within the study area, a field investigation was conducted. The aim was to collect input parameters for the slope stability analysis, including dip amount and dip direction of slope and discontinuities, the failure plane waviness, slope height, upper slope face inclination, and in-situ strength test and collecting representative rock sample determined in the field.

3.2.2.1. Identification of critical slope section and structural data collection.

According to Hoek & Bray (1989), the most crucial aspect of the stability analysis is to identify these geological characteristics, as their existence or absence has a significant impact on the stability of rock slopes. A field evaluation was conducted to identify potential slope instabilities based on the failure mechanism, which might be either non-structural controlled failure or structurally controlled failure. In the field, visual observations and measurements were made of discontinuity characteristics such as spacing, separation, roughness, continuity, and orientation, as well as ground water conditions.

During filed survey quarrying activity observed which create step slope with unfavourable orientation of discontinuity and different critical slope section was identified for furthers analysis of rock slope stability and to recommend appropriate remedial measure. Quarry operation continue excavation by poor bench design. The slope was created by poor mining activities and benching. Quarrying operations have resulted in a slope with a height of 20 to 55 meters. The slope is steep, with an inclination of 75^0 to 90^0 with jointed rock mass. This condition could result in failure due to slope instability caused by inappropriate quarrying procedures. Hear attached some critical slope section that shows structural and non-structural controlled slope section of quarry site figure 3.1. (A) represent overall quarry slope face , (B) structural controlled wedge mode of failure represented by QSS_1, (C) represent QSS_3 which shows wedge mode of failure, (D) represent QSS_2 planner mode of failure and (E) non-structural controlled slope section of QSS_4 and QSS_5.

(A)

(B)

(C)

(D)

(E)

Figure 3.1: Structural and non-structural slope section of quarry site that have highly jointed and create steep cut slope due to quarrying operation.

3.2.2.2. In-situ strength test

For determining the mechanical characteristics of rock material, the Schmidt hammer offers a rapid and affordable way to determine surface hardness (Aydin & Basu, 2005a). According to Aydin and Basu (2005), the N-type hammer proved to be more efficient than the L-type hammer in predicting uniaxial compressive strength because it caused less scatter in the data. So during the in situ strength test, an N-type Schmidt hammer was used in this study to determine the rebound value (R) of rocks at selected different critical quarry slope sections following the ASTM C 805 test process. The ASTM C805 test method is frequently chosen since it is flexible, quick, simple, and economical (ASTM, 2008). As shown in figure 3.2 a Schmidt hammer was gently strike the test surface while being applied perpendicular to it. At each sample location, two trials with ten readings each were carried out. Readings were taken for every trial test with a 20 mm space between the two impact test locations. The average of the rebound value (R) was used to determine the UCS after the rebound values were listed in ascending order. The empirical equation Barton & Choubey, 1977 it offers a useful and reliable technique for determining rock strength based on joint parameters. The joint roughness coefficient (JRC) and the joint wall compressive strength (JCS), two important variables affecting the shear strength of rock joints, are taken into consideration in this equation.

Finally, the empirical equation 4 used to calculate the uniaxial compressive strength of the rocks along the crucial slope portion (Barton & Choubey, 1977).

Figure 3.2: In-situ strength test using Schmidt hammer at different critical slope section of quarry

3.2.2.3. Rock sampling

To analyse slope stability sampling is an essential step. It involves the collection of representative rock samples from the site and their subsequent testing to investigate the engineering characteristics of the rocks in the research area, these samples taken from significant slope sections at the quarry site. Once the samples was collected, they are subjected to a range of laboratory tests to determine their physical and mechanical properties. Unit weight and point load, were measured as part of the laboratory tests.

3.2.3. **Rock Laboratory test**

After gathering representative samples from the field, the necessary laboratory tests was carried out in an Engineering Corporation of Oromia in accordance with the standards on a variety of samples taken from critical slope section of quarry site. Laboratory testing like unit weight test and point load test determined the physical and mechanical characteristics of rock samples, which were crucial for slope stability analysis.

3.2.3.1. Point load test

The point load test is an alternate method that can be used to adequately predict the uniaxial compressive strength of a rock material using portable and simpler equipment. In accordance with ASTM D 5731 (1995), a point load strength test of rocks was performed. As shown in figure 3.3 test procedure, irregular lumps and rock samples are put between two conical platens, and a concentrated force is given until failure. The rocks' point load strength was converted to their uniaxial compressive strength as part of the test. The point load strength index recorded over rock samples other than those having a 50 mm core diameter is termed the uncorrected point load strength index (Is) in ATM 5731 (1995). This index must be corrected to a 50 mm diameter point load strength index, or Is (50), using the correction factors F provided in equation 11.

$$\mathrm{I_S(KPa)} = \frac{P}{De^2} \tag{6}$$

Where, Is refers uncorrected point load strength P refers failure load and the equivalent core diameter De is calculated based on the shape of the specimen as:

$$D_e = \sqrt{\frac{4 \times A}{\pi}} \tag{7}$$

Where, A is the minimum cross-section area of a plane through the contact point of the planes and is calculated as:

$$A = \mathrm{W} \times \mathrm{D} \tag{8}$$

$$\mathrm{I_S}(50) = \mathrm{F} \times \mathrm{I_S} \tag{9}$$

Where, Is (50) corrected point load strength index and F is a size correction factor, which is calculated as:

$$\mathrm{F} = (D_e/50)^{0.45} \tag{10}$$

In this study uncorrected point load strength index was obtained and converted to corrected point load strength index, finally According to an empirical equation 12 relationship proposed by Broch and Franklin (1972), the uniaxial compressive strength (UCS) of rock can be calculated from the point load strength index as follows:

$$\mathrm{UCS} = 24 * \mathrm{Is}(50) \tag{11}$$

Where, UCS is uniaxial compressive strength of intact rocks and Is (50) is the size corrected point load strength.

Figure 3.3: Irregular sample taken from critical slope section of quarry and point load test.

3.2.3.2. Density and unit weight rock

The unit weight of the rock served as one of the input variables used to calculate the safety factor for calculations on the stability of rock slopes. The test were conducted on certain rock samples obtained from a significant quarry slope portion using buoyancy procedures as described in ASTM C 127-88 the standard as follows: The first step of the test was to name, weigh, and oven-dry the rock samples for 24 hours at 105°C. After that, the weight of the oven-dried rock samples was noted (M_{dry}). After inserting the oven-dried samples into the water-filled cylinder, the initial water volume (V_1, in ml), as well as the subsequent volume change (V_2, in ml), were measured. After that, determine how much the sample's volume has changed by putting an irregular, oven-dried rock in a cylinder of water that contains the equation 25.

Finally, the dry density (ρd) and unit weight (γd) of each rock sample were determined using equation 13 and 14, respectively.

$$\Delta V = V_2 - V_1 \quad 12$$

$$\rho d = M_{dry}/\Delta V \quad 13$$

$$\gamma d = \rho d * g \quad 14$$

Where, ΔV the difference between the volume before oven-dried sample was inserted into cylinder and the volume after rock sample was placed in cylinder, ρd dry density of rock in g/cm3, M_{dry} mass of oven-dried rock sample in g, γd dry unit weight of rock sample in KN/m3, and g-gravitational acceleration.

3.3. Data processing and analysis

Once all relevant information had been gathered through desk study, fieldwork, and laboratory testing, it had been organized and processed the slope stability assessment was conducted using Rocsciences software. The methods for analysing slope stability are kinematic, limit equilibrium and finite element approaches, which used to identify and determine stability conditions of the rhyolite quarries in Adama in terms of mode of failure and factor of safety.

3.4. Determining shear strength parameters along failure plane

Shear strength parameters like cohesion and friction angle are the main factors that define resisting force acting normal to the failure plane (Raghuvanshi, 2019). The following method was used to obtain the equivalent linear Mohr-Coulomb strength criterion or parameters (cohesion and friction angle) using Rocdata software, which uses nonlinear failure criteria (RocData, 2004). In this study, cohesion and friction angle along a failure plane were determined in accordance with built-in Rocdata software. The joint roughness coefficient, joint wall compressive strength, basic friction angle, unit weight of the rock, and slope height are the input parameters utilized by the RocData software to calculate the cohesion and friction angle. While joint wall compressive strength and slope height were measured in the field, the joint roughness coefficient (JRC) was qualitatively and visually assessed by comparing it with a standard profile. In a similar manner, the rock's unit weight was established in the lab. As a result, the Rocdata software's built-in table provided the fundamental friction angle as shown in figure 3.4.

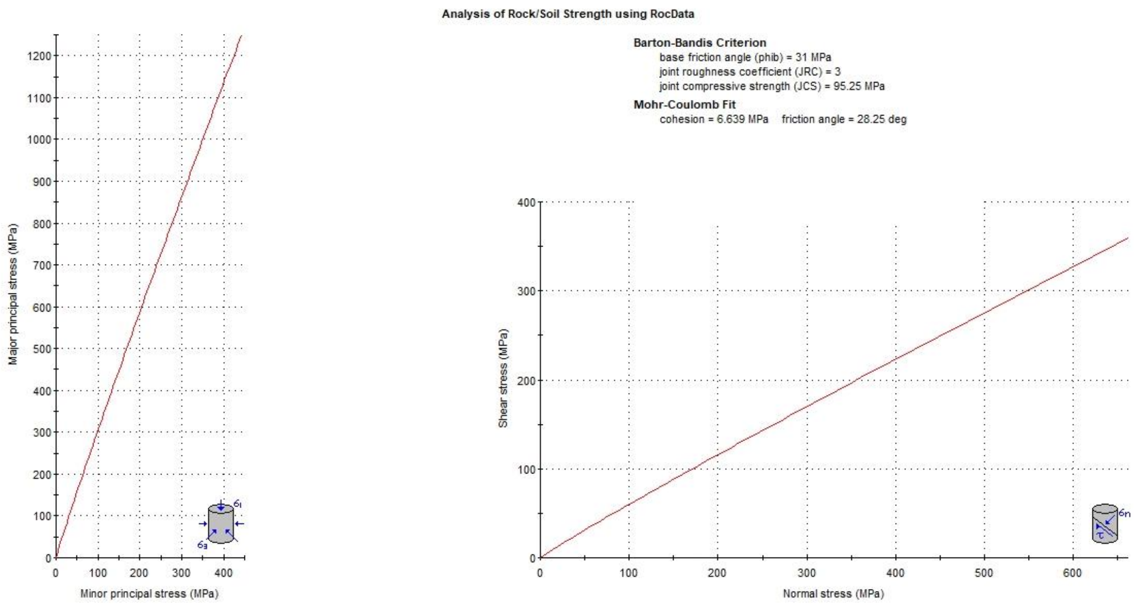

Figure 3.4: Shear strength parameter analyses using RocData software along a failure plane

For determining the basic friction of rock discontinuities, the basic friction angle of rhyolite rock units were estimated in this study to be 31° (Barton & Choubey, 1977; Ulusay & Karakul, 2015). Whereas the basic friction angle of igneous rocks has a range of 30° to 35° (Alejano et al., 2012; Barton & Choubey, 1977; Ulusay & Karakul, 2016). For dry, unweathered surfaces, the basic friction angle φb is close to equal to the residual friction angle φr (Barton & Choubey, 1977). The Barton-Bandis shear criterion can be used to evaluate the shear strength of a discontinuity using equation 15 (Barton & Bandis, 1990).

$$\tau = \sigma_n tan\left[\varphi_r + JRClog_{10}\left(\frac{JCS}{\sigma_n}\right)\right] \qquad 15$$

Where JRC is the joint roughness coefficient, JCS is the compressive strength of the joint surface, σ_n is the normal stress applied to the joint, and φ_r is the residual friction angle, which can be calculated by using equation 16:

$$\varphi_r = (\varphi_b - 20^0) + 20\frac{r}{R} \qquad 16$$

Where r is the Schmidt hammer rebound number recorded for a weathered and wet discontinuities, such as those typically seen in the field, and R is the Schmidt hammer rebound number recorded for the unweathered surfaces of the same rock, and φ_b is the basic friction angle.

3.5. Slope stability analysis method

The methods currently in used for slope stability analysis are kinematic analysis; limit equilibrium and finite element method. These methods of analysis was used for circumstances that are static dry, static saturated, dynamic dry, and dynamic saturated.

3.5.1. Kinematics analysis

Kinematic analysis of rock slopes was carried out for structurally controlled failure using the software Dips 6.0 to identify potential mode of failure. The input parameter for the analysis were obtained from filed measurement of orientations of discontinuity and slope face using burton compass. Whereas value for the friction angle, which can be obtained via RocData software were determined. One of the input parameters for the Dips program are orientation of discontinuities and slope face (dip and dip direction), and friction angle (Hoek, 1974 & Barton and Choubey, 1977).

3.5.2. Limit equilibrium method

The limit equilibrium method was utilized to carry out stability assessments for both structurally and non-structurally controlled slope sections using Rocscience Slide 6.0 software. Once the kinematic method identifies the mode of rock slope failure limit equilibrium, it can be used to determine the stability of the slope in terms of FOS, which is the ratio of resisting force to driving force along the failure plane (Price, 2009; Hoek and Bray, 1981). Input parameters, including cohesion, friction angle, unit weight, and slope geometry, were used to determine the safety factor. Those input parameters obtained were cohesion and friction angle from RocData software, unit weight from a rock laboratory test, and slope geometry measured from a field. The effect of these characteristics on the slope section is analysed using the safety factor for each of the static dry, static saturated, dynamic dry, and dynamic saturated circumstances. The rock slope section in this study was analysed using the most thorough limit equilibrium methods, such as Janbu generalized (JG), Morgenstern-Price (M-P), Spencer's, and general limit equilibrium (GLE) using the Slide 6.0 software program.

3.5.3. Finite element method

A finite-element-based numerical simulator in the Phase2 software program used to generate the critical shear SRF, which is equivalent to the FOS. This study used the Phase2 software to determine the slope stability conditions for selected critical slope sections. Phase2 software is a strong finite-element tool that can be used to model the slope stability at different conditions (You et al. 2018).

The deformation modulus rock mass used in the numerical analysis of slope stability was determined using the following equation 17 for $\sigma ci \leq 100$ MPa and $\sigma ci > 100$ MPa (Hoek and Brown, 1997)

For $\sigma ci \leq 100$ MPa, $$\mathrm{Em\ (GPa)} = \left(1 - \frac{D}{2}\right)\sqrt{\sigma\frac{ci}{100}} * 10^{(GSI-10/40)} \quad 17$$

$\sigma ci > 100$ MPa, $$\mathrm{Em\ (GPa)} = \left(1 - \frac{D}{2}\right) * 10^{(GSI-10/40)}$$

For this study, the Poisson's ratio of the rock mass can be calculated using equation 18 the relationship between the material constant (mi) and GSI proposed by Balazs (2009) as can be seen in

$$Vrm = -0.002GSI - 0.003m_i + 0.457 \quad 18$$

Where Vrm is the Poisson's ratio of the rock mass, mi is the material constant of an intact rock which was taken from the Rocdata software, and GSI is the Geological strength index of rocks estimated in the field.

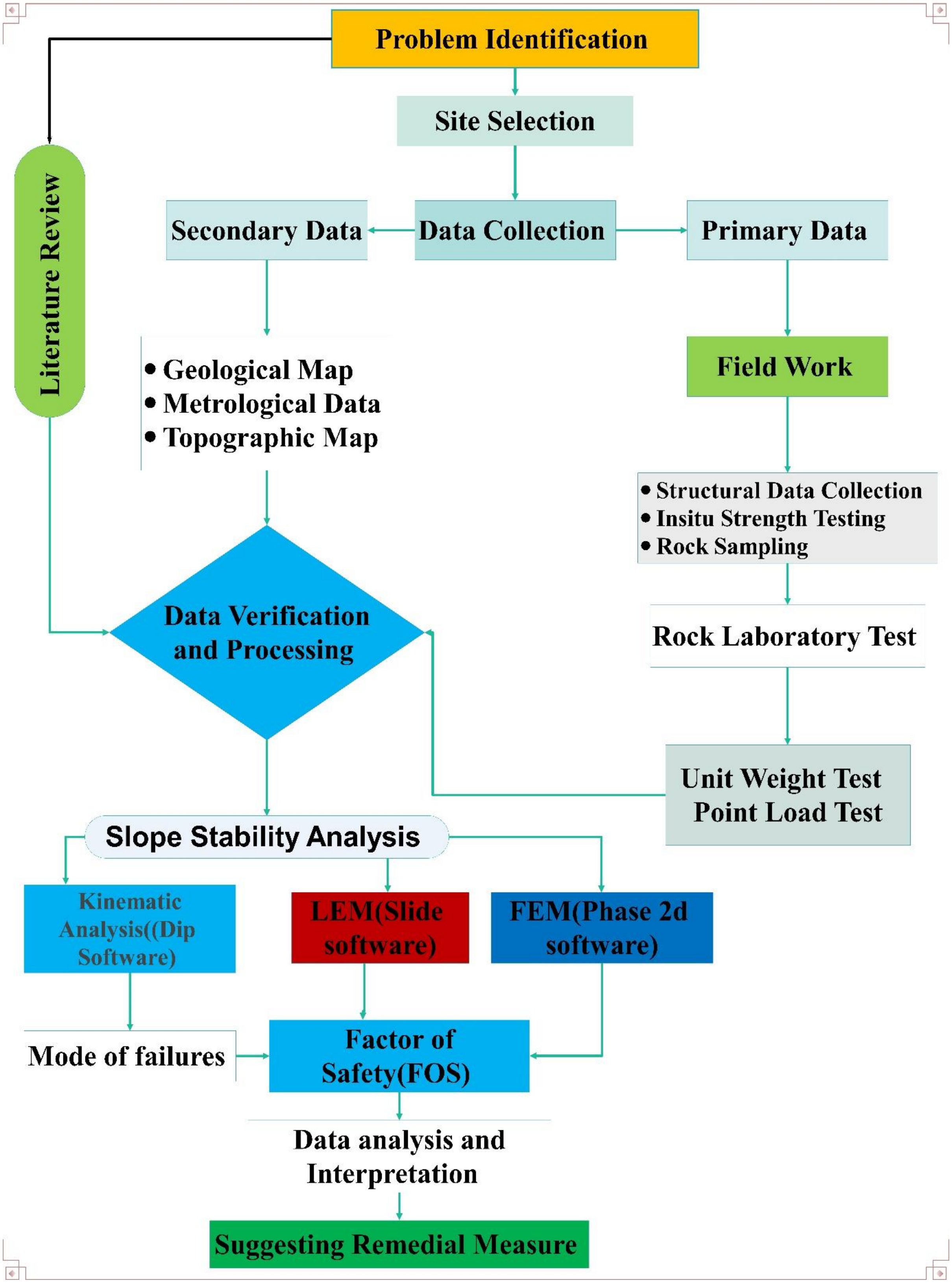

Figure 2: Methodology flow chart showing procedures to slope stability analysis of quarry site.

CHAPTER FOUR

4. DESCRIPTION OF THE STUDY AREA

4.1. Location and accessibility

The main centre of the study, Adama Town, is situated in the Main Ethiopian Rift of the Oromia National Regional State in the East Showa Zone. It is located 99 km from Addis Ababa along the road that connects Addis Ababa with the eastern towns of the nation and the port of Djibouti at an elevation of 1712 meters and 8.514477°N latitude and 39.269257°E longitude. As shown in figure 4.1(C) quarry site is located with coordinates of 8.544464°N and 39.301842°E and elevation of 1625 meters.

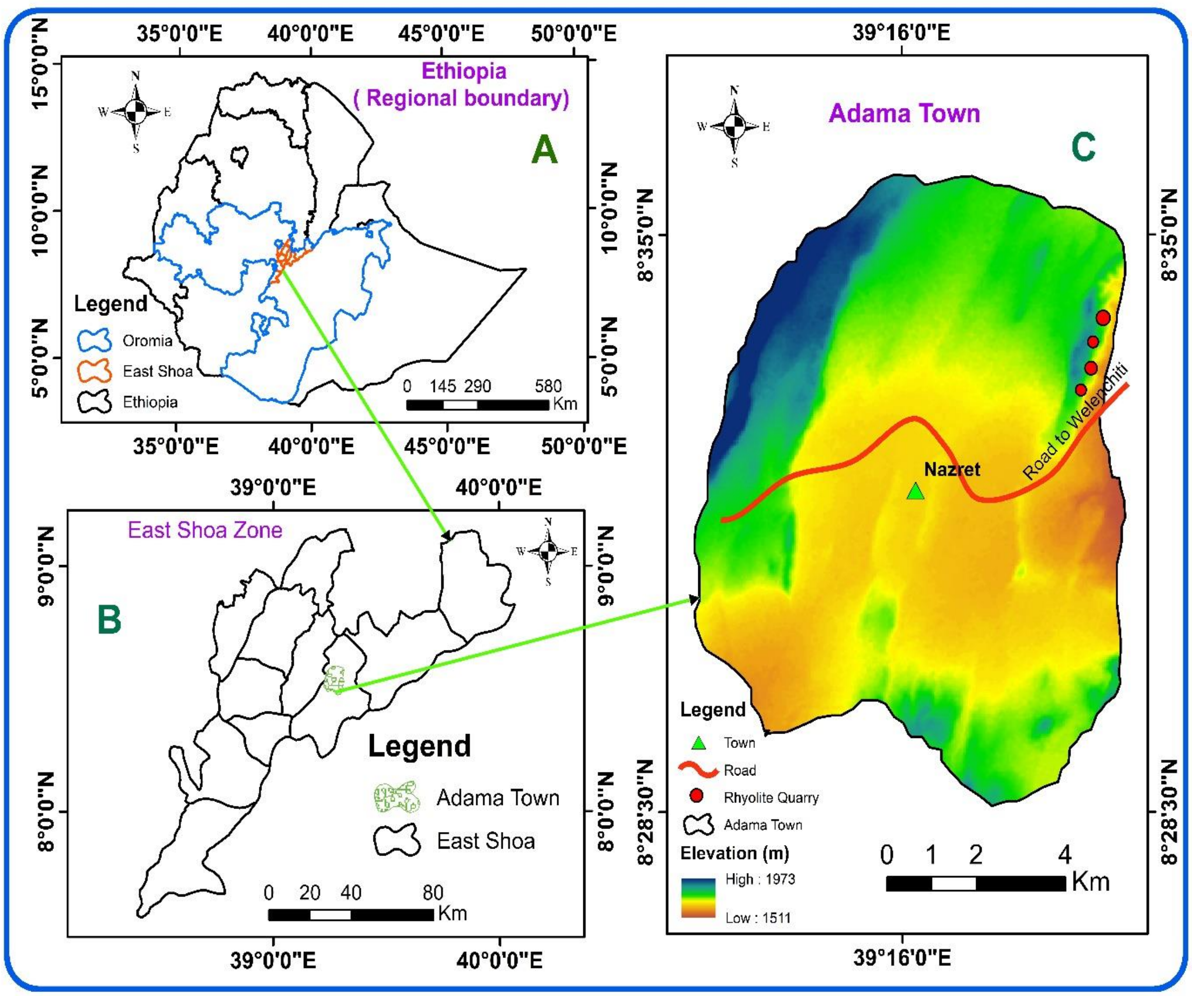

Figure 4.1: Location map of the study area (A is Ethiopian regional boundary; B is East Showa Zone (Woreda boundary); and C is Adama Town and Rhyolite quarry site).

4.2. Physiography of study area

Various factors such as structural features, geomorphology, and tectonic settings influence the physiography of Adama and its surroundings. The study area is at an elevation ranging from 1520 to 1920 m above sea level as shown in figure 4.2. Where the Adama town range of fault-bounded basins, volcanoes, and escarpments define the Rift Valley. Its location lies between the Great Rift Valley to the east and the foot of an escarpment to the west. The quarry site is located 1625 meters above sea level. Within the Great Rift Valley, Adama town is situated on flat terrain, is surrounded by mountains, and ridged topography.

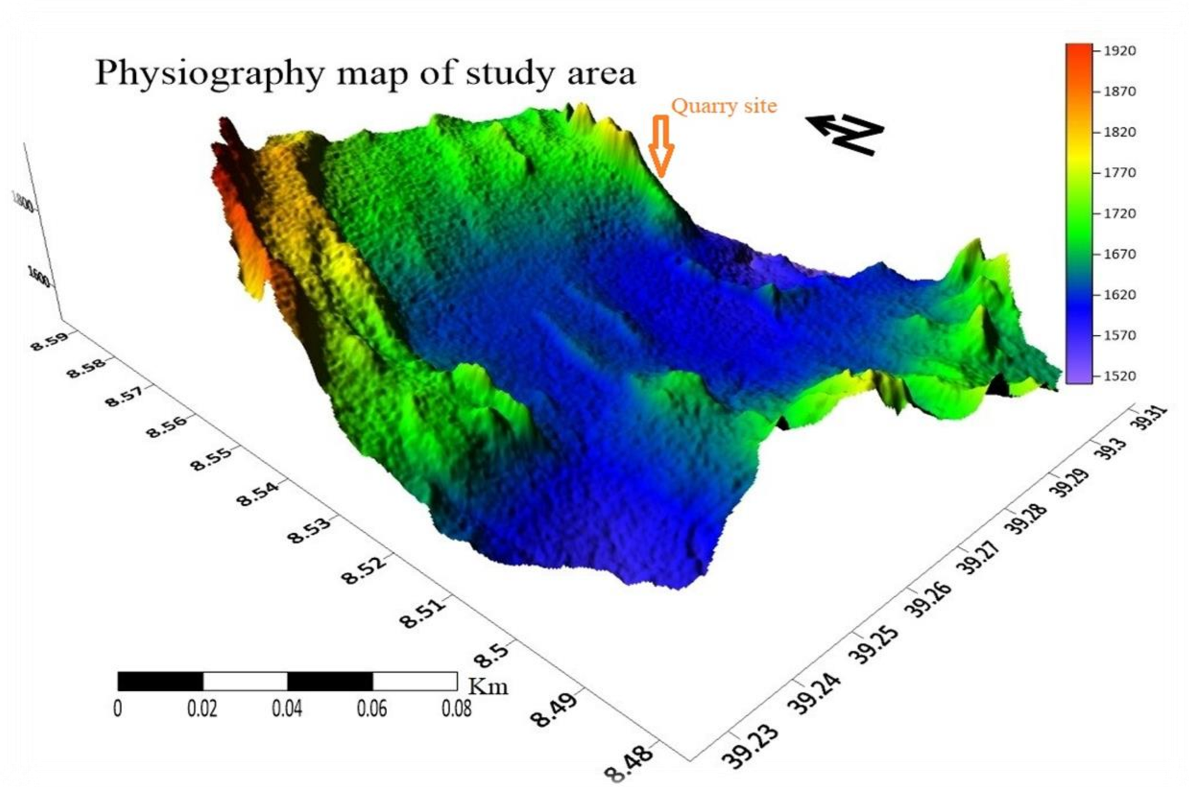

Figure 4.2: 3D Physiography map of study area

4.3. Drainage pattern of study area

The study area found in Ethiopia's Great Rift Valley, which has a dendritic drainage pattern as showed on figure 4.3. Smaller tributaries join larger ones as they flow downhill towards the main river channel, creating a pattern like a tree formed by the streams and rivers.

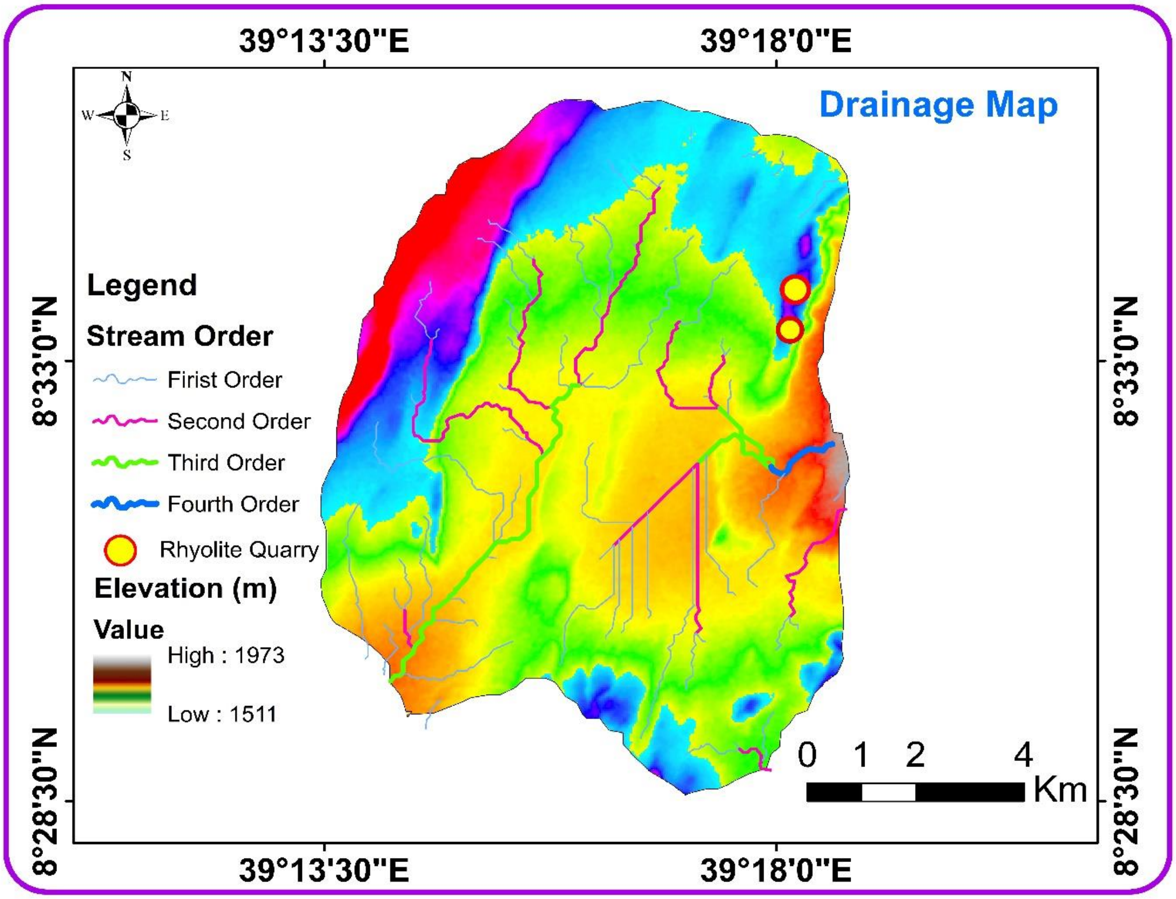

Figure 4.3: Drainage pattern of the study area

4.4. Seismicity of the study area

One of the elements that causes slope instability is seismic activity, especially in seismically active areas (Hoek & Bray, 1981). In accordance with location, the study region is found in the Main Ethiopian Rift (MER), an area prone to seismic hazard map zone 4 or zone of major damages. According to the report, Asfaw & Woldeyes(1986), Ethiopia seismic risk map for the study region (zone 4) as showed on figure 4.4, the design ground acceleration is expected to be 0.1 g for a 100-year return period. Therefore, slope stability issues in the quarry site, which may be triggered by seismic activity.

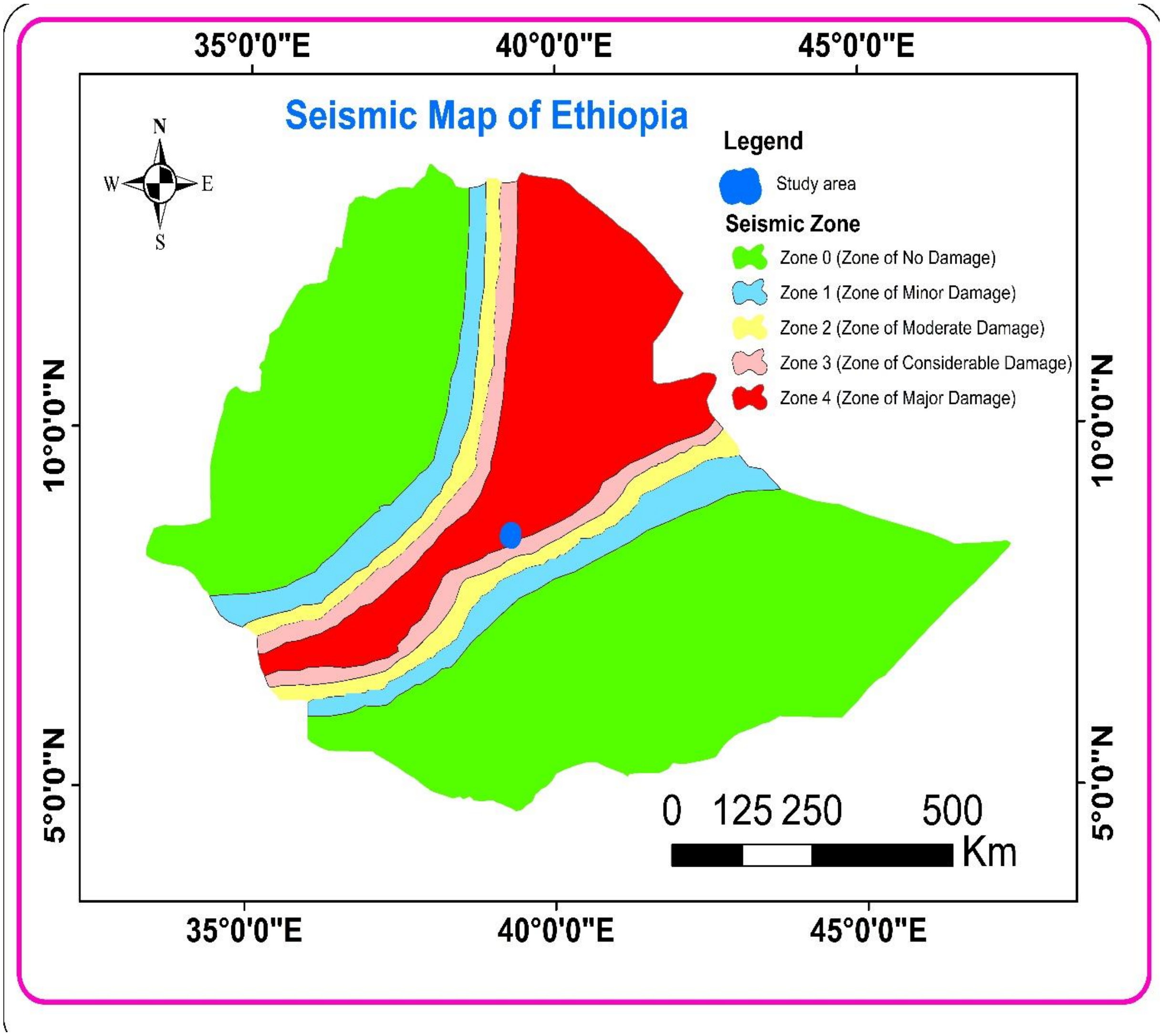

Figure 4.4: Seismic risk map of Ethiopia modified after (Asfaw & Woldeyes, 1986)

4.5. Rainfall of the study area

Slope instabilities are triggered by intense rainfall, and previous rainfall has impact on the occurrence of instability of slope (Bogaard & Greco, 2016). Based on field observations, it has been noted that slope instability in the area being studied is common during the summer months. According to 12 years rainfall data from 2011 to 2022, figure 4.5 and 4.6 constructed for study area data acquired from NASA, the minimum and maximum annual rainfall of the area is between 68mm and 216mm with average annual rainfall of 686mm.

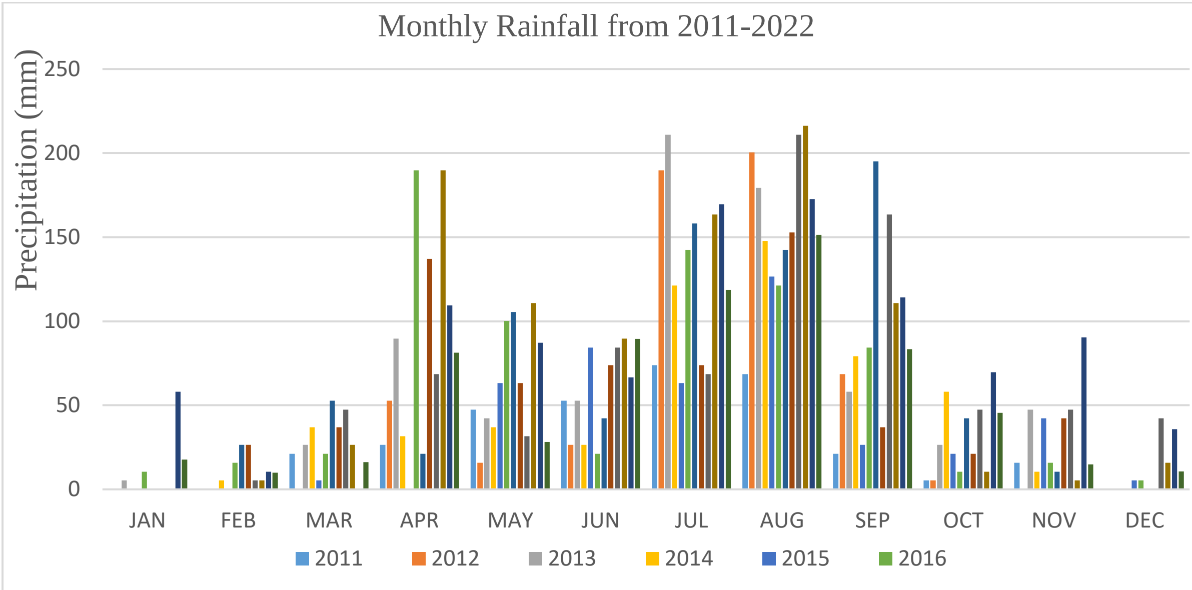

Figure 4.5: Monthly rainfall data of the study area (2011-2022) from NASA.

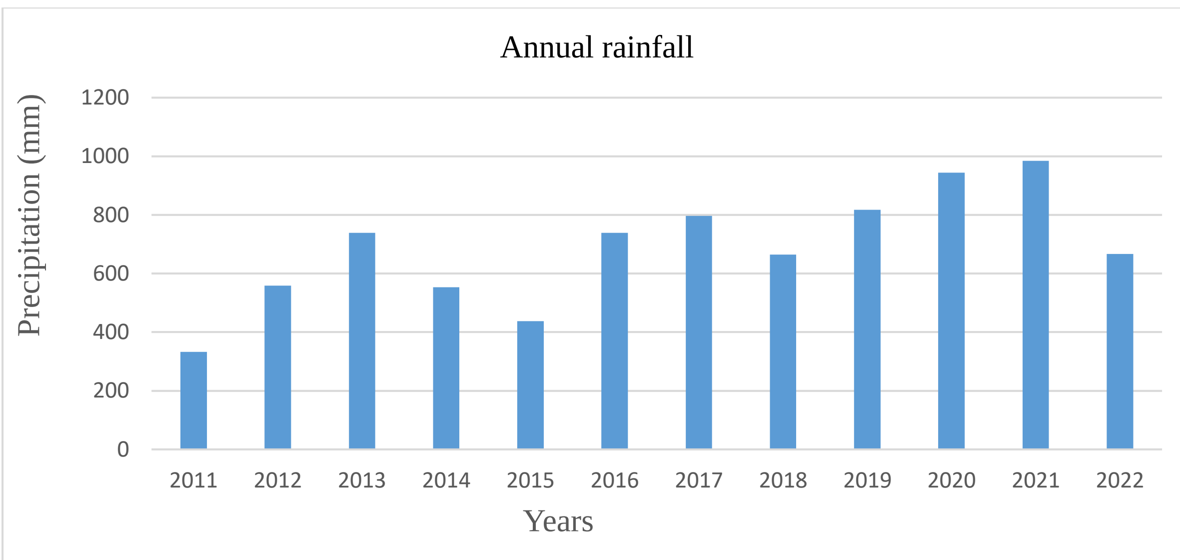

Figure 4.6: Annual rainfall of the study area (2011-2022) from NASA.

4.6. Regional geology and tectonic setting

The geology of Ethiopia is comprised of three major geological terrains, namely: the Proterozoic crystalline basement, Late-Paleozoic to Mesozoic marine and continental sedimentary rocks and Cenozoic, basic and felsic volcanic and associated sedimentary rocks (Abbate et al., 2015). The Main Ethiopian Rift (MER) exhibits a complex regional geology characterized by extensive volcanism, seismic activity, and ground fissuring consists of thick succession of flood basalts, alkaline to tholeiitic in composition, and lower amounts of rhyolites emplaced during Eocene to

Middle Miocene (Bonini et al., 2005; WoldeGabriel et al., 1991). According to Peccerillo et al. (2003), a bimodal basalt-rhyolite association with a noticeable absence of lavas with an intermediate composition primarily defines volcanism. Specifically, the Main Ethiopian Rift (MER), located in the northern portion of the EARS, exhibits variations in volcanism (mostly in composition and volume) in relation to the extent of rift extension. The majority of the northern MER's floor is made up of these basalts, which are mostly responsible for the region's large basaltic lava flows that are connected to shield volcanoes or erupting fissures (Hayward and Ebinger, 1996; Lahitte et al., 2003). On the other hand, the central and southern regions of the rift are mostly home to felsic central volcanoes, which typically distinguished by calderas and emit rhyolite ignimbrites (WoldeGabriel et al., 1990). Typically, sedimentary syn-rift deposits intercalated with these deposits (Turdu et al., 1999). According to recent field research, basalts typically connected to monogenetic vents and/or fissure eruptions on the side of the main central volcano. Furthermore, quaternary rocks commonly affected by faulting along this belt, which defines an important active volcano tectonic axis located within the broader rift valley bounded by border faults trending north-northeast to northeast (Mohr, 1974; 1977). Adama town situated in the southern extreme of the active volcano- tectonic segment of the northern Main Ethiopian Rift (MER). Rocks in the Adama region are classified from low to high strength using unconfined compressive strength tests, while the predominant soil types are low to medium plastic silty sand and sand (Chemeda, 2020). Because of the area's vulnerability to geohazards as landslides, flooding, seismic activity, and gully erosion, careful engineering and urban planning are required (Chemeda, 2020). However, the Adama region's geological features are mostly shaped by tectonic and volcanic activities. According to the works of Kazmin and Berhe (1978) reveal the following stratigraphic succession, which is more particular to the Adama area as shown in table 4.1 below.

Table 4.1. Lithostratigraphic sequence in the study area.

<table>
<tr><th>Age (Million)</th><th>Formation</th><th>Description</th></tr>
<tr><td>Recent</td><td></td><td>Lacustrine sediments</td></tr>
<tr><td>1.5</td><td rowspan="2">Wonji Group</td><td>Pleistocene to sub-recent basalts</td></tr>
<tr><td rowspan="2">1.5 - 2</td><td>Recent rhyolites, domes and flows</td></tr>
<tr><td rowspan="2">Nazareth Group</td><td>Older rhyolites, domes and flows</td></tr>
<tr><td>9 - 2</td><td>Ash flows, tuffs, pantleritic ignimbrites and un-welded tuffs</td></tr>
</table>

The Wonji Group, which includes the younger basalt and rhyolite, typically linked to the formation of the Wonji fault system in the rift valley. The older units, known as the Nazareth Group, are primarily upper Miocene to Pleistocene volcanic succession that widely distributed along the Main Ethiopian Rift Floor. According to Alula (1992), various rock types outcropping are subdivided into; alluvial and lacustrine deposits; Bofa basalt; rift floor ignimbrites; rhyolitic lava flows; tuffs and pumice fall deposit

4.6.1. Rift floor ignimbrites

The rift floor ignimbrites are the region's oldest outcropping unit. The main outcrops, which have elongated outcrops and surrounded by faults, are actually located west of Nazareth town. The ignimbrites are large and tightly welded, which is favourable as an aggregate. Alula et al., (1992) found a total thickness of roughly 100 m with a K/Ar age of 1.7 Ma. Due to caldera collapses and violent volcanic activity, the Main Ethiopian Rift's (MER) rift floor ignimbrites are important geological phenomena (Bedassa et al., 2023). With indications of fractional crystallization and magma mixing playing a role in their genesis, the ignimbrites are distinguished by a bimodal distribution of mafic and felsic compositions (Rienzo, 2019). According to Langone et al. (2024), the ignimbrites exhibit a variety of compositions from basaltic to rhyolitic, with intermediate forms also being recognized.

4.2.1. Rhyolitic lava flows

Rhyolitic lava flows in Ethiopia, particularly within the Ethiopian Rift, exhibit unique characteristics and formation processes characterized by a glassy texture and high silica content (Ayalew et al., 2021). The flow bands in Badi volcano's lavas arise from alternating vesicular and non-vesicular domains, indicating complex cooling histories. The Badi volcano in the Central Afar region is notable for its compositionally homogeneous rhyolitic obsidian lavas, which display well-developed flow bands resulting from variable vesicularity during cooling and degassing (Ayalew et al., 2021). Peralkaline rhyolite eruptions have also been found to occur on the Aluto volcano, which is noteworthy because of the possible risks they pose, such as pyroclastic density currents (PDCs) (Clarke, 2020). According to research, peralkaline rhyolites and basaltic magmas are genetically related due to intensive fractional crystallization processes (Rienzo, 2019). On the caldera's western rim, rhyolitic lava flows occur as a basal layer. The color of these flows is gray, having fine to medium texture, or microscopically, they have porphyritic texture, which generates steep slopes surrounding the rim (Alula et al., 1992).

4.2.2. Bofa basalt

Bofa basalt is a component of a complex volcanic system with a variety of magmatic compositions and processes (Mohr, 1983). A variety of basaltic lavas that have experienced substantial evolution because of fractional crystallization, crustal assimilation, and magma mixing are found in this region, especially inside the Main Ethiopian Rift (Kazmin et al., 1980). Due to fractional crystallization processes, the Bofa basalt has a bimodal composition that changes from basalt to peralkaline rhyolite (Tadesse et al., 2023). With melting taking place at depths of 21 to 25 km and temperatures of about 1150°C, basaltic lavas are mostly formed from a primitive mantle source (Rienzo, 2019). The geological diversity of the Ethiopian plateau is highlighted by the fact that, although the Bofa basalt is a notable volcanic feature, other parts of the country may display distinct magmatic features, such as the influence of subduction-related processes or different mantle sources (Tamirat et al., 2021).

4.2.3. Pumice fall deposits

Important geological features in Ethiopia are pumice fall deposits, which are the product of violent volcanic eruptions, especially along the Main Ethiopian Rift (Rooney et al., 2012). The stratigraphically broad deposit covers the lowest rhyolitic lava flow. In hydrothermally active areas, it underwent a complete transformation. The pumice fall deposit creates a softer slope even far from the caldera, with an exposed thickness of about 4.5 m (Alula et al., 1992). These deposits shed light on the region's magma development and eruptive history. Given that peralkaline rhyolite magmas predominate in the Ethiopian Rift's eruption record and have an impact on the properties of pumice deposits, their evolution is essential (Rooney et al., 2012). Pumice fall deposits are crucial for comprehending volcanic activity, but they also endanger the local population, therefore further research is needed to understand their dynamics and possible concerns from future eruptions (Clarke, 2020).

4.2.4. Tuffs

Pumice clasts and lithic fragments are abundant in this unit. The tuff is brown in colour and outcrops around the Boku caldera's eastern rim. The unit is approximately 80 m thick (Haile et al., 2002). The region's plains are completely covered in unwelded tuffs. These deposits, which are mostly made of pumice and volcanic ash, are essential for comprehending environmental changes and geological history. Volcanic ash, which may contain pumice and other pyroclastic debris, is the primary component that forms tuff deposits (Tamirat et al., 2021). They are caused by violent volcanic eruptions, in which ash is released and then settles to form tuff layers. This unit is found on the western side of the study area and seems to be discoloured due to weathering.

4.2.5. Lacustrine sediments

The area between Wonji and Awash Melkasa is covered with an extensive and thick lacustrine deposit. These compact lacustrine deposits are made up of clay, silt, fairly welded travertine, ashes, diatomite, and pumice intercalation (Alula et al., 1992). The majority of the lacustrine deposit is fine to medium-grained. Furthermore, the study area is located within Main Ethiopian Rift (MER) sector the influence of tectonics, lithology, and climate on landslide formation in the rift highlights the role of active faulting, steep slopes, and precipitation in triggering slope instability.

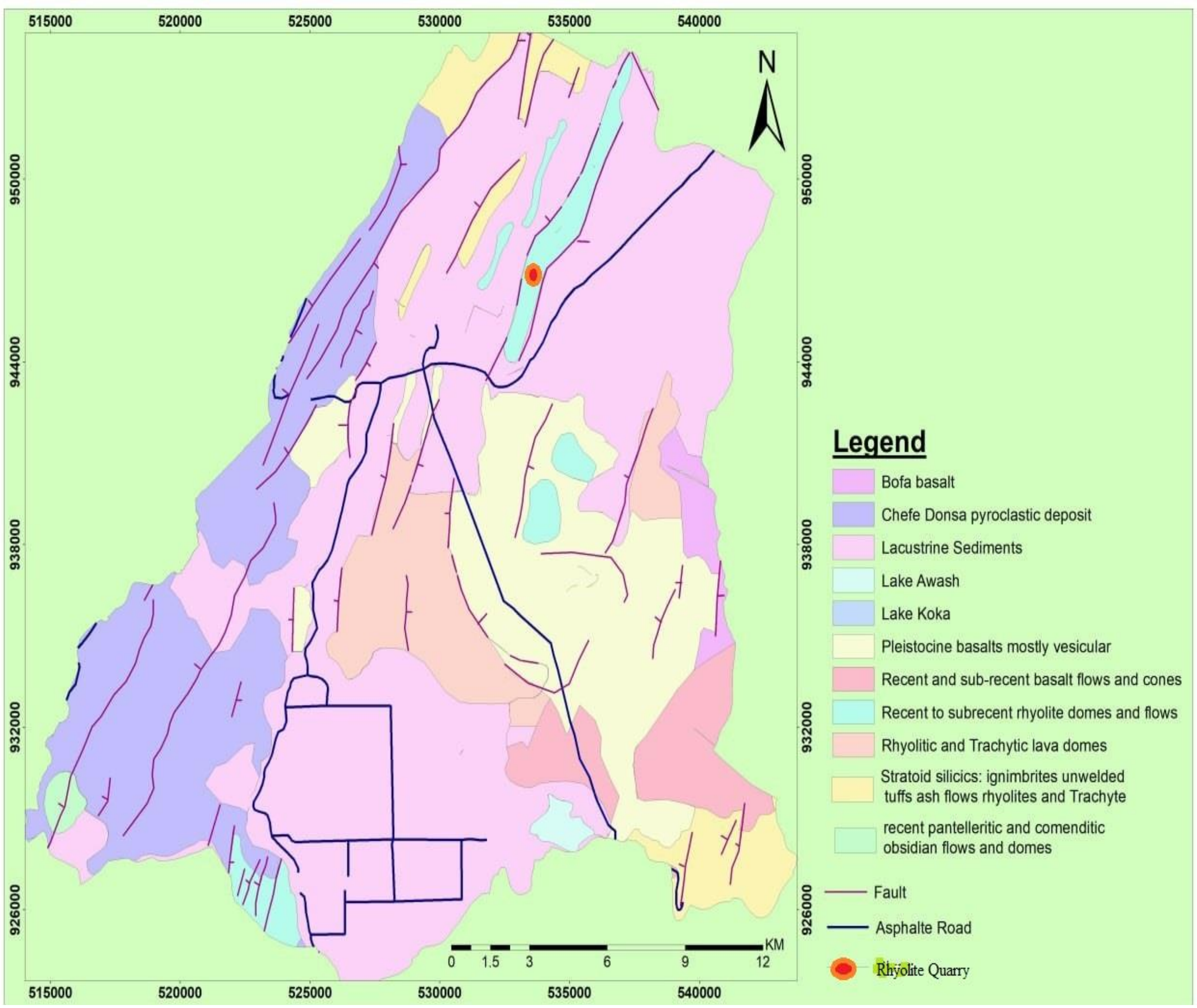

Figure 4,7. The Adama area regional geological map (modified after Damte et al., 1992).

4.3. Geology of study area

The research site is located inside the Nazret-Dera structural units from a stratigraphic and volcanic perspective. Geographically, it lies within the NMER. According to geology, ignimbrite, rhyolite, basalt, pumice, scoria, ash, and quaternary soil deposits make up the majority of the research region (Fig. 4.8). The rhyolite rock unit is a fine-grained, extrusive volcanic rock. It is exposed in a study area. It varies from fresh to moderately weathered, and at some places, it is interlayered with obsidian and ignimbrite. It is felsic in composition and light in color; it's very strong rock unit ranges between 83.28 MPa to 138.96 MPa. This rock unit is dominant fractured by two sets of joints (NE and SE striking), which are primarily vertical. There are three sets of some of vertical joints (striking NW, NNE, and SSE). The joint surfaces are rough and planner. The aperture is variable, ranging from open to extremely wide. Some joints are filled with fine materials, while the others are partially filled with rock fragments.

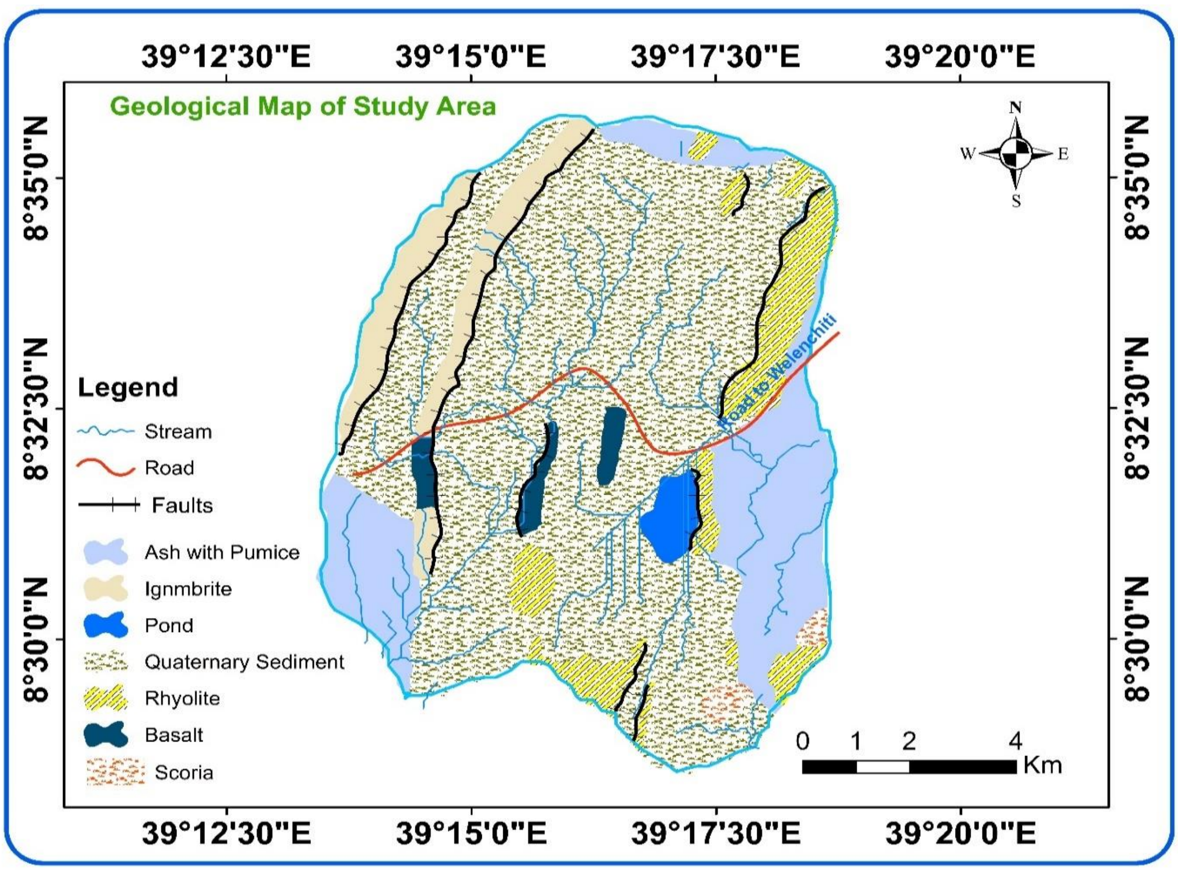

Figure 4.8: Geological map of the study area, scaled to 1:10,000 (modified from Chemeda, 2020)

4.4. Geological structures

Joints and faults are geological structures that play significant roles in rock deformation and influence slope stability of the quarry site. The dominating geological structures include extensional related minor and major normal faults that run approximately parallel to each other in a NNE-SSW direction, usually in a right-stepping manner (Wolde Gabriel et al., 1990), as well as joints and fractures. The fault's overall direction in the research region runs from N-S to NNE-SSW strike, with the majority of it vertical. The joints are the prevalent geological feature identified at the quarry site. The majority of the joints have a dangerous dipping angle and run parallel to the local faults. The major combined sets observed are N-NE strikes as shown in figure 4.9. Although there is a wide range of structural orientations, there are some notable NW striking joints, as illustrated in the rose diagram.

4.4.1. Joint

Joints are fractures in rocks that have not moved significantly, whereas faults are fractures that have changed position. The orientation of joint sets is critical in determining quarry slope stability under both static and dynamic loads. Furthermore, the interaction between joints is critical because increase the probability of instability, particularly when joint sets are present, allowing for a variety of joint combinations that may result in slope failure. Understanding the geometric conditions offered by joint sets in rock masses is critical for anticipating probable instability and designing appropriate slopes to reduce instability concerns. The general orientation of structures striking NE and SE are dominant as shown in figure 4.9.

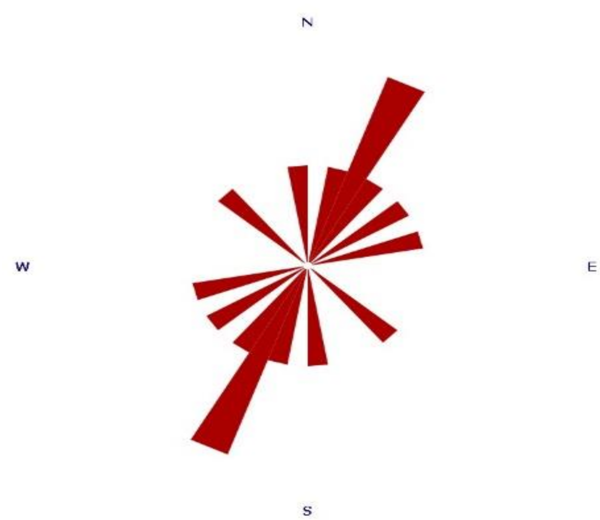

Figure 4.9: Rose plotted diagram, which indicate the joint orientation of quarry site.

4.4.2. Fault

Faults are geological structures. A fracture between two blocks of rock allows them to move relative to one another. The study site, Adama and its surroundings is located in the northern Main Ethiopian Rift (MER), where NNE-SSW striking normal fault characteristics are widespread (Corti et al., 2020). Overall strike of all the faults around Adama show N 22^0 E orientation (Erbello & Shube, 2019). In addition, Quarry site follows the general orientation of faults in the area as shown in figure 4.10 below.

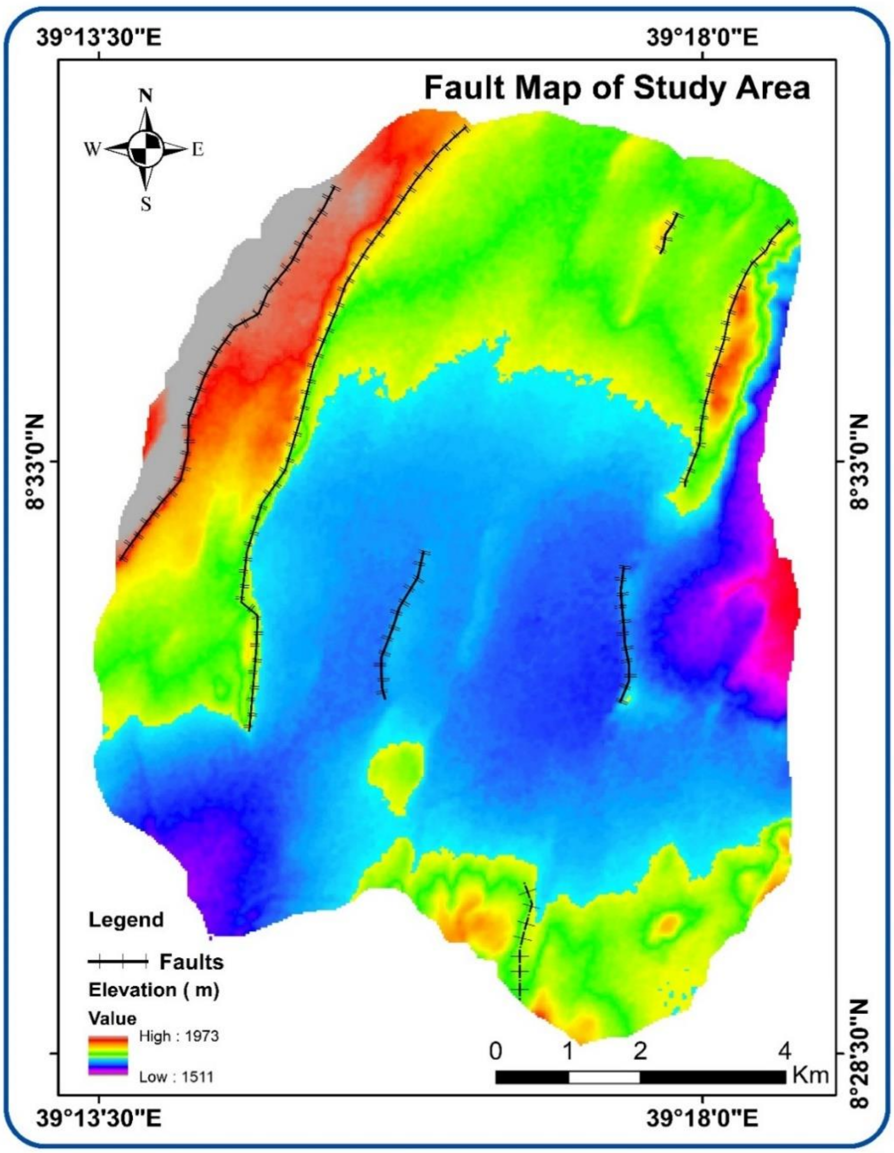

Figure 4.10: Fault map study area (modified after Chemeda, 2020; Erbello & Shube, 2019).

CHAPTER FIVE

5. RESULTS AND DISCUSSION

5.1. Introduction

In order to evaluate the stability of the critical quarry slope sections, a series of field surveying and laboratory tests were conducted. Through field survey, identification of critical slope section of quarry site, structural data collection, in situ strength test and taking representative rock sample conducted whereas rock laboratory tests were conducted to determine dry and saturated unit weight and compressive strength of rock sample taken from critical slope section of quarry. Kinematics analysis was used to determine the mode of failure of the critical slope section. Whereas, finite element and limit equilibrium methods were used to determine the Strength reducing factor and factors of safety of the critical slope section, respectively. In addition, the appropriate remedial measure was suggested based on finding of stability analysis of the quarry rock slope.

5.2. Engineering Geological Characterization of the Rock

Engineering geological characterization of rock was conducted to evaluating the mechanical and physical properties of the rock in order to determine essential slope stability within the quarry site and to characterize the geological characteristics of the rock. The type of rock, weathering, fractures, and groundwater conditions were all determined visually during the field survey. In addition, discontinuity conditions were noted in the field and laboratory tests was conducted on rock samples taken from the critical slope section of quarry site.

5.2.1. Discontinuity surveys

The discontinuity parameters obtained from the field survey, such as joint orientation, joint spacing, joint filling, aperture, joint roughness, groundwater, and weathering condition, were determined which are crucial for analysing the stability of critical rock slopes (structurally control) section as shown below by table 5.1.

Table 5.1: Discontinuity characteristics of the critical slope section.

Discontinuity parameters		Critical quarry slope sections		
		QSS_1	QSS_2	QSS_3
Joint spacing(cm)		10-83	40-95	15-80
Condition of discontinuity	Persistence (m)	0.6-1	0.8-2	0.4-1.5
	Joint aperture (cm)	0.1-1	0.2-1.5	0.5-1

	Filling materials	Soft filling	Soft filling	Soft filling
	Roughness	Slightly rough	Slightly rough	Slightly rough
	Degree of weathering	Slightly weathered	Slightly weathered	Slightly weathered
Groundwater condition		Dry	Dry	Dry
QSS ; Quarry slope section				

In addition, structural data collection was collected by field survey, which is important for slope stability analysis of quarry slope sections, such as dip amount, dip directions of joints, and slope as table 5.2.

Table 5.2: Orientation of the slope and discontinuities of critical rock slope (structurally controlled) section

Rock slope section	Joint set						Slope face	
	J1		J2		J3			
	D	DD	D	DD	D	DD	D	DD
QSS_1	72°	144°	66°	352°	-	-	78°	105°
QSS_2	58°	194°			-	-	67°	195°
QSS_3	76°	294°	30°	187°	68°	354°	72°	348°
QSS; Quarry slope section, D ; dip amount, and DD; dip direction								

5.2.2. Rock Quality Designation (RQD)

Palmstrom (1982) proposed that the RQD be approximated from the volumetric count technique (the number of discontinuities per unit volume) in cases when no core is available but discontinuity traces are visible in surface exposures. Based on the volumetric count obtained from the field on table 5.3 and calculated by equation 8, the RQD of the study area ranges from 68.8 to 88.6 that show fair to good rock quality.

Table 5.3: The rock quality designation of a critical slope section.

Slope section	JV (Av)/1m*m	RQD%	Class According to Deere (1988)
QSS_1	11	78.7	Good
QSS_2	8	88.6	Good
QSS_3	14	68.8	Fair
QSS; Quarry slope section, JV; volumetric count and RQD; Rock Quality Designation			

5.2.3. In-Situ Rock Strength Test

The uniaxial compressive strength (UCS) of the intact rock was determined by using an N-type Schmidt hammer in this study to determine the rebound value (R) of rocks to predict uniaxial compressive strength at selected different critical quarry slope sections following the ASTM C 805 test process. Tests were conducted. Depending on the average rebound value, the Schmidt hammer test record on table 5.4 and calculate by equation 10 the UCS of the intact rock range from 84.1 MPa to 138.8 MPa that shows strong to very strong rock.

Table 5.4: Schmidt hammer rebound value and UCS values of different critical quarry slope sections

Slope sections	Trials	Schmidt hammer rebound value from each trial	Ave(R) for each trial	Ave (R)	UCS (MPa)	Classifications (ISRM 1981)
QSS_1	1	43,49,49,50,51,52,54,56,56,57	51.7	52	125.23	Very strong
	2	42,51,51,53,53,54,54,55,55,56	52.4			
QSS_2	1	51,51,52,53,53,54,56,56,56,58	54	54.4	138.8	Very strong
	2	51,53,53,53,54,54,54,54,55,56	54.7			
QSS_3	1	51,52,54,54,55,56,56,57,58,59	55.2	54.45	117.46	Very strong
	2	50,52,52,53,53,54,54,55,57,57	53.7			
QSS_4	TRS	28,28,32,34,34,35,37,40,44,44	35.6	35.6	84.1	Strong
	RRS	42,44,44,47,49,49,51,53,53,54	48.6	48.6	126.24	Very strong
QSS_5	RRS	49,50,53,53,54,54,55,57,58,58	54.1	54.1	115.58	Very strong
QSS; quarry slope section; TRS; vitric tuff; R; rebound value; and UCS; uniaxial compressive strength.						

5.2.4. Rock mass classification

5.2.4.1. Rock mass rating (RMR)

The rock mass classification and shear strength parameter for rock mass were estimated at the critical slope section. For this study, according to Bieniawski (1989), the geomechanical classification of rock follows five basic parameters based on the geological condition of a structurally controlled quarry slope section. To determine the uniaxial compressive strength of rock mass, in-situ strength testing results were used because they can yield more realistic data on the characteristics of the rock mass because they take into account the real circumstances under which the rock falls. In addition, other parameters were estimated from the field. The data pertaining to RMR was collected from three structurally controlled slope sections in a field. Based on the data collected from the field, the RMR of the study area ranges from 75 to 84 as table 5.5.

Table 5.5: Rock mass rating classification of critical rock slope section

Rock slope section	Rating of five basic RMR values					RMR basic	Class	Rock quality according to Bieniawski(1989)
	UCS	RQD	SP	CON.D	GW.C			
QSS_1	12	17	10	25	15	79	II	Good
QSS_2	12	17	15	25	15	84	I	Very good
QSS_3	12	13	10	25	15	75	II	Good
QSS; quarry slope section, UCS; uniaxial compressive strength, RQD; rock quality designation, SP; spacing of discontinuity, CON.D; condition of discontinuity, GW.C; groundwater condition; and RMR; rock mass rating.								

5.2.4.2. Geological Strength Index (GSI)

The geological strength index (GSI) was used to assess the strength and stability of rock units. In this study, the GSI value ranges from 45 to 75, with higher values indicating stronger and more stable rock units based on data recorded on filed by table 5.6. It is determined by assessing the rock mass characteristics, such as the rock type and discontinuities. This parameter was identified from field observation of quarry site rock units in the study area. In this study, the GSI value was estimated using RocData software(RocData, 2004), which is used to calculate the shear strength of the rock mass, which is an important parameter in slope stability analysis and quarry slope design.

Table 5.6: Estimated GSI values of rock slope section.

Rock slope section	Rock types	Estimated GSI values	Rock mass quality (Hoek et al. 1995)	Disturbance factor(D)
QSS_1	Rhyolite highly jointed, slightly weathered	55	Fair	0.7
QSS_2	Rhyolite slightly jointed and weathered	75	Good	0.7

QSS_3	Rhyolite highly jointed and slightly weathered	50	Fair	0.7
QSS_4	Highly jointed and slightly weathered Rhyolite	48	Fair	0.7
	Vitric tuff, highly weathered	45	Fair	0.7
QSS_5	Rhyolite slightly jointed and weathered	65	Good	0.7

The disturbance factor, D was determined based on the specifications mechanical excavation shown in RocData (RocData, 2004) software.

5.3. Laboratory tests results from the rock sample

The laboratory tests conducted on these rock samples taken from significant slope sections of the quarry site, like the unit weight test and point load test, determined the physical and mechanical characteristics of the rock samples, which were crucial for slope stability analysis. Rock samples were taken from two non-structurally and three structurally controlled critical slope sections for this study for each slope section as described in table 5.7.

Table 5.7: Description and location of rock sample

Slope sections	Sample ID	Northing (N)	Easting (E)	Rock types and description of quarry site critical slope section
QSS_1	RRS_1	944277	533037	Rhyolite highly jointed, slightly weathered, unfavourable orientation of joints to slope face
QSS_2	RRS_2	944667	533132	Rhyolite slightly jointed and weathered, unfavourable orientation of joints to slope face
QSS_3	RRS_3	944811	533261	Rhyolite highly jointed and slightly weathered, unfavourable orientation of joints to slope face.
QSS_4	TRS_1	944419	533201	Rhyolite highly jointed and slightly weathered interlay with highly weathered vitric tuff.
	RRS_4	944804	533233	
QSS_5	RRS_5	944974	533316	Rhyolite slightly jointed and weathered
RRS: rhyolite rock sample; TRS: vitric tuff rock sample; QSS: quarry slope section.				

5.3.1. Point load test

The point load test is an alternate method that can be used to adequately predict the uniaxial compressive strength of a rock material using portable and simpler equipment. In accordance with ASTM D 5731 (1995), a point load strength test of rocks was performed. In this test procedure, irregular lumps and rock samples are put between two conical platens, and a concentrated force is given until failure. In this study, an uncorrected point load strength index was obtained and converted to a corrected point load strength index as determined on table 5.8 below. Finally, according to an empirical relationship proposed by Broch and Franklin (1972), the uniaxial compressive strength (UCS) of rock can be calculated from the point load strength index as follows:

$$\mathrm{UCS} = 24 * \mathrm{Is}(50) \qquad 19$$

Where, UCS is uniaxial compressive strength of intact rocks and Is (50) is the size corrected point load strength.

Table 5.8: Point load test result and its corresponding uniaxial compressive strength

Slope sections	Sample ID	I_S(50)Mpa	UCS(Mpa)	ISRM (1978)
QSS_1	RRS_1	4.82	115.68	Very strong
QSS_2	RRS_2	4.625	111	Very strong
QSS_3	RRS_3	5.76	138.96	Very strong
QSS_4	TRS_1	3.47	83.28	Strong
	RRS_4	5.39	129.36	Very strong
QSS_5	RRS_5	4.95	118.8	Very strong
RRS: Rhyolite rock sample; TRS: vitric tuff rock sample; QSS: quarry slope section.				

5.3.2. Unit weight rock

The unit weight of the rock test was conducted on certain rock samples obtained from a significant quarry slope portion using buoyancy procedures as described in ASTM C 127-88, the standard as follows: The first step of the test was to name, weigh, and oven-dry the rock samples for 24 hours at 105°C. After that, the weight of the oven-dried rock samples was noted ($\mathrm{M_{dry}}$). After inserting the oven-dried samples into the water-filled cylinder, the initial water volume ($\mathrm{V_2}$, in ml) as well as the subsequent volume change ($\mathrm{V_1}$, in ml) were measured. After that, determine how much the sample's volume has changed by putting an irregular, oven-dried rock in a cylinder of water that contains. The details are attached in Appendix B.

Table 5.9: Dry and wet unit weights of rocks from laboratory tests

Sample ID	Rock type	Dry unit weight (KN/m3)	Wet unit weight (KN/m3)
RRS 1	Rhyolite	23.78	24.38
RRS 2	Rhyolite	23.67	24.25
RRS_3	Rhyolite	22.12	22.53
RRS_4	Rhyolite	25.52	26.25
TRS 1	Vitric tuff	29.19	29.64

5.4. Determining shear strength parameters along failure plane

Using RocData 3.0 software, the shear strength of discontinuities/failure planes in this study was calculated in accordance with the non-linear failure criteria of Barton and Bandis (1990). The joint roughness coefficient (JRC) and the joint wall compressive strength (JCS), two important variables affecting the shear strength of rock joints, are taken into consideration. Because all of the joint walls of the rocks in the research area have slightly weathering, the JCS in this study is therefore calculated to be 75% of the UCS. Similarly, Ulusay and Karakul's (2015) research was used to determine the basic friction angle of 31 for rhyolite rock, which is the rock that is exposed in all quarry slope sections. Shear strength of discontinuities/failure planes determined on table 5.10 below.

Table 5.10: Input parameters for RocData 3.0 Software and output results

Rock slope section	Input parameters						Output	
	JS	JCS (Mpa)	JRC	γ(KN/m3)	Φ(b)	Sh (m)	Cohesion (Mpa)	Φ (^{0})
QSS_1	JS1	92	3	23.78	31	52	8.014	27.95
	JS2	95.73	5	23.78	31	52	12.947	26.01
QSS_2	JS1	103.5	7	23.67	31	34	12.384	26
QSS_3	JS1	95.25	3	22.12	31	45	6.639	28.25
	JS2	90.16	5	22.12	31	45	10.723	26.30
	JS3	85.12	6	22.12	31	45	12.625	25.23
JS Joint Set, JCS Joint Compressive Strength, JRC Joint Roughness Coefficient, γ Unit weight of the rock, Φ(b) Basic Friction Angle, Sh Slope Height, c Cohesion. Φ Friction angle								

5.5. Stability analysis of rock slopes

5.5.1. Kinematic analysis

A kinematic analysis is the first step in evaluating rock slope stability and was performed in Dips 6.0 software to identify the possible mode of failure. These analyses need a value for the friction angle, which can be obtained via RocData software as well as dip amount and dip direction of the discontinuity and slope were determined by field measurements. Based on kinematic analysis results, figure 5.1 (A) and (D) for QSS_1 and QSS_3 show wedge mode of failure, respectively. Whereas figure 5.1 (B) and (C) for QSS_2 and QSS_3 show planer mode of failure, respectively.

Table 5.12: Input parameters of Dips 6.0 software for conducting a kinematic analysis

Rock slope section	Joint set J1		J2		J3		Slope face		Friction angle
	D	DD	D	DD	D	DD	D	DD	
QSS_1	72°	144°	66°	352°	-	-	78°	105°	26°
QSS_2	58°	194°			-	-	67°	195°	26°
QSS_3	76°	294°	30°	187°	68°	354°	72°	348°	27°

QSS; Quarry slope section, D ; dip, and DD; dip direction)

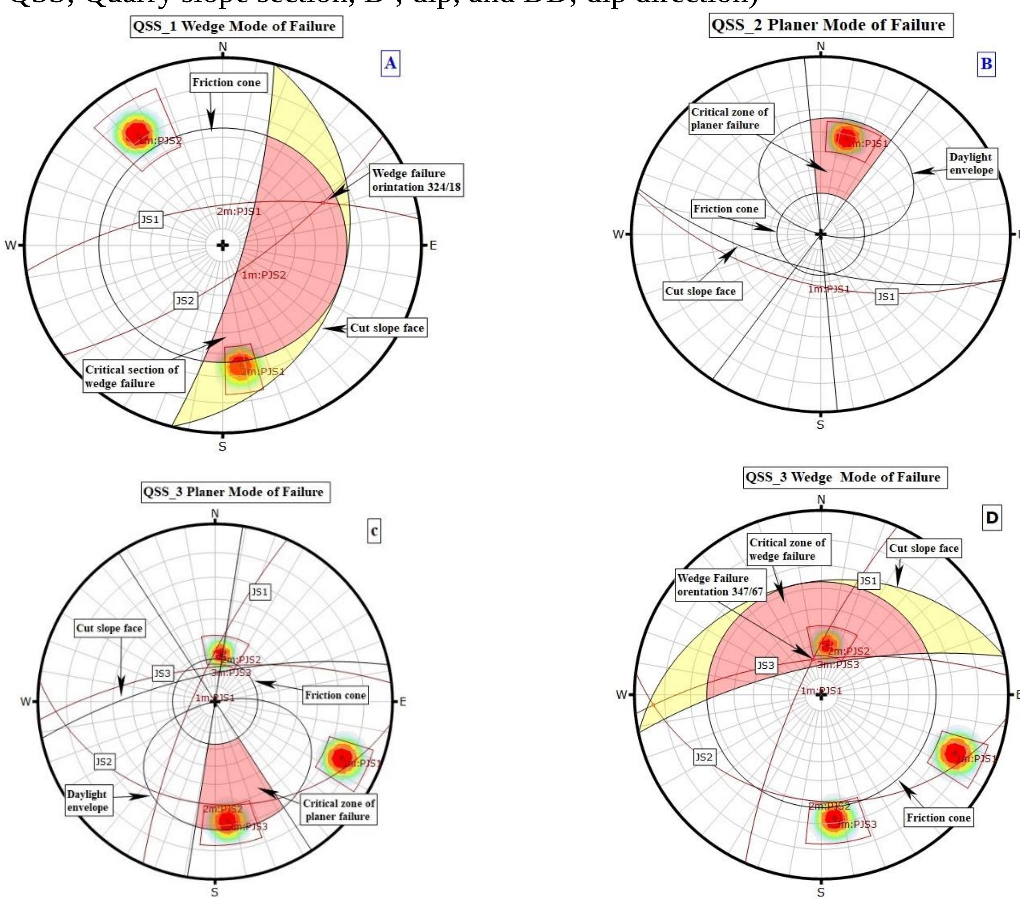

Figure 5.3: Kinematic analyses of different mode of failures at slope section of QSS_1, QSS_2 and QSS_3.

Table 5.12: Possible mode of failure from kinematic analyses result

Slope section	Possible failure mode from kinematic analyses
QSS_1	Wedge
QSS_2	Planer
QSS_3	Wedge and planer

5.5.2. LEM Modelling of Rock Slope

The LEM modelling was conducted on three different quarry slope sections, which showed different modes of failure. This analysis, conducted after kinematic analysis methods, identifies modes of failure on structurally controlled slope sections. For the analysis, a variety of circumstances, including static dry, static saturated, dynamic dry, and dynamic saturated, were examined for planer and wedge modes of failure using the RocPlane 2.0 and Swedge V.4.0 software, respectively.

5.5.2.1. LEM Modelling of Planer Failure

LEM modelling of planar failure involves examining using RocPlane 2.0 software after planar failure mode identified by kinematic analysis. In the study area, two planer modes of failure were identified through kinematic analysis at quarry slope sections QSS_2 and QSS_3. According to input parameter on table 5.13 LEM modelling of QSS_2 under a variety of circumstances, static dry, static saturated, dynamic dry, and dynamic saturated FOS are 1.45, 0.76, 1.26, and 0.58, respectively . Whereas QSS_3 FOS are 1.35, 0.48, 1.11, and 0.33, as shown in figure 5.2 and 5.3, respectively. Therefore, the results show both quarry slope sections are unstable at static saturated and dynamic saturated conditions and stable on other conditions.

Table 5.13: Input parameter used in RocPlane 2.0 software for planar mode of failure for QSS_2.

Slope section	Js	Slope geometry		Failure plane				Shear strength parameter			Forces	
		D (°)	H (m)	D (°)	W	γ(t/m^3)d/s	USA (°)	JRC	JCS (t/m^2)	φ (°)	γw (t/m^3)	α
QSS_2	J1	67	34	35	4	2.37/2.43	10	7	10554	26	1	0.1
Js joint set, γ unit weight, w waviness, USA; upper slope angle, c cohesion, φ friction angle, γw unit weight of water, α seismic coefficient.												

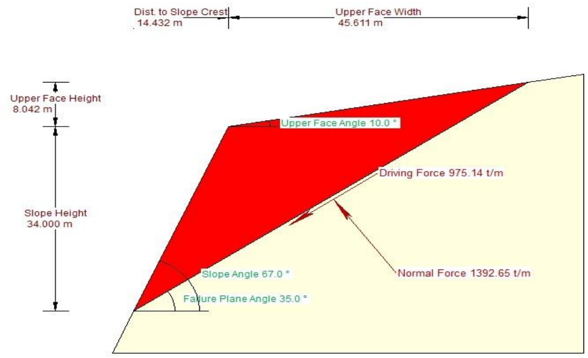

Factor of Safety	1.54
Driving Force	975.14t/m
Resisting Force	1500.41t/m
Wedge Weight	1700.11t/m
Wedge Volume	717.35m^3/m
Shear Strength	1403.03t/m^2
Normal Force	1392.65t/m
Plane Waviness	4.0°

Static dry

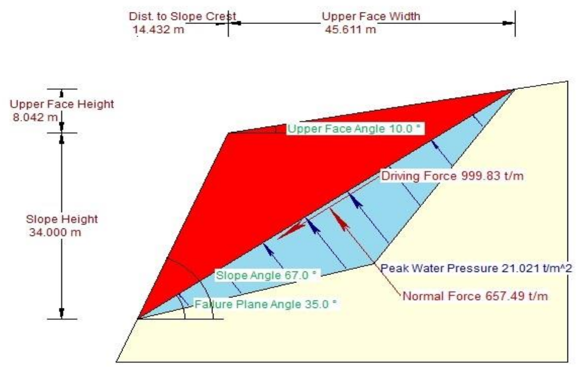

Factor of Safety	0.76
Driving Force	999.83t/m
Resisting Force	763.36t/m
Wedge Weight	1743.15t/m
Wedge Volume	717.35m^3/m
Shear Strength	717.39t/m^2
Normal Force	657.49t/m
Plane Waviness	4.0°
Water Force on Failure Plane	770.41t/m

Static saturated

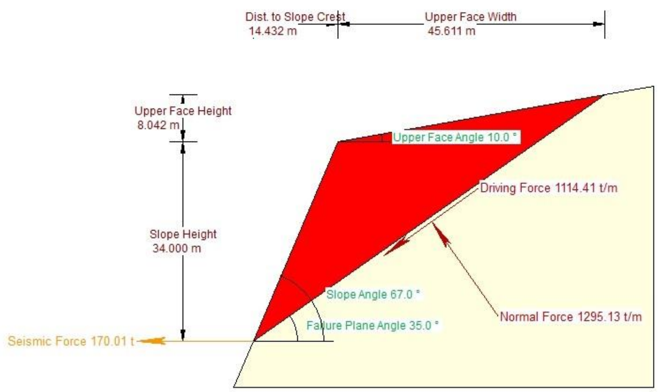

Factor of Safety	1.26
Driving Force	1114.41t/m
Resisting Force	1405.44t/m
Wedge Weight	1700.11t/m
Wedge Volume	717.35m^3/m
Shear Strength	1314.88t/m^2
Normal Force	1295.13t/m
Seismic Force	170.01t
Plane Waviness	4.0°

Dynamic dry

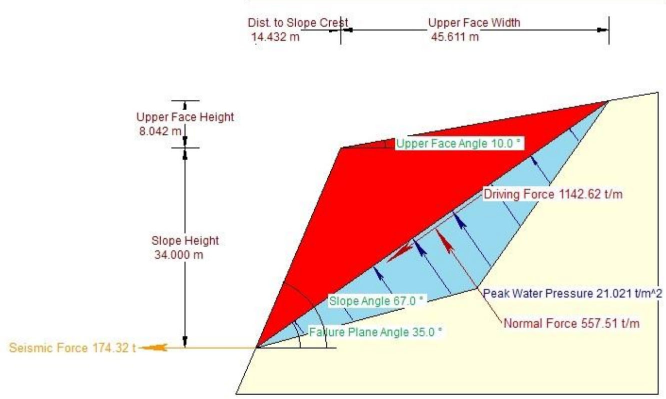

Factor of Safety	0.58
Driving Force	1142.62t/m
Resisting Force	658.07t/m
Wedge Weight	1743.15t/m
Wedge Volume	717.35m^3/m
Shear Strength	619.09t/m^2
Normal Force	557.51t/m
Seismic Force	174.32t
Plane Waviness	4.0°
Water Force on Failure Plane	770.41t/m

Dynamic saturated

Figure 5.2: LEM modelling of the planar mode of failure for QSS_2_J1 using RocPlane 2.0 software under different conditions.

Table 5.143: Summary of FOS obtained for QSS_2_J1 under different anticipated conditions

Slope section	FOS results under different anticipated conditions			
	Static dry	Static saturated	Dynamic dry	Dynamic saturated
QSS_2	1.45	0.76	1.26	0.58

Table 5.154: Input parameter used in RocPlane 2.0 software for planar mode of failure for QSS3_J3

Slope section	Js	Slope geometry		Failure plane				Shear strength parameter			Forces	
		D (°)	H (m)	D (°)	W	γ(t/m^3)d/s	USA (°)	JRC	JCS (t/m^2)	Φ, (°)	γw (t/m^3)	α
QSS_3	J3	72	45	37	6	2.21/2.253	16	6	8680	27	1	0.1

Js joint set, γ rock unit weight, w waviness, USA; upper slope angle, c cohesion, φ friction angle, γw unit weight of water, s saturated, d dry αs seismic coefficient.

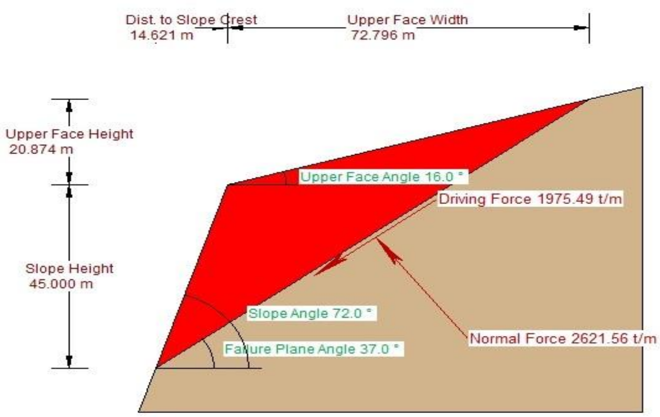

Factor of Safety	1.35
Driving Force	1975.49t/m
Resisting Force	2665.60t/m
Wedge Weight	3282.55t/m
Wedge Volume	1485.32m^3/m
Shear Strength	2390.06t/m^2
Normal Force	2621.56t/m
Plane Waviness	6.0°

Static dry

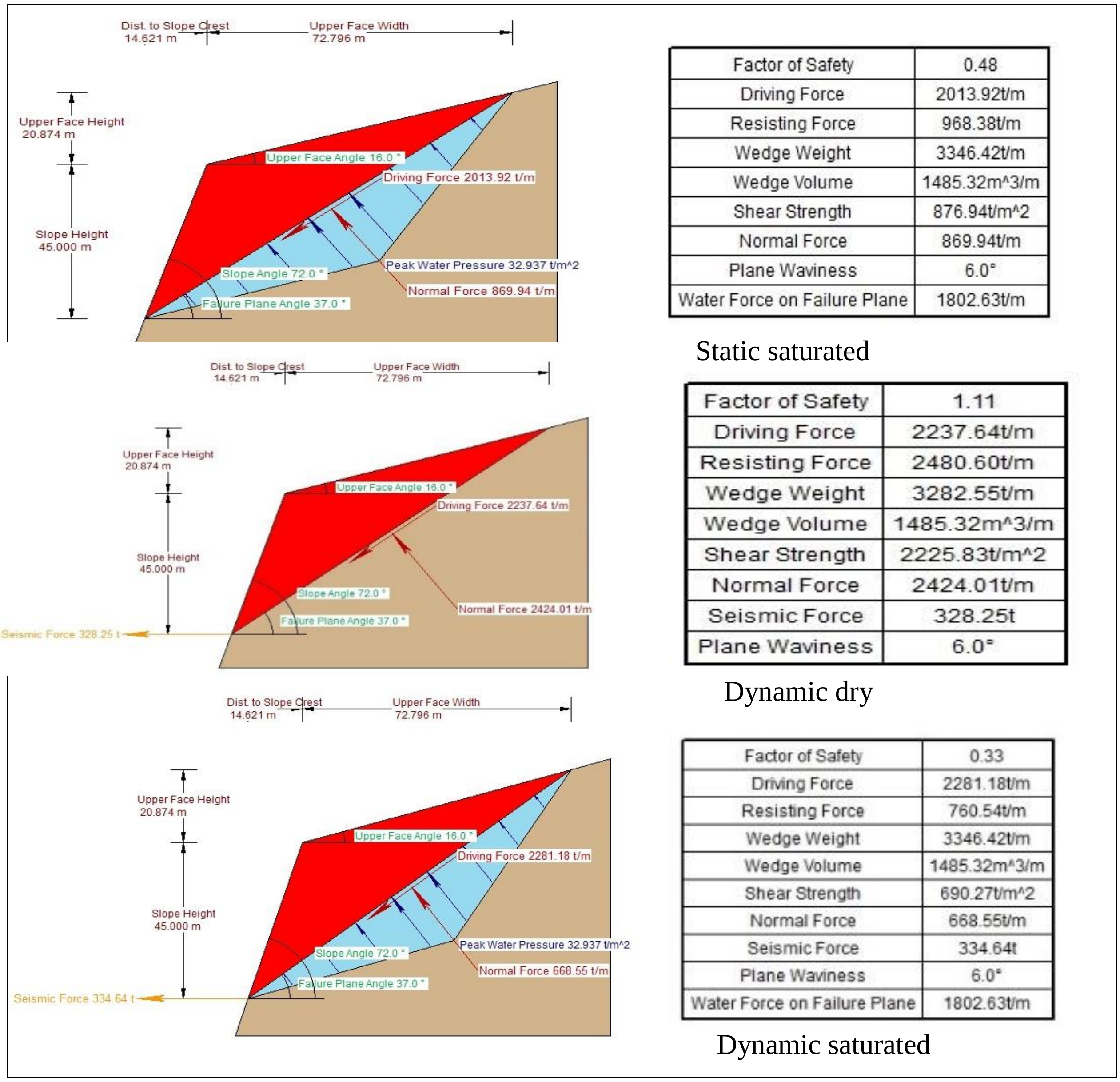

Figure 5.3: LEM modelling of the planar mode of failure for QSS3_J3 using RocPlane 2.0 software under different conditions.

Table 5.16: Summary of FOS obtained for QSS3_J3 under different anticipated conditions

Slope section	FOS results under different anticipated conditions			
	Static dry	Static saturated	Dynamic dry	Dynamic saturated
QSS_3_J3	1.35	0.48	1.11	0.33

Under both static and dynamic saturation conditions, the safety factor for slope sections QSS_2 and QSS_3 was less than one, according to Rocplane analysis of the safety factors based on the input parameters (Tables 5.15 and 5.16). These show that the slope was unstable in the given circumstances, particularly during the rainy seasons. Factor of safety larger than unity reveals a stable slope; while factor of safety equal to one shows that the slope is nearing failure (Hoek & Bray, 1981; Wyllie & Mah, 2004). As a result, slope sections QSS_2 and QSS_3 are stable in static and dynamic dry situations. According to Raghuvanshi (2017), intense saturation and seismic loading conditions are the main causes of slope failures. Furthermore, the simulation demonstrates a major impact of pore water pressure on slope instability by demonstrating that saturated situations have a much lower FOS than dry conditions.

5.5.2.2. LEM modelling of wedge failure

Kinematic analysis shows wedge mode failure on quarry slope sections QSS1 and QSS3. For this study, a LEM modelling of wedge failure was assessed using Swedge V.4.0 software under different conditions according to input parameter on table 5.17. Based on the finding, the FOS of QSS_1 and QSS_3 under dynamic saturated conditions are 0.95 and 0.248, respectively, which are unstable as shown in figure 5.4.

Table 5.17: Input parameter of Swedge V. 4.0 software for wedge mode of failure QSS1 and QSS3

Slope section	Js	Joint	Slope geometry		SF	USF	Shear strength parameter			Forces
		D/DD	H (m)	γ (t/m^3)d/s	D/ DD	USA (°)	C (Mpa)	Φ (°)	γw (t/m^3)	α
QSS1	J_1	72/144	52	2.42/2.48	78/ 105	10	8.017	27.9	1	0.1
	J_2	66/352	52	2.42/2.48	78/ 105	10	12.9	26	1	0.1
QSS3	J1	76/294	45	2.2/2.25	72/348	12	6.6	28	1	0.1
	J3	68/354	45	2.2/2.25	72/348	12	12.62	25	1	0.1

JS Joint Set, , γ Unit Weight Rock, s saturated, d dry, SF Slope Face, USF Upper Slope Face, D Dip Amount, DD Dip Direction, C Cohesion, Φ Friction Angle, γw Unit Weight of Water, αs Seismic Coefficient.

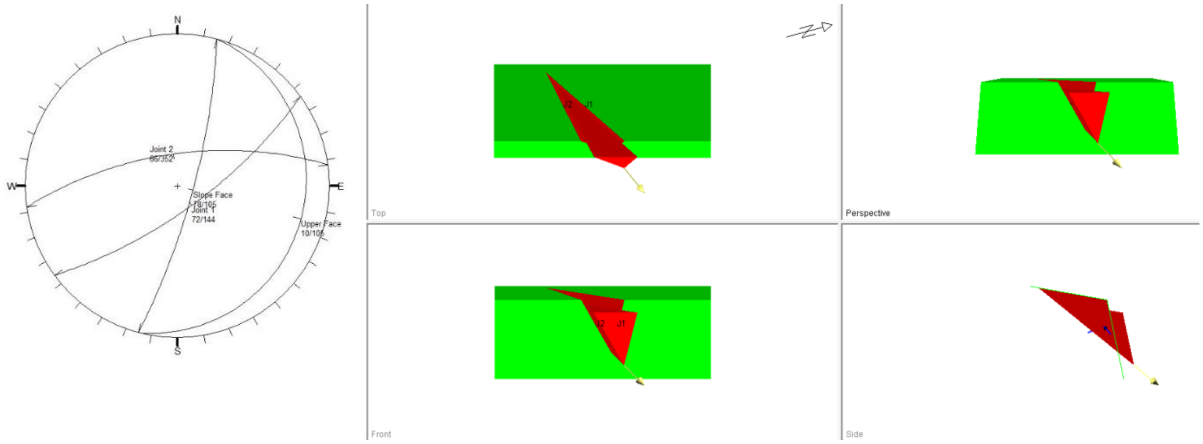

QSS_1_ Dynamic saturate condition FoS = 0.95

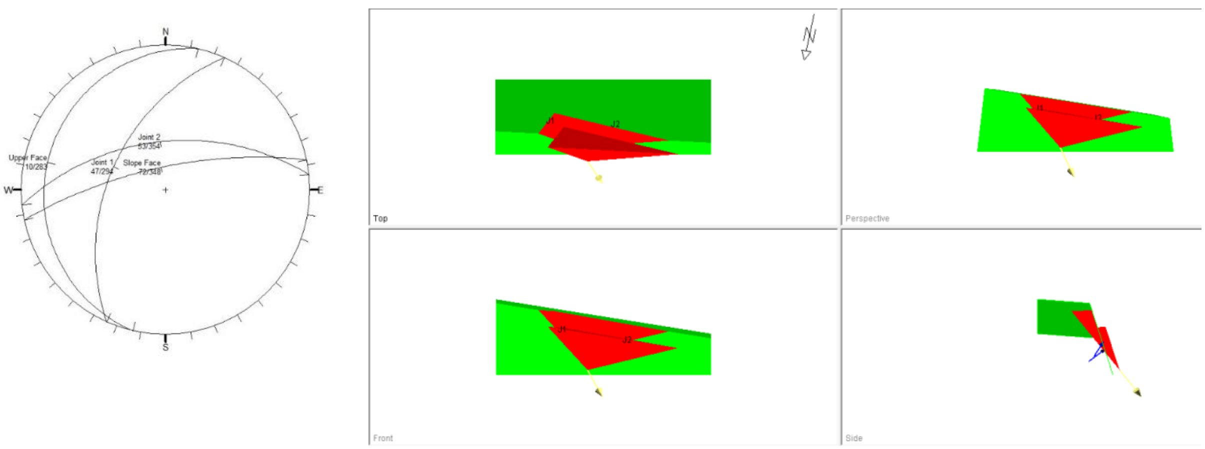

QSS_3_Dynamic saturate condition FoS = 0.248

Figure 5.4: Stereographic projection and wedge mode of failure using Swedge software under dynamic saturate condition.

Table 5.185: Summary of Factor of safety for under different anticipated conditions for wedge mode of failures

Slope section	Joint set intersection	FOS results under different anticipated conditions			
		Static dry	Static saturated	Dynamic dry	Dynamic saturated
QSS_1	J1&J2	1.93	1.13	1.62	0.95
QSS_3	J1&J3	1.92	0.281	1.69	0.248

The results of the kinematic analysis showed that the QSS1 and QSS3 slope portions are where the wedge mode of rock slope failure occurs (Fig. 5.4). Therefore, the factor of safety was computed independently for both slope portions utilizing Swedge, which shows that for both dynamic saturated conditions and under QSS_3 expected static saturated conditions, the factor of safety was less than one (Table 5.18). This indicates that the adversely oriented slope, discontinuities, and rainfall that saturates the slope all worked together to create unstable slopes. Therefore, under saturated conditions (i.e., static and dynamic saturated conditions), the wedge of this slope section is simply unstable. Furthermore, saturated conditions have substantially lower FOS than dry ones, as shown by the findings. Therefore, the saturation is mostly responsible for the low FOS of this slope wedge. Furthermore, because of the intersection of joints, the slope section is vulnerable to wedge mode failure, as demonstrated by the kinematic modelling. Based on the research conducted by Raghuvanshi et al. (2014), it can be inferred that variables such failure plane features and slope geometry, rather than seismicity and water pressure, are the main determinants of this wedge's stability.

5.5.3. Non-structural controlled stability analysis

Using Slide 6.0 and Phase 2D software, an analysis of instability for a non-structurally controlled quarry slope section was carried out under static and dynamic load circumstances. The load on each element was determined for static conditions by its weight and the force of gravity, which also covers the stress in the field. When the rhyolite quarry was being excavated in the Adama area, blasting was not used. Consequently, analysis under dynamic loading conditions was performed without taking into account the peak ground vibration that was caused by blasting. In the process of computing the analysis for the dynamic loading condition, external loads such as equipment loads and materials loaded upon it were also applied to the slope. Excavators and Sino trucks used in quarrying had an average exterior load of 214.8 kN and 245.3 kN, respectively. According to the equipment loading capacity, the external loads resulting from the materials placed on the Sino truck were predicted to be 360 kN for the quarry slope section and the vehicle. In addition, horizontal seismic forces were applied as an acceleration coefficient ($\alpha = 0.1$) for earthquakes.

5.5.3.1. LEM and FEM stability analysis

The stability condition of the rock slope under static and dynamic load conditions was examined by calculating a factor of safety for each slope section using various LEM, including Bishop's, Janbu's Simplified, Spencer, and Morgenstern-Price, using Slide 6.0 software for QSS_4 and QSS_5 for non-structurally controlled slope sections. The stability along specific slope sections of quarry site, which consist of a rock mass that, is highly fractured and moderately weathered, was examined by accounting for circular or nearly circular modes of failure. The Hoek-Brown failure criteria used to calculate the shear strength values used in this approach, where input parameters are collected using RocData software. Unit weight from rock laboratory. Similarly, the horizontal seismic acceleration (α) for the study region came from Asfaw (1986) as shown in table 5.19. The analysis, the results show that QSS_4 and QSS_5 are unstable under both static and dynamic loads as shown in figure 5.5 below.

Table 5.196: Input parameter for QSS_4 slope stability analysis using Slide 6.0 software.

Slope section	Rock types	Strength model	Unit weight (KN/m3)	Strength parameter		Forces
			γd/s	C(Mpa)	Φ, (°)	α
QSS_4	MW-Rhyolite and highly fractured	Mohr- coulomb	25.52/26.25	5.78	29.28	0.1
	Vitric tuff	Mohr- coulomb	29.19/29.64	4.27	22.66	0.1
QSS_5	MW-Rhyolite and highly fractured	Mohr- coulomb	22.16/22.53	1.106	62.04	0.1

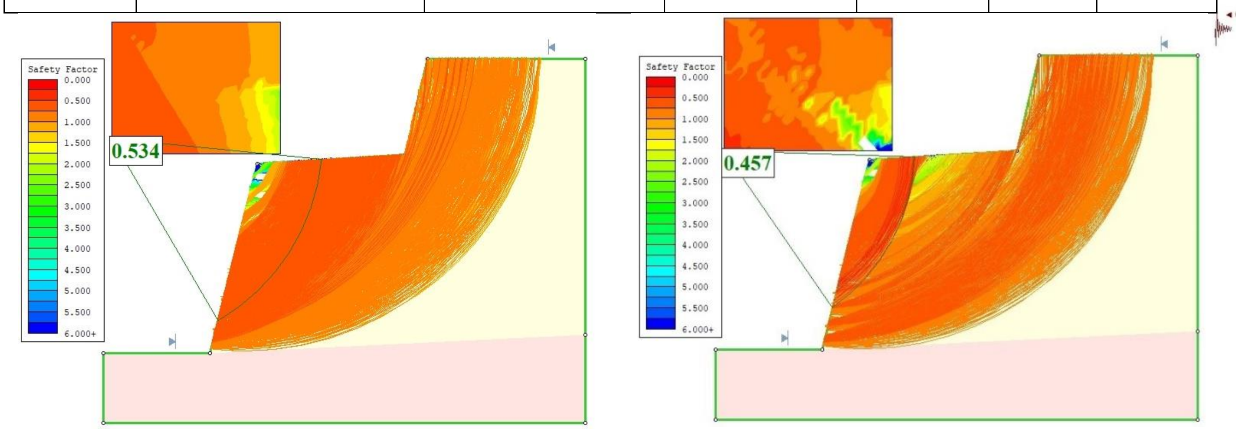

(A) (B)

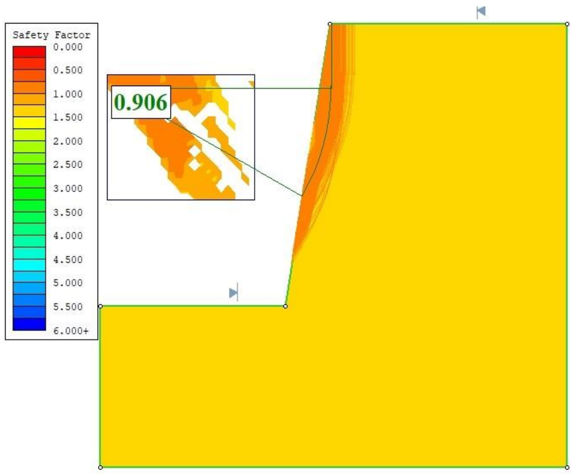

(A)

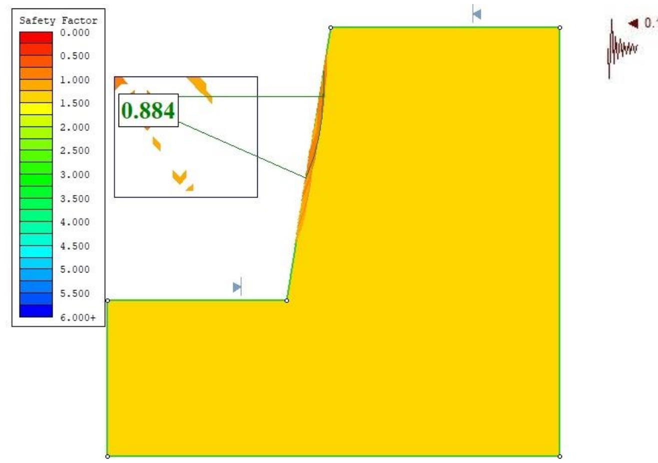

(B)

Figure 4: The factor of safety for the QSS_4 and QSS_5 determined using Slide 6.0 software (A) and (B) under static and dynamic condition, respectively.

Table 5.207: Summary of Factor of safety QSS_4 and QSS_5 of limit equilibrium method

Methods	FOS of different LEM for a different condition			
	QSS_4		QSS_5	
	Static	Dynamic	Static	Dynamic
Bishop's	0.509	0.461	0.992	0.812
Janbu's Simplified	0.525	0.451	0.845	0.733
Spencer	0.534	0.457	0.906	0.884
Morgenstern-Price	0.537	0.458	0.909	0.817

The FOS result under various circumstances was determined for each corresponding quarry slope section. With static load conditions, the FOS at QSS_4 and QSS_5 thus becomes 0.532 and 0.906, respectively, however under dynamic loading conditions; it is 0.457 and 0.884, respectively. When the analysis was conduct under dynamic loading conditions, their FOS the amount tended to decrease.

Additionally, in order to validate the results of the LEM analysis, the strength reduction factor (SRF) of the rock slope condition was evaluated using the FEM stability analysis by Phase 2D software under both static and dynamic loading circumstances. Wherein the following input parameters obtained from different sources, like slope height, groundwater condition, Young's modulus (Erm), Poisson's ratio (v), unit weight of rock (γ), shear strength parameter, and uniaxial compressive strength of entire rock (σci). Additionally, analyses under dynamic loading conditions conducted using loads equivalent to those in limit equilibrium analyses. According as shown in figure 5.6 below under dynamic loading condition, the SRF of QSS_4 and QSS_5 were 0.4 and 0.86, respectively.

Table 5.21: Input parameter for rock slope stability analysis using FEM using phase 2d software

Slope section	Rock types	Erm (Mpa)	V (µ)	Unit weight (KN/m3)	Strength parameter		Forces
				γ-d/s	C(Mpa)	Φ(°)	α
QSS_4	MW-Rhyolite and highly fractured	5793	0.436	25.52/26.26	5.78	29.28	0.1
	Vitric tuff	4467	0.424	29.19/29.64	4.27	22.66	0.1
QSS_5	MW- Rhyolite and highly fractured	15413	0.402	22.12/22.53	1.106	62.04	0.1

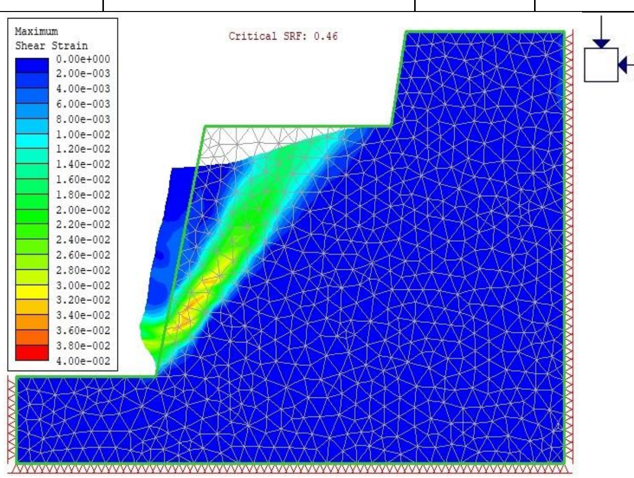

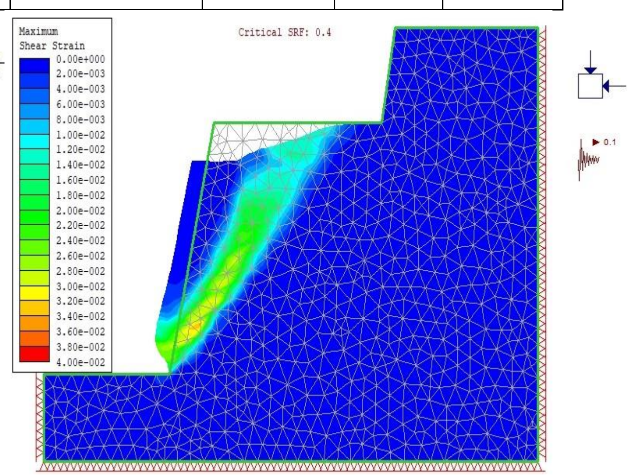

(A) (B)

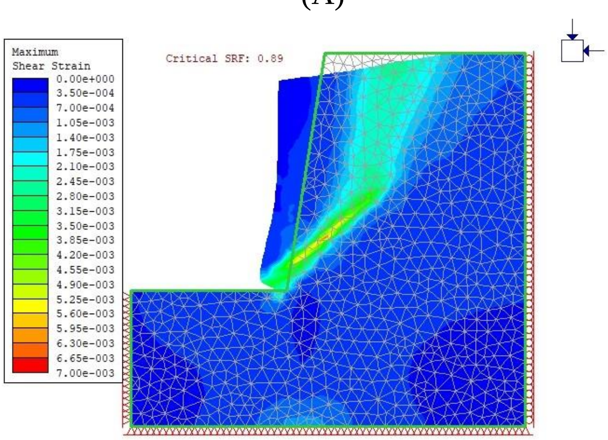

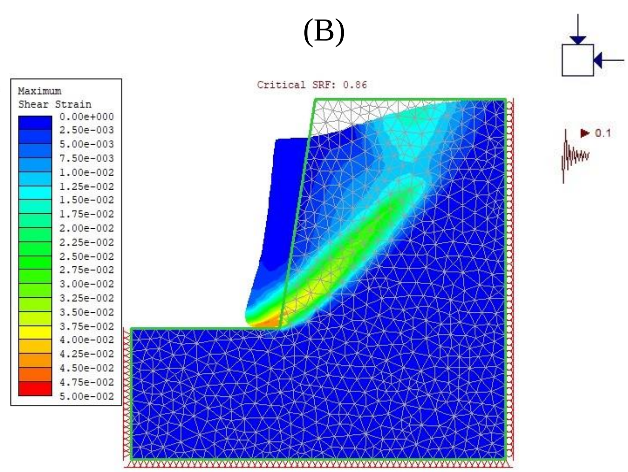

(A) (B)

Figure 5.65: The FEM determined using Phase 2d software under static (A) and dynamic (B) loading conditions for QSS_ 4 and QSS_5.

Table 5.22: Summary of SRF obtained for QSS_ 4 and QSS_5 under static and dynamic condition.

Slope section	SRF results under different conditions	
	Static	Dynamic
QSS_4	0.46	0.4
QSS_5	0.89	0.86

5.5.4. Comparison of LEM and FEM

The LEM has inherent limitations because it does not take into account the material's stress-strain relationship, whereas the FEM for slope stability analysis is widely used because it accounts for the material's stress-strain behaviour, the formation of failure zones based on the limiting material properties, and is considered more accurate and reliable(Tang et al., 2017; Wyllie & Mah, 2004). Comparison of these conducted under different anticipated condition static dry, static saturated, dynamic dry and dynamic saturated for structural based on analysis result on table 5.23. Additionally, under dynamic and static load for non-structural controlled slope section table 5.24. Similar to that, the FOS and SRF decreases from a static to a dynamic condition.

Table 5.238: Summary of FOS of structural controlled slope section

Slope section	Mode of failure	FOS results under different anticipated conditions			
		Static dry	Static saturated	Dynamic dry	Dynamic saturated
QSS_2	Planar	1.45	0.76	1.26	0.58
QSS_3	Planar	1.35	0.48	1.11	0.33
QSS_1	Wedge	1.93	1.13	1.62	0.95
QSS_3	Wedge	1.92	0.281	1.69	0.248

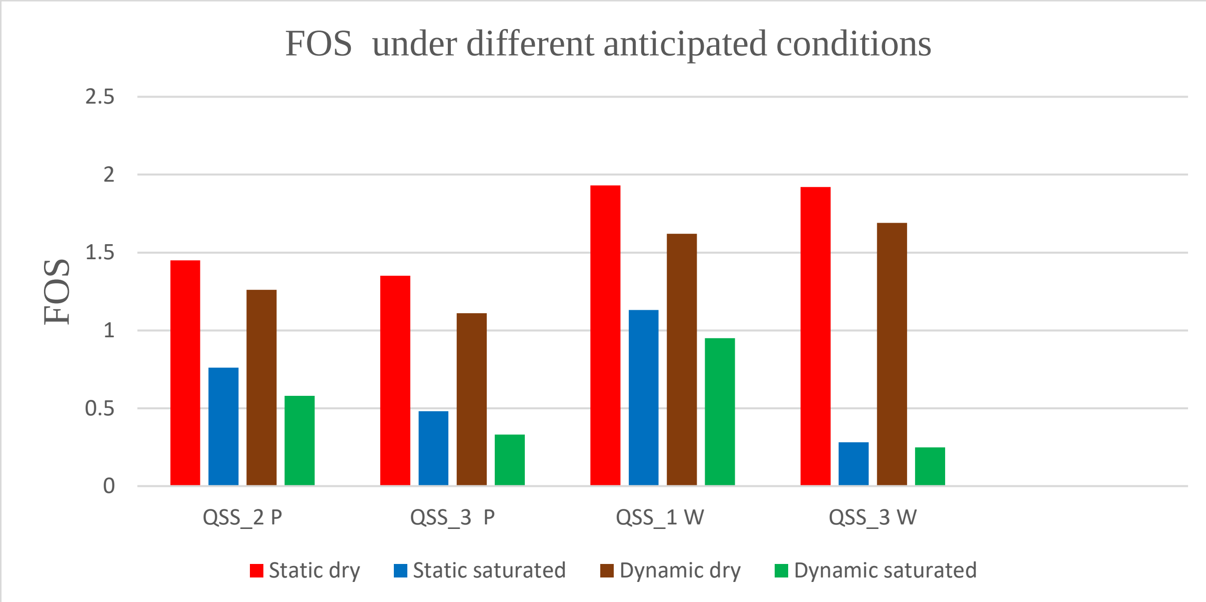

Figure 5.7: Comparison of FOS for structural controlled slope section

Table 9: Summary of FOS and SRF of non-structural controlled slope section

Slope section	FOS		SRF	
	Static load	Dynamic load	Static load	Seismic load
QSS_4	0.534	0.457	0.46	0.4
QSS_5	0.906	0.844	0.89	0.86

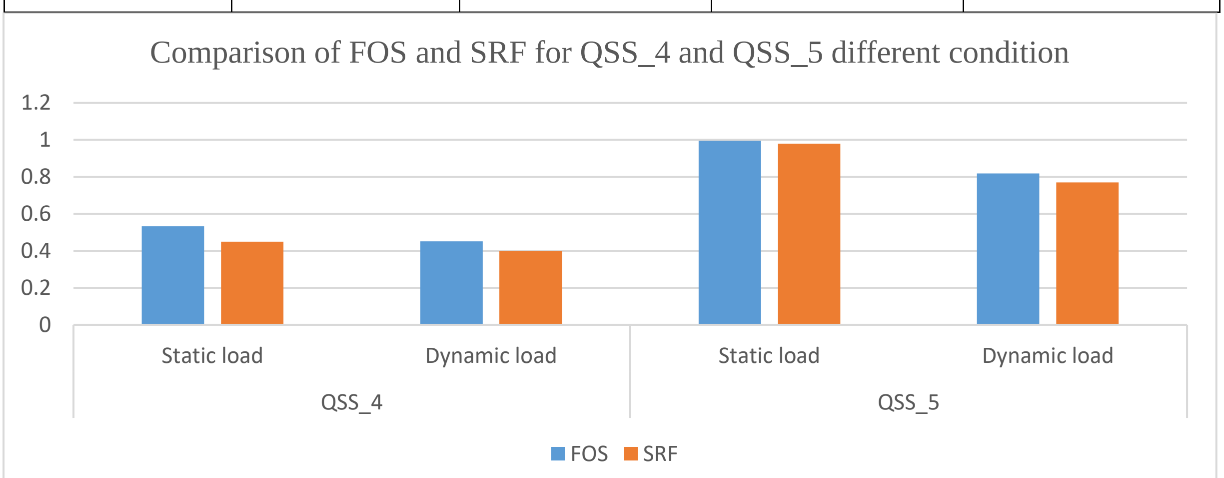

Figure 5.86: Comparison of FOS for QSS_4 and QSS_5 dynamic and static load condition

5.6. Remedial measures

The crucial slope sections of the quarry site are unstable under various anticipated conditions, according to an analysis on the stability of the quarry slope. Implementing appropriate remedial measures is essential to ensure worker safety, minimize the risk of slope failures, and sustain the long-term stability of the quarry site under all circumstances. As a result, appropriate mitigation measures taken. The most effective remedial measures are slope modifications to obtain the safest slope cut angle during extraction by optimizing bench width, flattening the slope angle, and minimizing bench height.

5.6.1. Multi-bench slope (reducing bench height)

Optimizing quarry slope by multi-bench slope technique used in quarry to improve the stability and safety issues brought on by steep slopes. The benches built by gradually removing materials, and safety berms added to prevent any possible rock falls. In addition to stability, the width of the benches is important to accommodate larger mining equipment, which can lead to improved productivity, cost efficiency, and play a crucial role in enhancing slope stability and managing quarry operations effectively by reducing the risk of slope failures. According to the analysis result, as increasing the number of benches from one to three, FOS also increased from 0.457 to 1.012 in QSS-4 and 0.884 to 1.125 in QSS_5 under dynamic load condition as shown in table 5.9 and 5.10, respectively. Based on the results, obtained in the analysis. FOS direct relation with the number of benches, but inversely related to bench height.

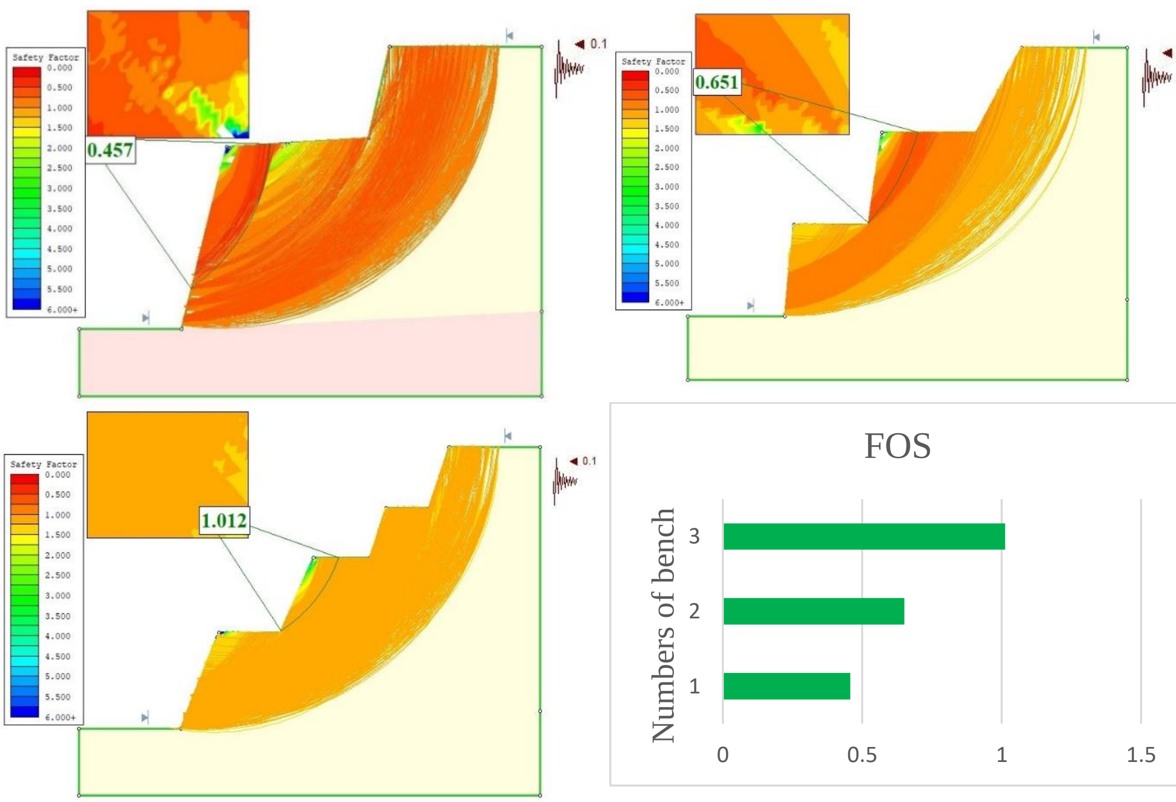

Figure 5.97: LEM slope models that show how increasing more benches stabilizes the slope at QSS_4.

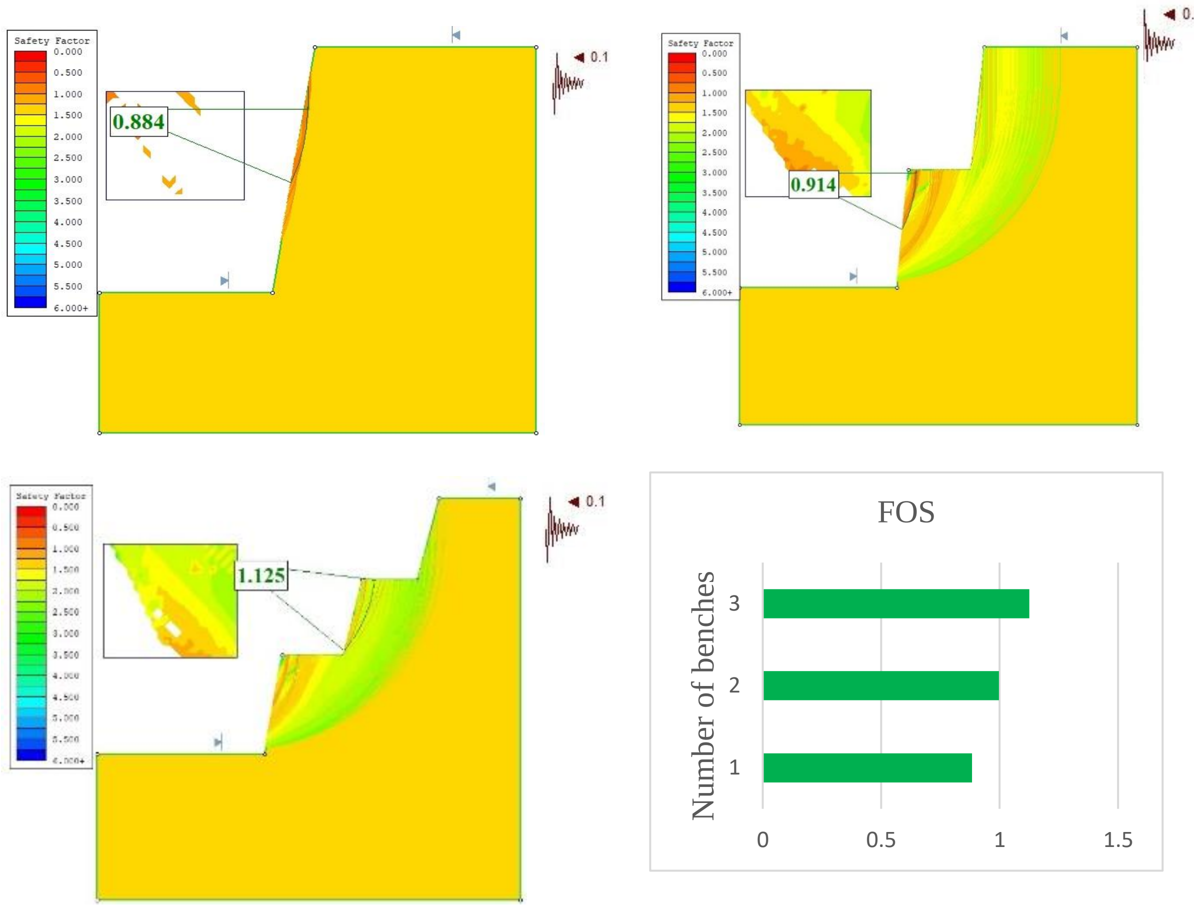

Figure 5.10: LEM slope models that show how increasing more benches stabilizes the slope at QSS_5.

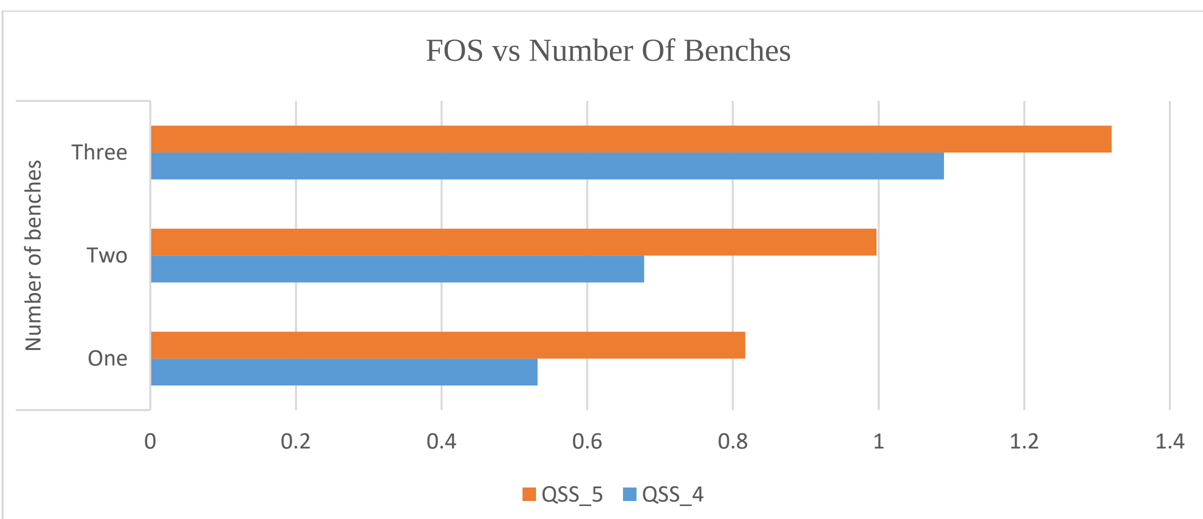

Figure 5.11: Summary of FOS versus bench number for QSS_4 and QSS_5

5.6.2. Flattening slope angle

In a quarry, flattening the slope angle is the process of making the slope less steep in order to increase stability and safety and lower the possibility of rock falls. The stability modelling, which utilized both the LEM and the FEM, showed that slope sections are unstable in a variety of situations. This study was addressed by looking at possible corrective actions. One important corrective strategy to reduce slope instability and maintain a safe and successful quarrying operation is to flatten the slope angle, which is a crucial component of good mining practices. For QSS_4 and QSS_5, analysis was therefore carried out, taking into account the unstable at both static and dynamic load conditions. LEM-based Slide 6.0 software was used to perform the analysis, which increased the FOS from 0.457 to 1.027 and 0.884 to 1.26 for QSS_4 and QSS_5, respectively, by gradually decreasing the slope angle from 54^0 to 38^0 for QSS_4 and from 65^0 to 55^0 for QSS_5 as shown in figure 5.12 and 5.13, respectively. According to Raghuvanshi (2017), the gravitational force acting on a slope is directly proportional to its inclination; hence, higher slopes increase the possibility of slope failure. Based on the findings from the analysis, FOS rises as the slope angle decreases.

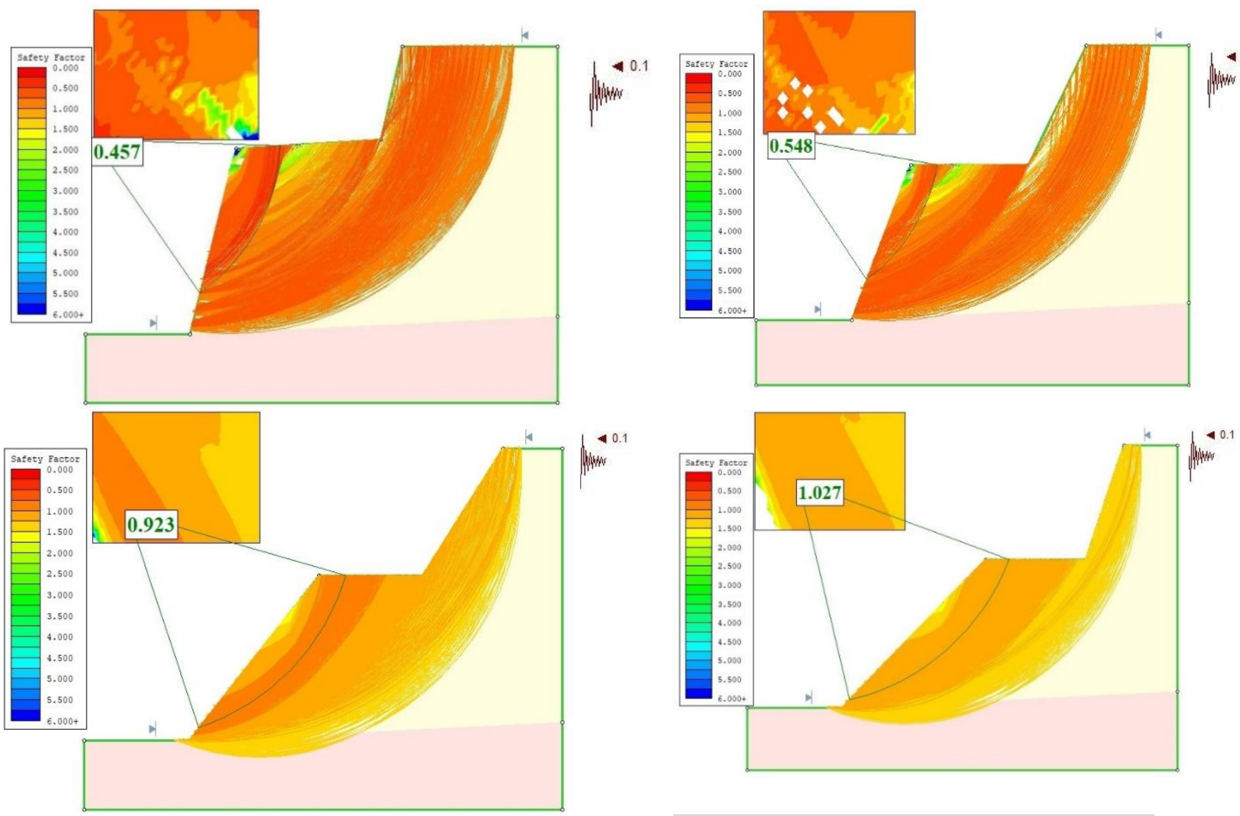

	Slope angle	FOS
A	54^0	0.457
B	48^0	0.548
C	43^0	0.923
D	38^0	1.027

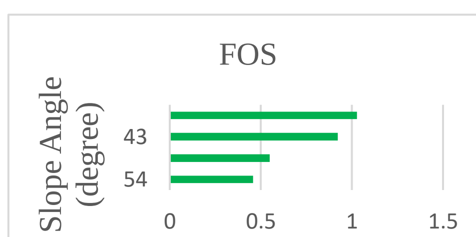

Figure 5.12: LEM models that illustrate a stabilized slope using the slope flattening technique from QSS_4.

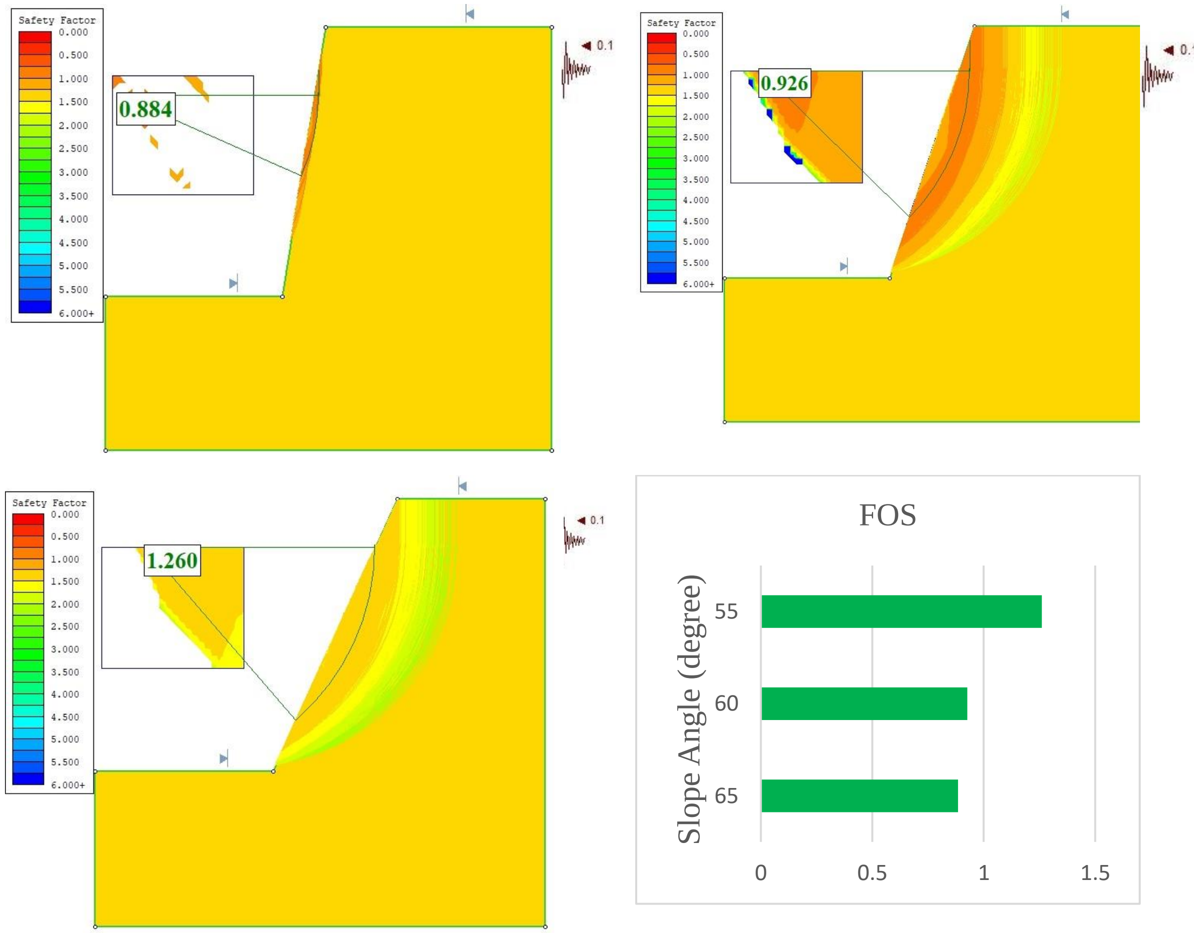

Figure 5.13: LEM models that illustrate a stabilized slope using the slope flattening technique from QSS_5.

5.7. Quarry safe cut slope design

Quarry slope design is essential for successful quarrying operations as the mining depths of the quarry are continuously increasing. In mining industries, multi-benched excavation systems are commonly used for quarrying activity. Based on factors of safety, structural characteristics, and strength properties of rock masses, safe cut slope quarries sites designed to maximize economic benefits determine the cut slope angle for the steepest, continuous, and stable slope without intermediate slope benches. This study focuses on analysing the stability of existing quarry cut slopes and designing quarry-safe cut slopes. It is commonly believed that a quarry slope is stable overall if the factor of safety (FOS) for the significant failure modes is greater than 1.5. This indicates that the resisting forces are significantly greater than the driving forces. generally regarded as safe and stable for long-term use(Abramson et al., 2001; Samarawickrama et al., 2014). The aim of the FOS values suggested for a rhyolite quarry is to represent a reasonable level of stability that offers a sufficient margin of safety for the quarry's long-term operation.

According to analysis, result below figure 5.14-quarry safe cut was designed at SRF of 1.76 and FOS of 1.455 and 1.27 under static and dynamic load conditions, respectively. Geometric design of quarry safe cut slope designed as figure 5.15 over all slope angle of 46^0, bench width and height of 8 m and 12 m, respectively.

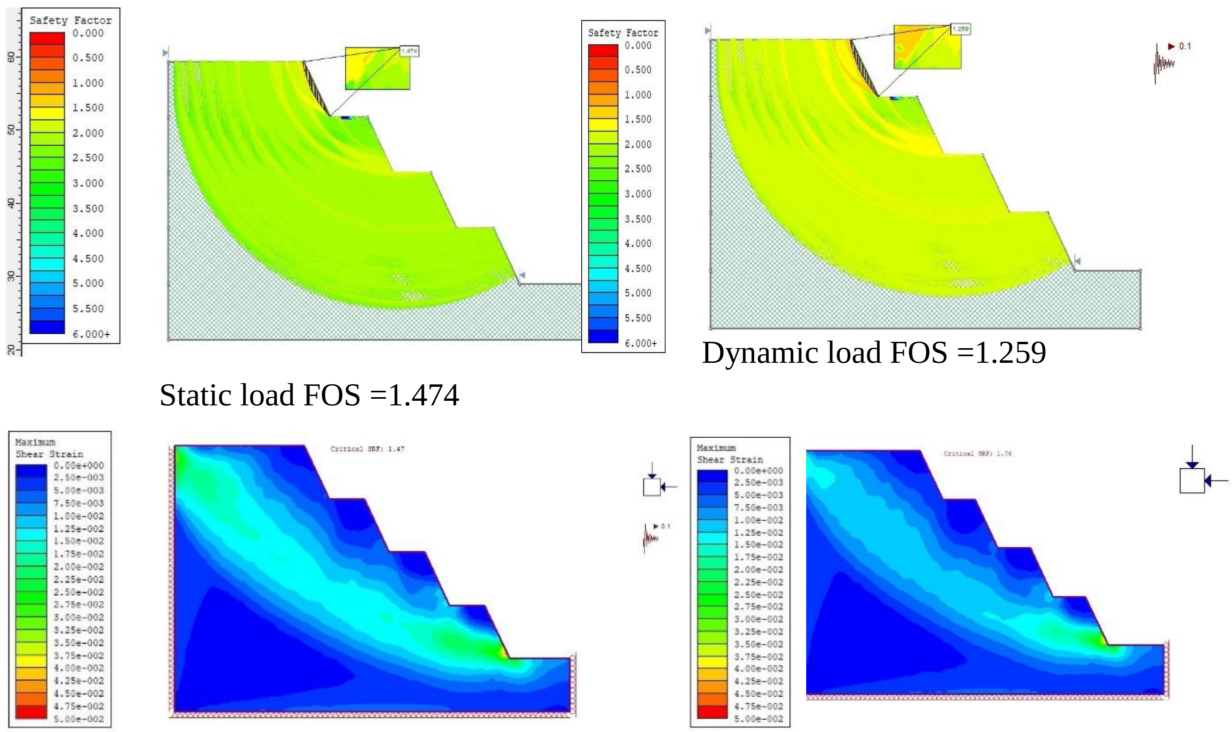

Dynamic load FOS =1.259

Static load FOS =1.474

Static load S=1.76

Dynamic load SRF =1.47

Figure 5.148: SRF and FOS under static and dynamic load conditions of safe cut design of quarry at over all slope angle of 46^0.

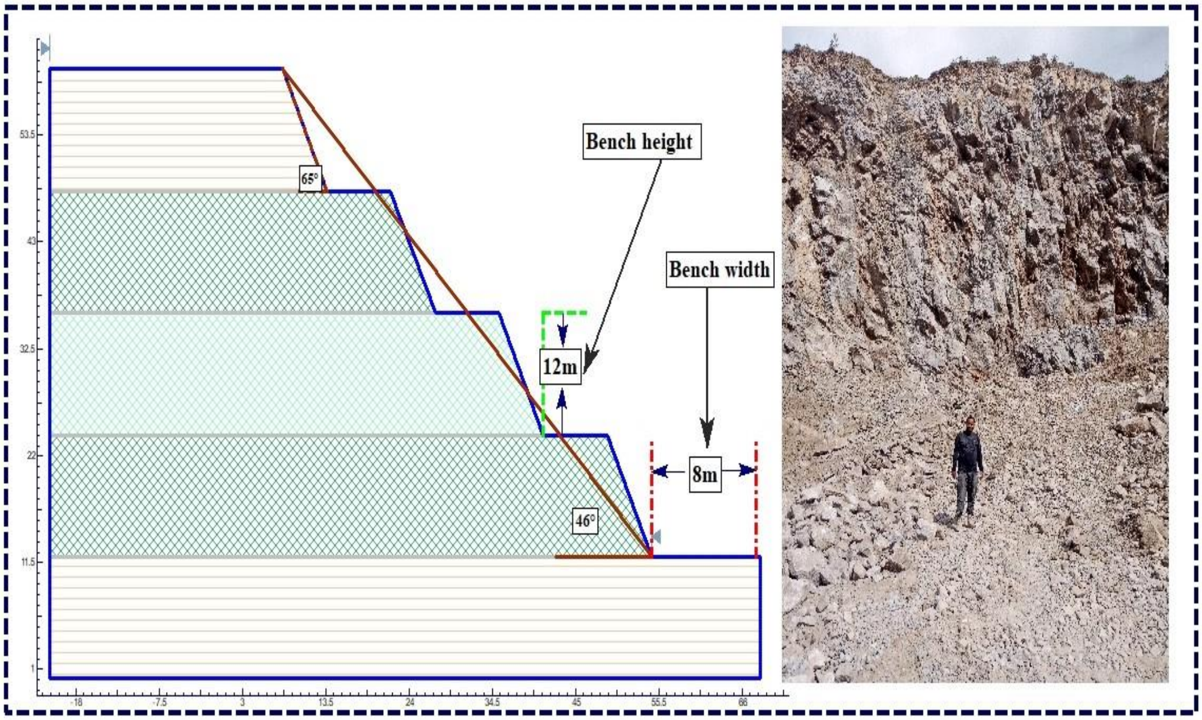

Figure 5.15: Geometric design of quarry safe cut slope.

CHAPTER SIX

6. CONCLUSION AND RECOMMENDATION

6.1. Conclusion

In conclusion, the stability assessment of rock slopes in quarry sites is a conducted by integrating detailed filed investigations, in situ strength tests, structural data collection, rock sampling, and laboratory testing of rock samples to evaluate the rock mass characteristics, discontinuities, and overall stability of the slopes for stability analysis and implementing appropriate remedial measures. The study's aim to evaluate the stability of rhyolite quarry slopes in the chosen section of quarry using kinematic, limit equilibrium, and the finite element method. The UCS of quarry site though in situ strength test using Schmidt hammer range from 84.1Mpa to 138.8Mpa. Whereas point load strength test the UCS of rock sample ranges from 83.28Mpa to 138.96Mpa, which shows strong to very strong rock. In addition, the average unit weight 24KN/m3, cohesion (c) 6.6 MPa and friction Angle (φ) of 26°. The quarry site dominantly rhyolite rock with slightly weathered. Quarrying activity has created a slope with a height of 20 to 55 meters and with poor bench design. The slope has a steep angle with an inclination of 75^{o} to 90^{o}. The top of the rock mass is moderately weathered, while the bottom of the slope is fresh to slightly weathered rhyolite rock unit. This condition could lead to failure, due to improper quarrying methods. Various methods such as Rock Mass Rating (RMR), Geological Strength Index (GSI), kinematic analysis, limit equilibrium and finite element analyses performed on the critical quarry slope section. Based on Kinematic analysis results QSS_1 and QSS_3 shows wedge mode of failure where as QSS_2 and QSS_3 shows planer mode of failure. Based on LEM modelling QSS_2 under variety of circumstances static dry, static saturated, dynamic dry, and dynamic saturated FoS are 1.45,0.76,1.26 and 0.58 respectively. Whereas QSS_3 FoS are 1.35, 0.48, 1.11 and 0.33 respectively. Therefore, the results shows both quarry slope section are unstable at static saturated and dynamic saturated condition and stable on other condition. Using Slide 6.0 and Phase2 software for QSS_4 and QSS_5 for non-structural controlled slope section, Based on the finding both slope section are unstable under Static and dynamic load. The key factors that can affect slope stability in quarry operation are slope geometry, discontinuity orientation with respect to the slope face, removal of rock material through excavation, intense rain, seismic activity, and poorly designed slopes are factors that significantly affect slope stability in quarry operations. To overcome stability condition of the quarry branching and reducing slope angle are most important aspect to stabilize and effective mining

6.2. Recommendations

Based on the results of this study, to address the impacts of slope instability on quarrying activities, it is recommended that the quarry operators implement the following slope stabilization techniques:

- ✓ Proper slope design, considering factors like slope angle, height, and bench layout, is essential for maintaining stable rock slopes.
- ✓ Overall slope angle, not exceeding 46 degrees, to reduce the driving forces acting on the slope.
- ✓ Incorporate well-designed benches with adequate height 12 meters and width 8 meters to provide intermediate stability and access for slope monitoring and maintenance.
- ✓ Excavation method: Implement protocols to minimize the impact of vibrations of machinery on the rock slopes, such as controlled quarrying techniques.

By implementing these recommendations, quarry operations can significantly enhance the long-term stability of their rock slopes, minimize the risk of failures, and promote the safe and sustainable extraction of resources.

References

Abebe, B., Dramis, F., Fubelli, G., Umer, M., & Asrat, A. (2010). Landslides in the Ethiopian highlands and the Rift margins. *Journal of African Earth Sciences*, *56*(4–5), 131–138. https://doi.org/10.1016/j.jafrearsci.2009.06.006

Abramson, L. W., Lee, T. S., Sharma, S., & Boyce, G. M. (2001a). *Slope stability and stabilization methods*. John Wiley & Sons.

Abramson, L. W., Lee, T. S., Sharma, S., & Boyce, G. M. (2001b). *SLOPE STABILITY AND STABILIZATION METHODS Second Edition f PREFACE xvii ACKNOWLEDGMENTS xix*.

Abzalov, M. (2016). *Applied mining geology* (Vol. 12). Springer.

Admassu, Y., & Shakoor, A. (2013). DIPANALYST: A computer program for quantitative kinematic analysis of rock slope failures. *Computers & Geosciences*, *54*, 196–202.

Alejano, L. R., Pons, B., Bastante, F. G., Alonso, E., & Stockhausen, H. W. (2007). Slope geometry design as a means for controlling rockfalls in quarries. *International Journal of Rock Mechanics and Mining Sciences*, *44*(6), 903–921.

Anbalagan, R. (1992). Landslide hazard evaluation and zonation mapping in mountainous terrain. *Engineering Geology*, *32*(4), 269–277.

Asfaw, L. M., & Woldeyes, G. (1986). Catalogue of Ethiopian earthquakes, earthquake parameters, strain release and seismic risk. *Geophysical Observatory, Faculty of Science, Addis Ababa University*.

Asmare, D., & Hailemariam, T. (2021). Assessment of rock slope stability using slope stability probability classification (SSPC) system, around AlemKetema, North Shoa, Ethiopia. *Scientific African*, *12*, e00730.

Ayalew, L. (1999). The effect of seasonal rainfall on landslides in the highlands of Ethiopia. *Bulletin of Engineering Geology and the Environment*, *58*, 9–19.

Ayele, S., Raghuvanshi, T. K., & Kala, P. M. (2014). Application of remote sensing and GIS for landslide disaster management: a case from Abay Gorge, Gohatsion–Dejen Section, Ethiopia. *Landscape Ecology and Water Management: Proceedings of IGU Rohtak Conference, Vol. 2*, 15–32.

Bar, N., & Barton, N. (2017). The Q-Slope Method for Rock Slope Engineering. *Rock Mechanics and Rock Engineering*, *50*(12), 3307–3322. https://doi.org/10.1007/s00603-

017-1305-0

Baraza, J., Lee, H. J., Kayen, R. E., & Hampton, M. A. (1990). Geotechnical characteristics and slope stability on the Ebro margin, western Mediterranean. *Marine Geology*, *95*(3–4), 379–393.

Barton, N., & Choubey, V. (1977). The shear strength of rock joints in theory and practice. *Rock Mechanics*, *10*, 1–54.

Barton, N., Lien, R., & Lunde, J. (1974). Engineering classification of rock masses for the design of tunnel support. *Rock Mechanics*, *6*, 189–236.

Bezie, G., Chala, E. T., Jilo, N. Z., Birhanu, S., Berta, K. K., Assefa, S. M., & Gissila, B. (2024). Rock slope stability analysis of a limestone quarry in a case study of a National Cement Factory in Eastern Ethiopia. *Scientific Reports*, *14*(1), 18541.

Bienawski, Z. T. (1976). *Rock mass classifications in rock engineering.*

Bieniawski, Z. T. (1975). The point-load test in geotechnical practice. *Engineering Geology*, *9*(1), 1–11.

Bieniawski, Z. T. (1989). *Engineering rock mass classifications: a complete manual for engineers and geologists in mining, civil, and petroleum engineering*. John Wiley & Sons.

Bizimana, H., & Sönmez, O. (2015). Landslide occurrences in the hilly areas of Rwanda, their causes and protection measures. *Disaster Science and Engineering*, *1*(1), 1–7.

Bommer, J. J., Rolo, R., Mitroulia, A., & Berdousis, P. (2002). Geotechnical properties and seismic slope stability of volcanic soils. *Proceedings of the 12th European Conference on Earthquake Engineering, London*.

Bozorgebrahimi, E., Hall, R. A., & Blackwell, G. H. (2003). Sizing equipment for open pit mining–a review of critical parameters. *Mining Technology*, *112*(3), 171–179.

Broch, E., & Franklin, J. A. (1972). The point-load strength test. *International Journal of Rock Mechanics and Mining Sciences & Geomechanics Abstracts*, *9*(6), 669–676.

Budetta, P. (2004). Assessment of rockfall risk along roads. *Natural Hazards and Earth System Science*, *4*(1), 71–81. https://doi.org/10.5194/nhess-4-71-2004

Bushira, K. M., Gebregiorgis, Y. B., Verma, R. K., & Sheng, Z. (2018). Cut soil slope stability analysis along national Highway at wozeka–gidole road, Ethiopia. *Modeling Earth Systems and Environment*, *4*, 591–600.

Bye, A. R., & Bell, F. G. (2001). Stability assessment and slope design at Sandsloot open pit, South Africa. *International Journal of Rock Mechanics and Mining Sciences*, *38*(3), 449–466.

C Samarawickrama, M. N., Amarasinghe, U. B., & Bandara, K. N. (2014). *MBA (Moratuwa), Senior Lecturer in Civil Engineering*. *XLVII*(03).

Chaulya, S., & Prasad, G. M. (2016). *Sensing and monitoring technologies for mines and hazardous areas: monitoring and prediction technologies*. Elsevier.

Chemeda, Y. C., & Info, A. (2020). *Engineering Geological Investigation of Adama Town : Implication to Engineering*. *7*(2).

Corominas, J., & Moya, J. (2008). A review of assessing landslide frequency for hazard zoning purposes. *Engineering Geology*, *102*(3–4), 193–213.

Corti, G., Sani, F., Florio, A. A., Greenfield, T., Keir, D., Erbello, A., Muluneh, A. A., & Ayele, A. (2020). Tectonics of the Asela-Langano Margin, Main Ethiopian Rift (East Africa). *Tectonics*, *39*(8), 1–23. https://doi.org/10.1029/2020TC006075

Damte, A., Boccaletti, M., Getaneh, A., Mazzuoli, R., & Tortorici, L. (1992). Geological Map of the Nazareth Dera Region (Main Ethiopian Rift), Scale 1: 50,000. *SELCA, Florence, Italy*.

Deere, D. U. (1964). Technical description of rock cores for engineering purpose. *Rock Mechanics and Enginee-Ring Geology*, *1*(1), 17–22.

Deere, D. U., & Deere, D. W. (1989). *Rock quality designation (RQD) after twenty years* (Issue 89). US Army Engineer Waterways Experiment Station.

Dellero, H., & El Kharim, Y. (2013). Rockfall hazard in an old abandoned aggregate quarry in the city of Tetouan, Morocco. *International Journal of Geosciences*, *4*(8), 1228–1232.

Duncan, J. M., Wright, S. G., & Brandon, T. L. (2014). *Soil strength and slope stability*. John Wiley & Sons.

Duncan, W. C., & Norman, N. I. (1996). Rock Slope Stability Analysis. *Landslides: Investigation and Mitigation*, 391–425.

Erbello, A., & Shube, H. (2019). Mapping Faults around Adama Town : Implication for Future Earthquake Triggering. *Ethiopian Journal of Science and Sustainable Development*, *6*(1).

Garcia, B., Villard, P., Richefeu, V., & Daudon, D. (2022). Comparison of full-scale rockfall tests with 3D complex-shaped discrete element simulations. *Engineering Geology*, *310*, 106855.

Gebreyohannes, D., Getahun, E., & Jothimani, M. (2024). Slope stability assessment in the seismically and landslide-prone road segment of Gerese to Belta, Rift Valley, Ethiopia. *PLoS One*, *19*(2), e0296807.

Genetu, M., & Mewa, G. (n.d.). Landslide Study on the Selected Site Along the Alem Ketema-Wereilu Road, North Shewa, Ethiopia. *North Shewa*, *Ethiopia*.

Giani, G. P. (1992). *Rock slope stability analysis*. CRC Press.

Gibson, W., De Bruyn, I. A., & Walker, D. J. H. (2006). Considerations in the optimisation of bench face angle and berm width geometries for open pit mines. *International Symposium on Stability of Rock Slopes in Open Pit Mining and Civil Engineering, The South African Institute of Mining and Metallurgy, Johannesburg*, 557–578.

Girma, F., Raghuvanshi, T. K., Ayenew, T., & Hailemariam, T. (2015). Landslide hazard zonation in Ada Berga District, Central Ethiopia–a GIS based statistical approach. *J Geom*, *9*(i), 25–38.

Goodman, R. E. (1989). Introduction to Rock Mechanics, vol. 2 Wiley. *New York*.

GRIFFITHS, D. V., & P.A.LANE. (2013). Slope stability analysis by ® nite elements. *GeÂotechnique*, *49*(3), 387–403.

Hack, R., Alkema, D., Kruse, G. A. M., Leenders, N., & Luzi, L. (2007). Influence of earthquakes on the stability of slopes. *Engineering Geology*, *91*(1), 4–15.

Hayati, N. (2021). A Review Study for Rock Slope Stability Assessments and Stabilization Methods. *Geotechnical Geology*, *17*(2), 487–493.

He, L., Coggan, J., Francioni, M., & Eyre, M. (2021). Maximizing impacts of remote sensing surveys in slope stability—a novel method to incorporate discontinuities into machine learning landslide prediction. *ISPRS International Journal of Geo-Information*, *10*(4). https://doi.org/10.3390/ijgi10040232

Hoek, E., & BRAY, J. (1989). *ROCK SLOPES DESIGN, EXCAVATION, STABILIZATION.*

Hoek, E., & Bray, J. D. (1981). *Rock slope engineering*. CRC press.

Hoek, E., & Brown, E. T. (1997). Practical estimates of rock mass strength. *International Journal of Rock Mechanics and Mining Sciences*, *34*(8), 1165–1186. https://doi.org/10.1016/S1365-1609(97)80069-X

Hoek, E., & Brown, E. T. (2019). The Hoek–Brown failure criterion and GSI – 2018 edition. *Journal of Rock Mechanics and Geotechnical Engineering*, *11*(3), 445–463.

https://doi.org/10.1016/j.jrmge.2018.08.001

Hoek, E., Carranza, C., & Corkum, B. (2002). Hoek-brown failure criterion – 2002 edition. *Narms-Tac*, 267–273.

Hoek, E., Read, J., Karzulovic, A., & Chen, Z. Y. (2000). Rock slopes in civil and mining engineering. *ISRM International Symposium*, ISRM-IS.

Holtz, R. D., & Schuster, R. L. (1996). Stabilization of soil slopes. *Landslides Investigation and Mitigation, Eds. Turner AK and Schuster, RL, Special Report, 247*.

Iverson, R. M., & Reid, M. E. (1992). Gravity-driven groundwater flow and slope failure potential: 1. Elastic Effective-Stress Model. *Water Resources Research*, *28*(3), 925–938.

Jaeger, J. C., Cook, N. G. W., & Zimmerman, R. (2009). *Fundamentals of rock mechanics*. John Wiley & Sons.

Kanungo, D. P., Pain, A., & Sharma, S. (2013). Finite element modeling approach to assess the stability of debris and rock slopes: A case study from the Indian Himalayas. *Natural Hazards*, *69*(1), 1–24. https://doi.org/10.1007/s11069-013-0680-4

Karacan, C. Ö., Ruiz, F. A., Cotè, M., & Phipps, S. (2011). Coal mine methane: a review of capture and utilization practices with benefits to mining safety and to greenhouse gas reduction. *International Journal of Coal Geology*, *86*(2–3), 121–156.

Kassa, M., & Meten, M. (2023). Slope stability analysis using kinematic, limit equilibrium, and finite element models at Dessie town, northern Ethiopia. *Arabian Journal of Geosciences*, *16*(12), 675.

Khanna, R., & Dubey, R. K. (2021). Comparative assessment of slope stability along road-cuts through rock slope classification systems in Kullu Himalayas, Himachal Pradesh, India. *Bulletin of Engineering Geology and the Environment*, *80*, 993–1017.

Kliche, C. A. (1999). *Rock slope stability*.

Kolapo, P., Oniyide, G. O., Said, K. O., Lawal, A. I., Onifade, M., & Munemo, P. (2022). An overview of slope failure in mining operations. *Mining*, *2*(2), 350–384.

Kumar, M. S., & Raj Kumar, M. (2022). Factors Affecting Slope Stability of an Opencast Mine: A Brief Study. *Int. J. Innov. Sci. Res. Technol.*, *7*, 878–882.

Kveldsvik, V., Nilsen, B., Einstein, H. H., & Nadim, F. (2008). Alternative approaches for analyses of a 100,000 m 3 rock slide based on Barton–Bandis shear strength criterion. *Landslides*, *5*, 161–176.

Labuz, J. F., & Zang, A. (2012). Mohr–Coulomb failure criterion. *Rock Mechanics and Rock Engineering*, *45*, 975–979.

Labuz, J. F., & Zang, A. (2014). Mohr–Coulomb failure criterion. In *The ISRM Suggested Methods for Rock Characterization, Testing and Monitoring: 2007-2014* (pp. 227–231). Springer.

Lamessa, G., & Meten, M. (2021). Stability analysis of rock slope along selected road sections from Gutane Migiru town to Fincha sugar factory, Oromiya, Ethiopia. *SN Applied Sciences*, *3*(2), 151.

Liu, S. Y., Shao, L. T., & Li, H. J. (2015). Slope stability analysis using the limit equilibrium method and two finite element methods. *Computers and Geotechnics*, *63*, 291–298.

Lunardi, P. (2008). *Design and construction of tunnels: Analysis of Controlled Deformations in Rock and Soils (ADECO-RS)*. Springer Science & Business Media.

Mandal, S., & Maiti, R. (2015). *Semi-quantitative approaches for landslide assessment and prediction*. Springer.

Mebrahtu, T. K., Heinze, T., Wohnlich, S., & Alber, M. (2022). Slope stability analysis of deep-seated landslides using limit equilibrium and finite element methods in Debre Sina area, Ethiopia. *Bulletin of Engineering Geology and the Environment*, *81*(10), 403.

Norrish, N. I., & Wyllie, D. C. (1996). Landslides: Investigation and Mitigation. Chapter 15-Rock slope stability analysis. *Transportation Research Board Special Report*, *247*.

Palmstrom, A. (1982). The volumetric joint count—a useful and simple measure of the degree of rock mass jointing. *International Association of Engineering Geology. International Congress. 4*, 221–228.

Pan, Y., Wu, G., Zhao, Z., & He, L. (2020). Analysis of rock slope stability under rainfall conditions considering the water-induced weakening of rock. *Computers and Geotechnics*, *128*, 103806.

Pantelidis, L. (2009). Rock slope stability assessment through rock mass classification systems. *International Journal of Rock Mechanics and Mining Sciences*, *46*(2), 315–325.

Park, H.-J., West, T. R., & Woo, I. (2005). Probabilistic analysis of rock slope stability and random properties of discontinuity parameters, Interstate Highway 40, Western North Carolina, USA. *Engineering Geology*, *79*(3–4), 230–250.

Pradhan, S. P., & Siddique, T. (2020). Stability assessment of landslide-prone road cut rock slopes in Himalayan terrain: a finite element method based approach. *Journal of Rock Mechanics and Geotechnical Engineering*, *12*(1), 59–73.

Prassetyo, S. H., Gutierrez, M., & Barton, N. (2017). Nonlinear shear behavior of rock joints using a linearized implementation of the Barton–Bandis model. *Journal of Rock Mechanics and Geotechnical Engineering*, *9*(4), 671–682.

Pun, W. K., & Urciuoli, G. (2008). Soil nailing and subsurface drainage for slope stabilization. *Proceedings of 10th International Symposium on Landslides and Engineered Slopes*, *30*, 85–126.

Raghuvanshi, T. K. (2019a). Plane failure in rock slopes–A review on stability analysis techniques. *Journal of King Saud University-Science*, *31*(1), 101–109.

Raghuvanshi, T. K. (2019b). Plane failure in rock slopes – A review on stability analysis techniques. *Journal of King Saud University - Science*, *31*(1), 101–109. https://doi.org/10.1016/j.jksus.2017.06.004

Raghuvanshi, T. K., Ibrahim, J., & Ayalew, D. (2014). Slope stability susceptibility evaluation parameter (SSEP) rating scheme–an approach for landslide hazard zonation. *Journal of African Earth Sciences*, *99*, 595–612.

Rahardjo, H., Li, X. W., Toll, D. G., & Leong, E. C. (2001). The effect of antecedent rainfall on slope stability. *Unsaturated Soil Concepts and Their Application in Geotechnical Practice*, 371–399.

Rahardjo, H., Ong, T. H., Rezaur, R. B., & Leong, E. C. (2007). Factors controlling instability of homogeneous soil slopes under rainfall. *Journal of Geotechnical and Geoenvironmental Engineering*, *133*(12), 1532–1543.

RocData, R. I. (2004). 3.0 user's guide of RocData: strength analysis of rock and soil masses using the generalized Hoek–Brown, Mohr–Coulomb, Barton–Bandis and power curve failure criteria. *Rocscience Inc, Toronto/Ontario*.

Rocscience. (2004). 3.0 user's guide of RocData: strength analysis of rock and soil masses using the generalized Hoek–Brown, Mohr–Coulomb, Barton–Bandis and power curve failure criteria. *Rocscience Inc, Toronto/Ontario*.

Romana, M., Tomás, R., & Serón, J. B. (2015). Slope Mass Rating (SMR) geomechanics classification: Thirty years review. *13th ISRM International Congress of Rock Mechanics*, *2015-MAY*, 1–10.

Selby, M. J. (1982). Controls on the stability and inclinations of hillslopes formed on hard rock. *Earth Surface Processes and Landforms*, *7*(5), 449–467.

Shariati, M., & Fereidooni, D. (2021). Rock slope stability evaluation using kinematic and kinetic methods along the Kamyaran-Marivan road, west of Iran. *Journal of Mountain Science*, *18*(3), 779–793.

Sharon, R., & Eberhardt, E. (2020). *Guidelines for Slope Performance Monitoring*. CSIRO PUBLISHING.

SIMON, N., Ghani, M. F. A., HUSSIN, A., LAI, G. O. H. T., RAFEK, A. G., SURIP, N., MONAM, T. R. T., & ERN, L. E. E. K. (2015). *Assessment of rockfall potential of limestone hills in the Kinta Valley*.

Singh, V. K. (1992). *Influence of geotechnical factors on open pit slope stability*. PhD Thesis, Department of Mining Engineering, Institute of Technology ….

Sjöberg, J. (1996). *Large scale slope stability in open pit mining: a review*.

Sophocleous, M. (2002). Interactions between groundwater and surface water: the state of the science. *Hydrogeology Journal*, *10*, 52–67.

Stead, D., Eberhardt, E., & Coggan, J. S. (2006). Developments in the characterization of complex rock slope deformation and failure using numerical modelling techniques. *Engineering Geology*, *83*(1–3), 217–235.

Stead, D., & Wolter, A. (2015). A critical review of rock slope failure mechanisms: the importance of structural geology. *Journal of Structural Geology*, *74*, 1–23.

Steffen, O. K. H., Contreras, L. F., Terbrugge, P. J., & Venter, J. (2008). A risk evaluation approach for pit slope design. *ARMA US Rock Mechanics/Geomechanics Symposium*, ARMA-08.

Tang, H., Yong, R., & Ez Eldin, M. A. M. (2017). Stability analysis of stratified rock slopes with spatially variable strength parameters: the case of Qianjiangping landslide. *Bulletin of Engineering Geology and the Environment*, *76*, 839–853.

Terzaghi, K. (1946). Rock defects and loads on tunnel supports. *Rock Tunneling with Steel Supports*.

Tesfaye, M., Regassa, B., & Garo, T. (2024). Rock slope stability modeling using kinematic and limit equilibrium methods along Woliso to Wonchi lake road, central Ethiopia. *Modeling Earth Systems and Environment*, *10*(1), 331–347.

Ullah, S., Khan, M. U., & Rehman, G. (2020a). a Brief Review of the Slope Stability Analysis Methods. *Geological Behavior*, *4*(2), 73–77. https://doi.org/10.26480/gbr.02.2020.73.77

Ullah, S., Khan, M. U., & Rehman, G. (2020b). A brief review of the slope stability analysis methods. *Geological Behavior (GBR)*, *4*(2), 73–77.

Waltham, T. (2009). *Foundations of engineering geology*. CRC press.

Wang, X., & Niu, R. (2009). Spatial forecast of landslides in Three Gorges based on spatial data mining. *Sensors*, *9*(3), 2035–2061. https://doi.org/10.3390/s90302035

Wyllie, D. C., & Mah, C. (2004). *Rock slope engineering*. CRC Press.

Yalcin, A. (2011). A geotechnical study on the landslides in the Trabzon Province, NE, Turkey. *Applied Clay Science*, *52*(1–2), 11–19.

Zhao, L. heng, Jiao, K. fu, Li, D. jian, & Zuo, S. (2020). System reliability analysis of seismic pseudo-static stability of rock wedge based on nonlinear Barton—Bandis criterion. *Journal of Central South University*, *27*(11), 3450–3463. https://doi.org/10.1007/s11771-020-4558-9

Appendix

Appendix A: Monthly Rainfall data of the study area at coordinate of (x- 39.2667, y- 8.5507& z- 1730)

					ADAMA								
YEAR	JAN	FEB	MAR	APR	MAY	JUN	JUL	AUG	SEP	OCT	NOV	DEC	ANN
2011	0	0	21.09	26.37	47.46	52.73	73.83	68.55	21.09	5.27	15.82	0	332.23
2012	0	0	0	52.73	15.82	26.37	189.84	200.39	68.55	5.27	0	0	558.98
2013	5.27	0	26.37	89.65	42.19	52.73	210.94	179.3	58.01	26.37	47.46	0	738.28
2014	0	5.27	36.91	31.64	36.91	26.37	121.29	147.66	79.1	58.01	10.55	0	553.71
2015	0	0	5.27	0	63.28	84.38	63.28	126.56	26.37	21.09	42.19	5.27	437.7
2016	10.55	15.82	21.09	189.84	100.2	21.09	142.38	121.29	84.38	10.55	15.82	5.27	738.28
2017	0	26.37	52.73	21.09	105.47	42.19	158.2	142.38	195.12	42.19	10.55	0	796.29
2018	0	26.37	36.91	137.11	63.28	73.83	73.83	152.93	36.91	21.09	42.19	0	664.45
2019	0	5.27	47.46	68.55	31.64	84.38	68.55	210.94	163.48	47.46	47.46	42.19	817.38
2020	0	5.27	26.37	189.84	110.74	89.65	163.48	216.21	110.74	10.55	5.27	15.82	943.95
2021	58.01	10.55	0	109.39	87.2	66.55	169.64	172.64	114.24	69.64	90.48	35.76	984.1
2022	17.7	9.83	16.28	81.2	28.24	89.42	118.53	151.35	83.35	45.46	14.82	10.73	666.89

Appendix B: Unit weight of rock sample taken from critical slope section laboratory test results

ECO

Korporeeshiinii Injiinariingii Oromiyaa
የኦሮሚያ ኢንጂነሪንግ ኮርፖሬሽን
Engineering Corporation of Oromia

External Letter

Document No.
OF/ECO/GM/035

Issue 1 No. 1 Page No. Page 1 of 1

Lak.ቁጥር/Ref. No. ECO/BO-061907
Guyyaa/ቀን/Date 19/07/2024

To: Fikeru Kefyalew Deresso
Finfinne

Subject: **Test Results Report**

As per your request with letter Ref. No. PGR/28047/15 dated 11/06//2024 to test for five rock samples collected from "Rock slope stability analysis of quarry sites around Adama, central Ethiopia" and tested for dry unit weight and wet unit weight parameters.

Therefore, please find attached herewith the test result conducted using the required standard.

With regards,

Engineering Corporation of Oromia
Laboratory Service
TIN 0002964649

Likissa Fanta Tasgara
Mining, Geotechnical &
Laboratory Service Division
Executive Officer

CC

- Mining Geo-technical and Laboratory Service Division
- Laboratory Service Directorate

ECO

ስልክ /Lakk bilbila/ + 251-11- 439-21-62/2470
Email:contactus@ecoet.org

Faaksii /ፋክስ/ + 251-11- 439-2008 ፖ.ሣ.ቁ p.o.box 850/1270
Website www.ecoet.org

Compan Name **KorporeshiniiIngineeringiiOromiyaa** **ኦሮሚያኢንጅነሪንግኮርፖሬሽን** **Engineering Corporation of Oromia**	Form No.: OF/ECO/TL/7.8/02 Lab No: 287	
Form Title :- **Particle size distribution,Specific Gravity, Water Absorption And Unit Weight of Aggregate,**	Issue No: 1	Page No: 1

Project	Research on Rock Slope Stabiity analysis of quarry sites around Adama, central Ethopia	**Sampled By**	
Client	Fikeru Kefyalew Deresso	**Lab Code**	RCK/251/287
Contructor		**Sampel ID**	RRS 4&5
Consultant		**RF Pro No**	IECOLB/287/2016
Location		**Date Receviod**	11/06/2024
Material Sourse		**Tested date**	26/06/2024
SAmpling Station	quarry site around Adama	**Date Reported**	01/07/2024

Test Method ASTM C 127-88 And Result

	DRY Unit Weight of ROCK			**WET Unit Weight of ROCK**		
SAMPLE ID	**Volume of rock(m^3)**	**M1 (kg)**	**Unit Weight(kg/m^3)**	**Volume of rock(m3)**	**M2(kg)**	**Unit Weight(kg/m3)**
RRS 4&5	**0.00135648m^3**	**3.21**	**2366.40**	**0.00135648m^3**	**3.29**	**2425.40**

M1=Mass of oven dry rock sample Kg

M2=Mass of saturated surface Dry(SSD) Rock sample

volume of water (m3) =0.0045216m^3

volume of water (m3)+volume of sample =0.00587808m3

Remark : The volume of rock was calculated by using the water displacement method in the known volume of water in the cyliner.

(volume of rock= volume of water displament-volume of water)

Tested By	**Reported By**	**Checked By** 10/11/16	**Approved By**
Tesfaye Leta	Tesfaye Leta	Sefia Feyo	Directorate Director
Laboratort Technician	Laboratort Technician	Laboratory Coordinator	

ante (phD)
Laboratory Service Leader
Engineering Corporation
Of Oromia

Campus Name

KorporeshiniiIngineeringiiOromiyaa

ኦሮሚያኢንጅነሪንግኮርፖሬሽን

Engineering Corporation of Oromia

Form No: OF/ECO/TL/7.8/02

Lab No :287

Form Title :-	Particle size distribution,Specific Gravity, Water Absorption And Unit Weight of Aggregate,	Issue No: 1	Page No: 1

Project	Research on Rock Slope Stabiity analysis of quarry sites around Adama, central Ethopia	Sampe By	
Client	Fikeru Kefyalew Deresso	Lab Code	RCK/249/287
Contructor		Sampel ID	TRS 1&2
Consultant		RF Pro No	EECOLB/287/2016
Location		Date Receviod	11/06/2016
Material Sourse		Tested date	18/06/2016
SAmpling Station	quarry site around Adama	Date Reported	28/06/2016

Test Method ASTM C 127-88 And Result

SAMPLE ID	DRY Unit Weight of ROCK			WET Unit Weight of ROCK		
	Volume of rock(m^3)	M1 (kg)	Unit Weight(kg/m^3)	Volume of rock(m3)	M2(kg)	Unit Weight(kg/m3)
TRS 1&2	$0.0011304m^3$	3.30	2919.30	0.0011304m3	3.35	2963.60

M1=Mass of oven dry rock sample

M2=Mass of saturated surface Dry(SSD) Rock sample

volume of water (m3) $=0.0045216m^3$

volume of water (m3)+volume of sample =0.00562m3

Remark : The volume of rock was calculated by using the water displacement method in the known volume of water in the cyliner.

(volume of rock= volume of water displacement-volume of water)

Tested By	Reported By	Checked By	Approved By
Tesfaye Leta	Tesfaye Leta	Sefia Feyo 10/11/16	Abdenna Deressa Amante (phD)
Laboratort Technician	Laboratort Technician	Laboratory Coordinator	Laboratory Directorate Director / Team Leader at Engineering Corporation Of Oromia

Campan Name	KorporeshiniiIngineeringiiOromiyaa ኦሮሚያኢንጅነሪንግኮርፖሬሽን **Engineering Corporation of Oromia**	Form No: OF/ECO/TL/7.8/02 Lab No :287	
Form Title :-	**Particle size distribution,Specific Gravity, Water Absorption And Unit Weight of Aggregate,**	Issue No: 1	Page No: 1

Project	Research on Rock Slope Stabiity analysis of quarry sites around Adama, central Ethopia	**Sampe By**	
Client	Fikeru Kefyalew Deresso	**Lab Code**	RCK/250/287
Contructor		**Sampel ID**	RRS 1&2
Consultant		**RF Pro No**	EECOLB/287/2016
Location		**Date Receviod**	11/06/2016
Material Sourse		**Tested date**	18/06/2016
SAmpling Station	quarry site around Adama	**Date Reported**	28/06/2016

Test Method ASTM C 127-88 And Result

	DRY Unit Weight of ROCK			WET Unit Weight of ROCK		
SAMPLE ID	**Volume of rock(m^3)**	**M1 (kg)**	**Unit Weight(kg/m^3)**	**Volume of rock(m3)**	**M2(kg)**	**Unit Weight(kg/m3)**
TRS 1&2	**0.0018086**	**4.30**	**2377.50**	**0.0018086**	**4.41**	**2438.40**

M1=Mass of oven dry rock sample

M2=Mass of saturated surface Dry(SSD) Rock sample

volume of water (m3) =0.0045216m^3

volume of water (m3)+volume of sample =0.00633024m^3

Remark : The volume of rock was calculated by using the water displacement method in the known volume of water in the cyliner.

(volume of rock= volume of water displacement-volume of water)

Tested By	**Reported By**	**Checked By**	**Approved By**
Tesfaye Leta	Tesfaye Leta	Sefia Feyo 10/11/16	Abdenna Deressa (phD)
Laboratort Technician	Laboratort Technician	Laboratory Coordinator	Laboratory Directorate Director / Leader at Engineering Corporation Of Oromia

Company Name

KorporeshiniiIngineeringiiOromiyaa
ኦሮሚያ ኢንጅነሪንግ ኮርፖሬሽን
Engineering Corporation of Oromia

Form No.: OF/ECO/TL/7.8/02

Lab No :287

Form Title:- Particle size distribution,Specific Gravity, Water Absorption And Unit Weight of Aggregate,

Issue No: 1

Page No: 1

Project	Research on Rock Slope Stabiity analysis of quarry sites around Adama, central Ethopia	Sampe By	
Client	Fikeru Kefyalew Deresso	Lab Code	RCK/252/287
Contructor		Sampel ID	RRS 7&8
Consultant		RF Pro No	IECOLB/287/2016
Location		Date Receviod	11/06/2024
Material Sourse		Tested date	26/06/2024
SAmpling Station	quarry site around Adama	Date Reported	01/07/2024

Test Method ASTM C 127-88 And Result

DRY Unit Weight of ROCK **WET Unit Weight of ROCK**

SAMPLE ID	Volume of rock(m^3)	M1 (kg)	Unit Weight(kg/m^3)	Volume of rock(m3)	M2(kg)	Unit Weight(kg/m3)
RRS 4&5	0.001446912m^3	3.20	2211.60	0.001446912m^3	3.26	2253.10

M1=Mass of oven dry rock sample Kg

M2=Mass of saturated surface Dry(SSD) Rock sample

volume of water (m3) =0.0045216m^3

volume of water (m3)+volume of sample =0.005968512m^3

Remark : The volume of rock was calculated by using the water displacement method in the known volume of water in the cyliner.

(volume of rock= volume of water displament-volume of water)

Tested By	Reported By	Checked By	Approved By
Tesfaye Leta	Tesfaye Leta	Sefia Feyo 10/11/16	Abdeina Deressa Amante (phD)
Laboratort Technician	Laboratort Technician	Laboratory Coordinator	Laboratory Sector Leader at Engineering Corporation Of Oromia

Company Name

KorporeshiniiIngineeringiiOromiyaa

ኦሮሚያኢንጅነሪንግኮርፖሬሽን

Engineering Corporation of Oromia

Form No: OF/ECO/TL/7.8/02

Lab No: 287

Form Title	Unit Weight of Aggregate and Rock	Issue No: 1	Page No: 1

Project	Research on Rock Slope Stability analysis of quarry sites around Adama, central Ethiopia	Sampled By	
Client	Fikeru Kefyalew Deresso	Lab Code	[illegible]
Contructor		Sampel ID	[illegible]
Consultant		RF Pro No	[illegible]
Location		Date Receviod	[illegible]
Material Sourse		Tested date	[illegible]
Sampling Station	quarry site around Adama	Date Reported	[illegible]

Test Method ASTM C 127-88 And Result

DRY Unit Weight of ROCK				WET Unit Weight of ROCK		
SAMPLE ID	Volume of rock(m^3)	M1 (kg)	Unit Weight(kg/m^3)	Volume of rock(m3)	M2(kg)	Unit Weight(kg/m3)
NIRS-1	0.000678m^3	1.73	2551.60	0.000678m^3	1.78	2625.40

M1=Mass of oven dry rock sample Kg

M2=Mass of saturated surface Dry(SSD) Rock sample

volume of water (m3) =0.0045216m^3

volume of water (m3)+volume of sample =[illegible]

Remark : The volume of rock was calculated by using the water displacement method in the known volume of water in the cyliner

(volume of rock= volume of water displament-volume of water)

Tested By	Reported By	Checked By	Approved By
Tesfaye Leta	Tesfaye Leta	Sefia Feyo 10/11/16	
Laboratort Technician	Laboratort Technician	Laboratory Coordinator	

Abdenna Deressa Gemechu (phD) Laboratory Service Leader Director Engineering Corporation Of Oromia

Appendix C: GSI value from RocData Software

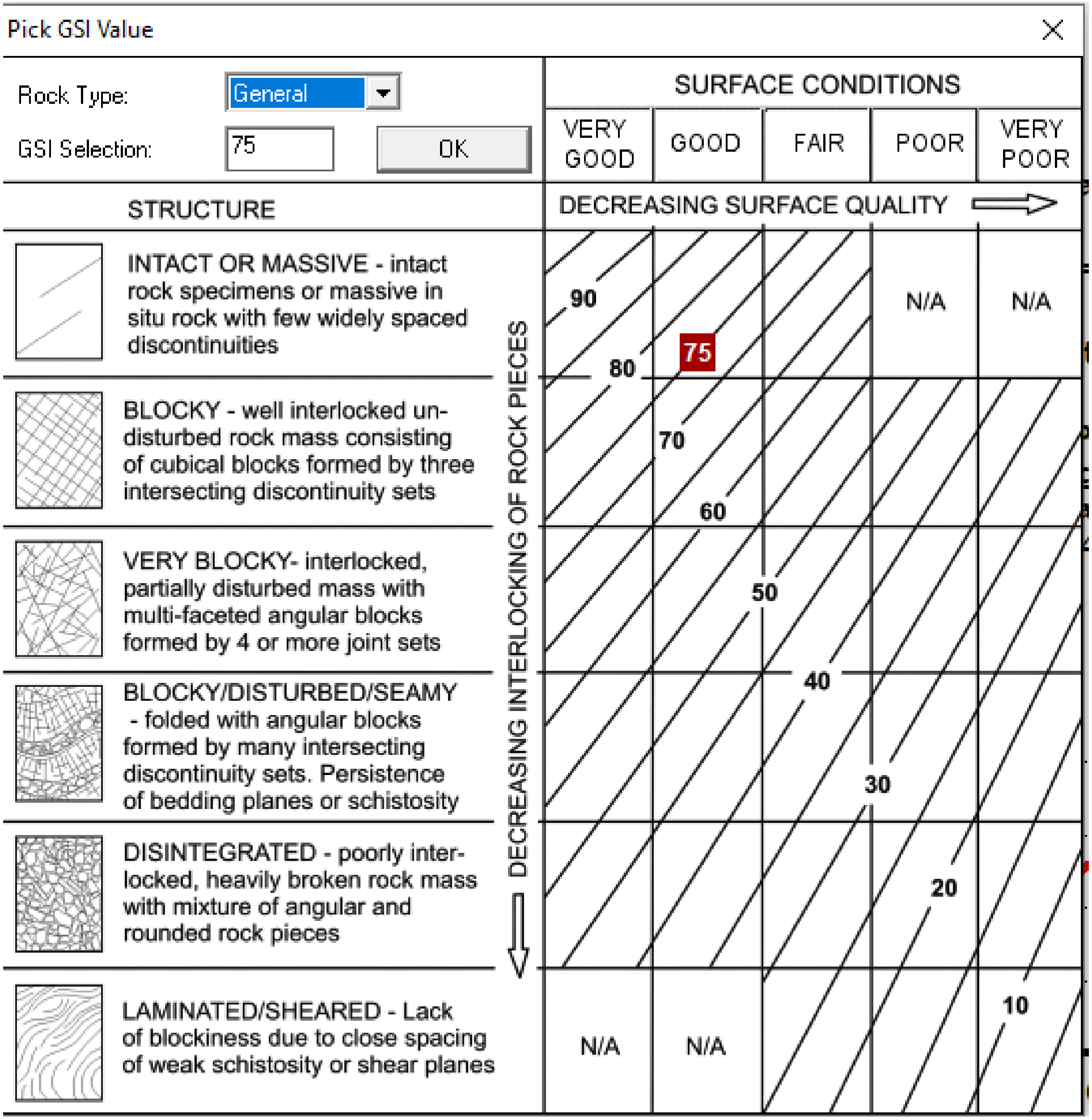

Appendix D: Rock mass quality classification according to RQD (Deere et al. 1967)

RQD	Rock Mass Quality
< 25	Very poor
25 – 50	Poor
50 – 75	Fair
75 – 90	Good
99 – 100	Excellent

Appendix E: Rock-mass rating system (after Bieniawski 1989)

No.	Parameter	Ranges of values						
1	Strength of intact rock material, uniaxial compressive strength (MPa)	>250	100–250	50–100	25–50	5–25	1–5	<1
	Rating	15	12	7	4	2	1	0
2	Rock quality designation, RQD (%)	90–100	75–90	50–75	25–50	<25		
	Rating	20	17	13	8	3		
3	Spacing of discontinuities	>2 m	0.6–2 m	200–600 mm	60–200 mm	<60 mm		
	Rating	20	15	10	8	5		
4	Condition of discontinuities	Very rough surfaces, not continuous, no separation, unweathered wall rock	Slightly rough surfaces, separation <1 mm, slightly weathered walls	Slightly rough surfaces, separation <1 mm, highly weathered walls	Slickensided surfaces or gouge <5 mm thick orseparation 1–5 mm, continuous	Soft gouge >5 mm thick or separa-tion >5 mm, continuous		
	Rating	30	25	20	10	0		
5	Groundwater in joint	Completely dry	Damp	Wet	Dripping	Flowing		
	Rating	15	10	7	4	0		

Appendix F: Disturbance factor (D) value from RocData Software

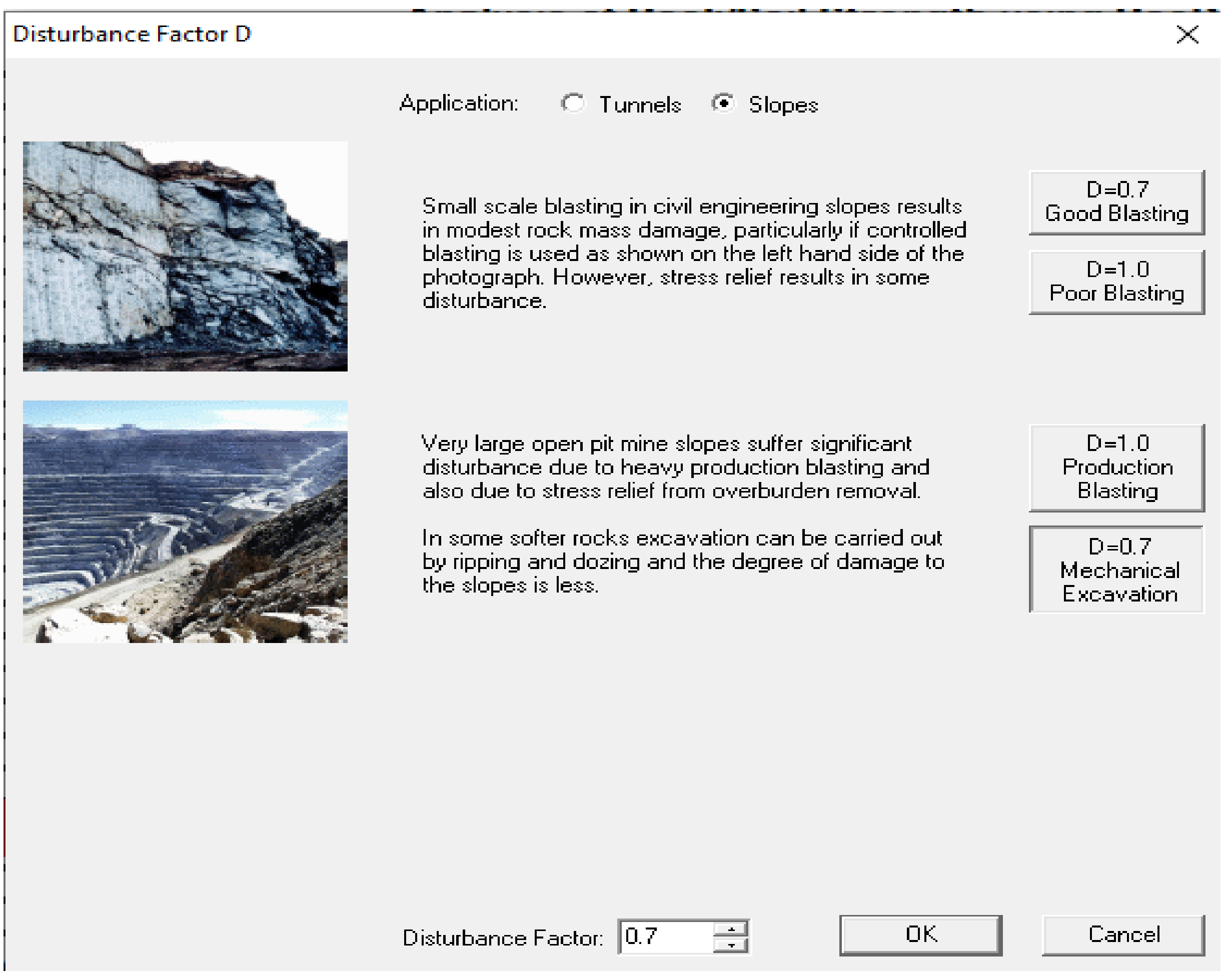

Appendix G: The shear strength parameters estimated using RocData software (Using Barton-Bandis method).

QSS1_J1

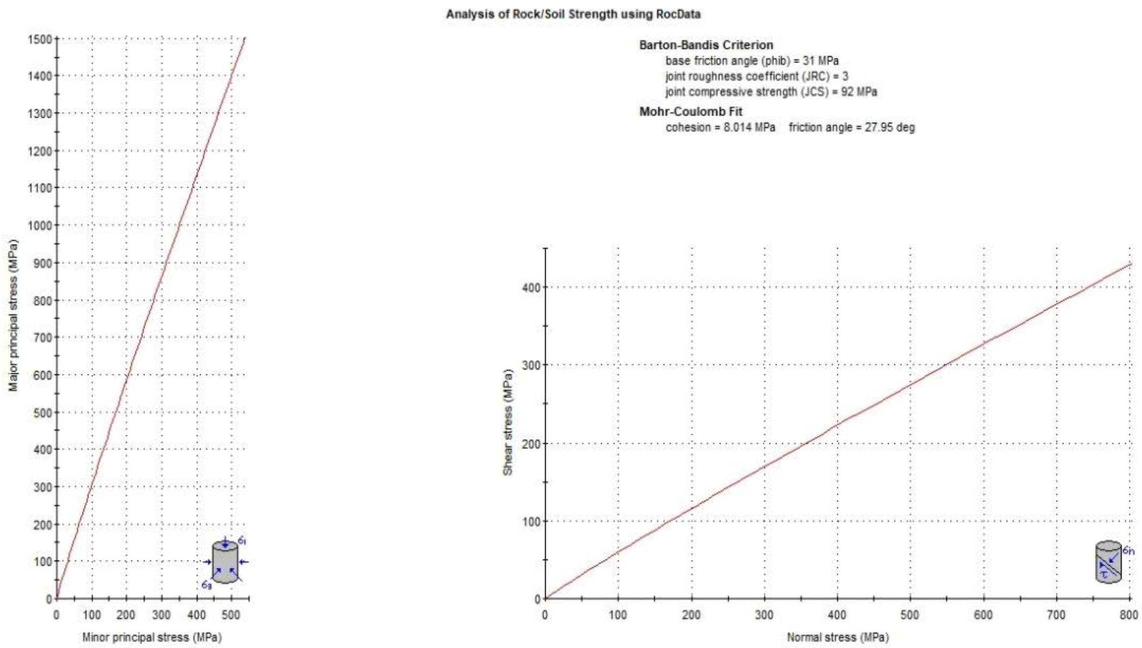

QSS1_J2

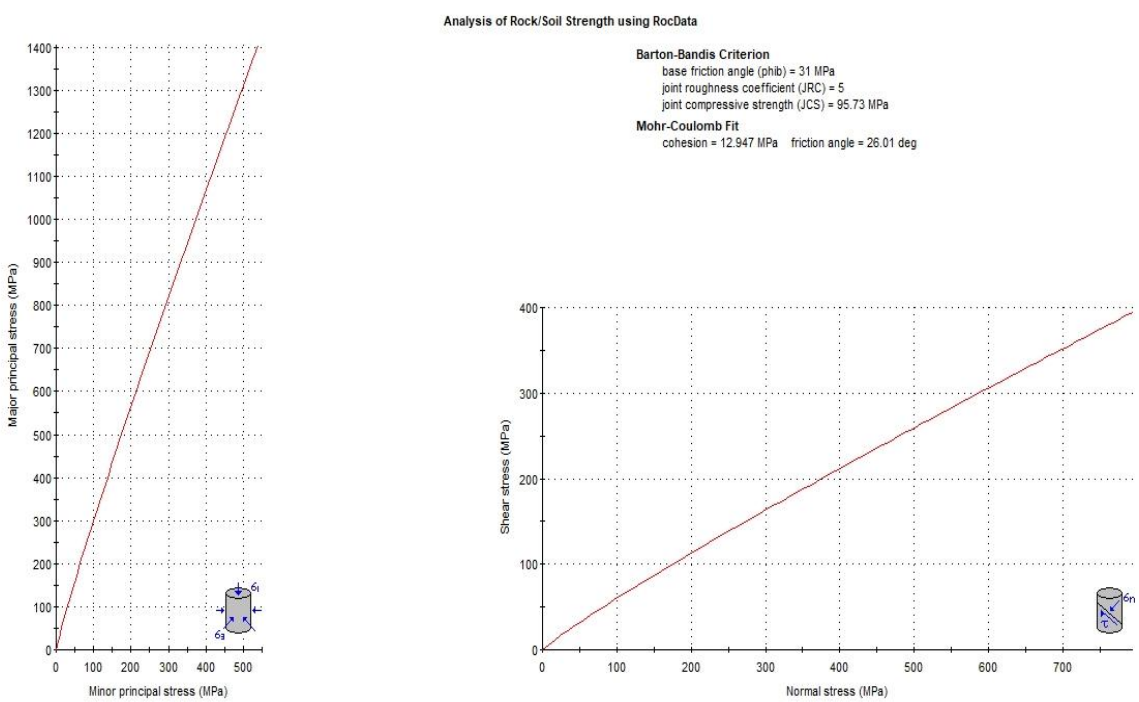

QSS2_J1

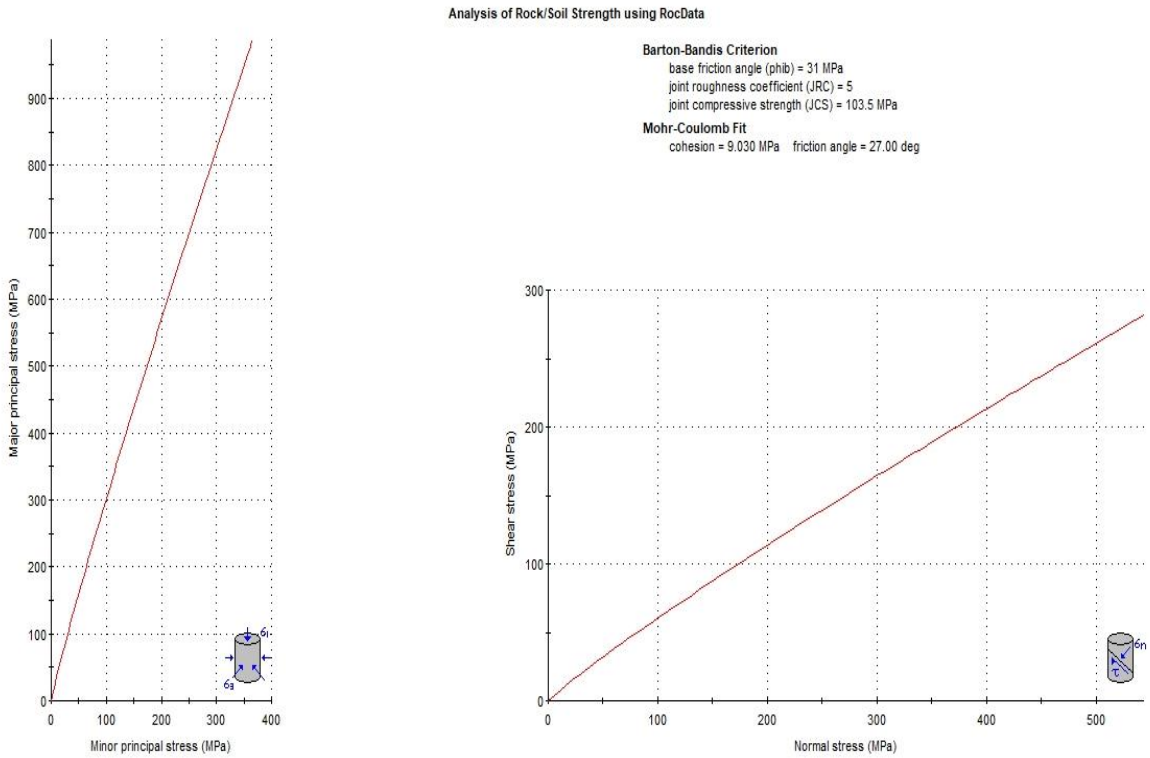

QSS2_2

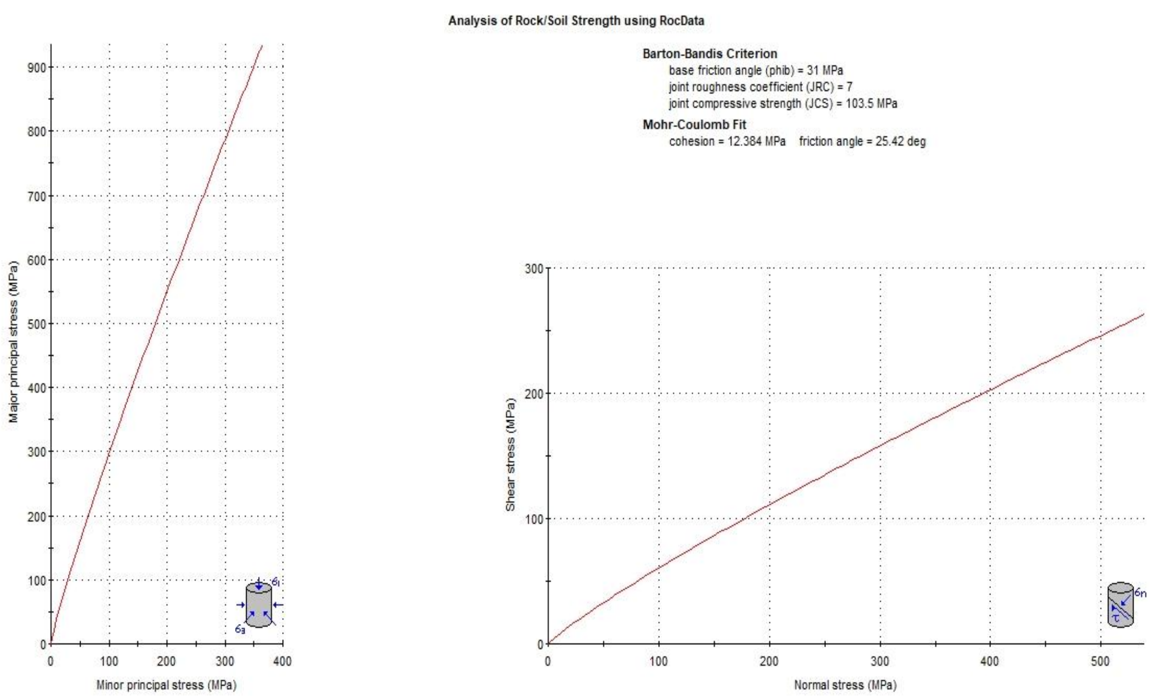

QSS3_J1

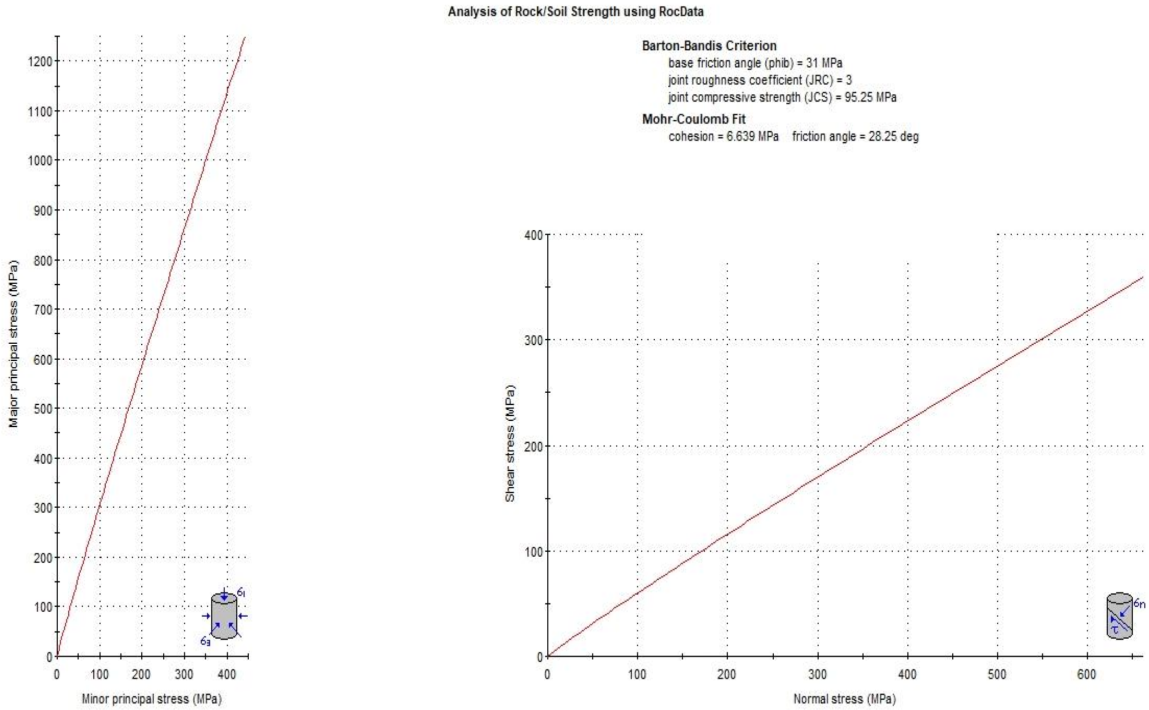

QSS3_J2

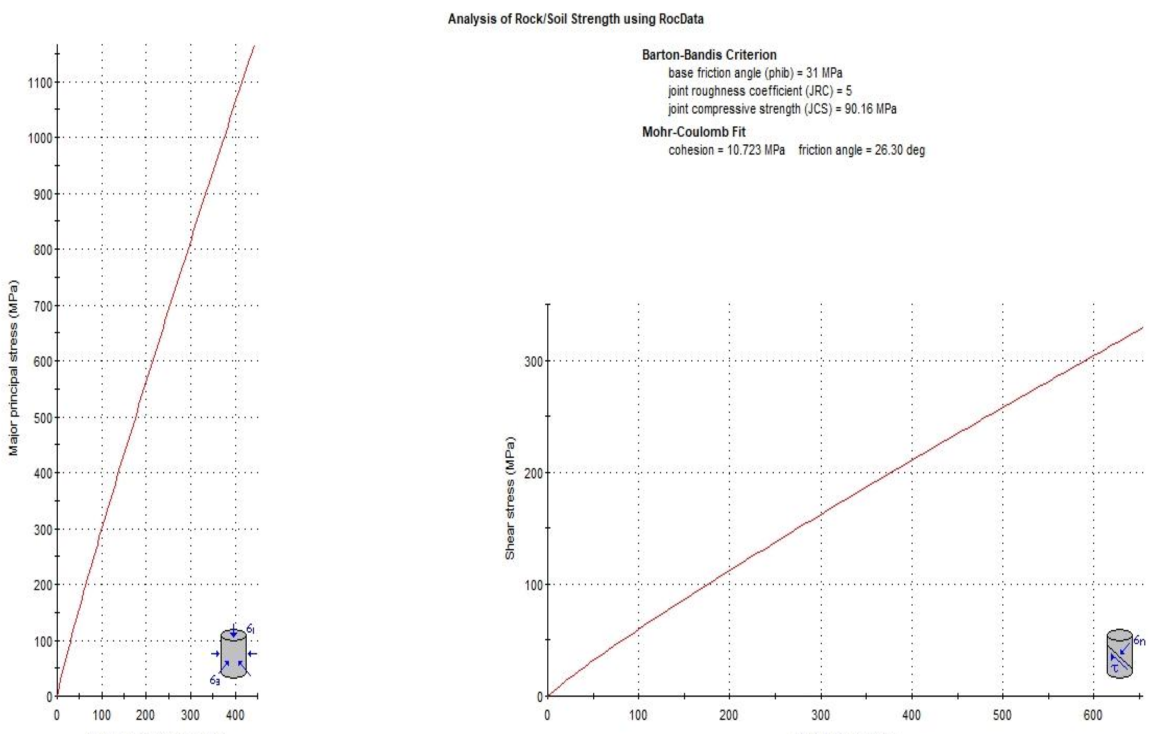

QSS3_J3

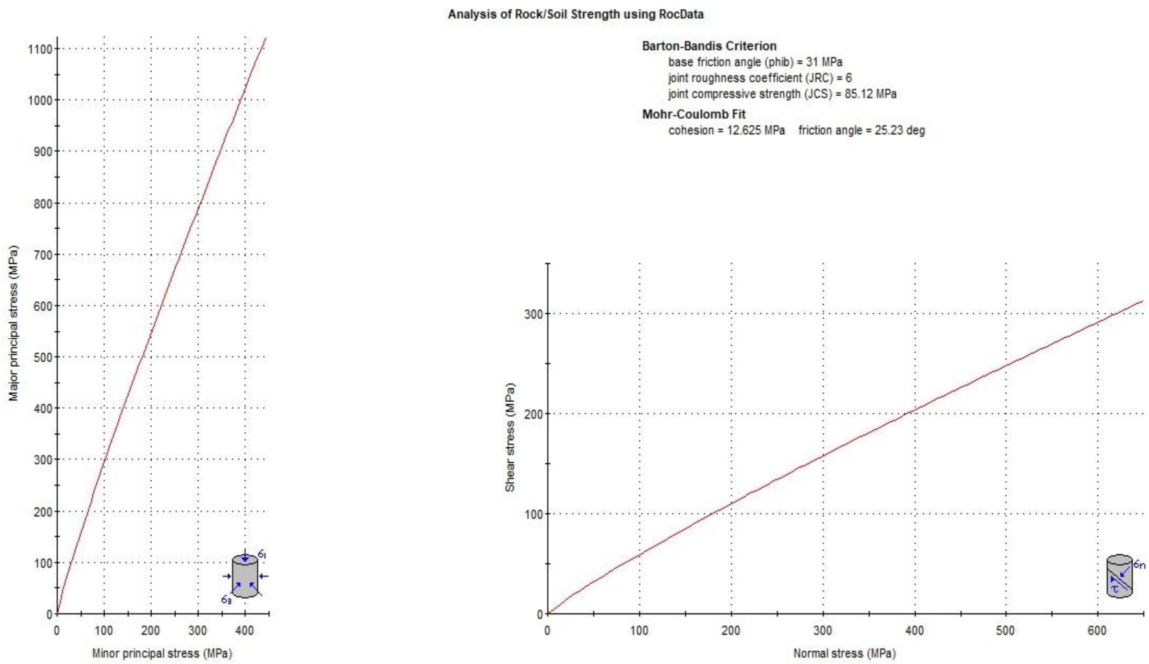

Appendix H: The shear strength parameters estimated using RocData software (Using Hoek-Brown methods).

QSS_4

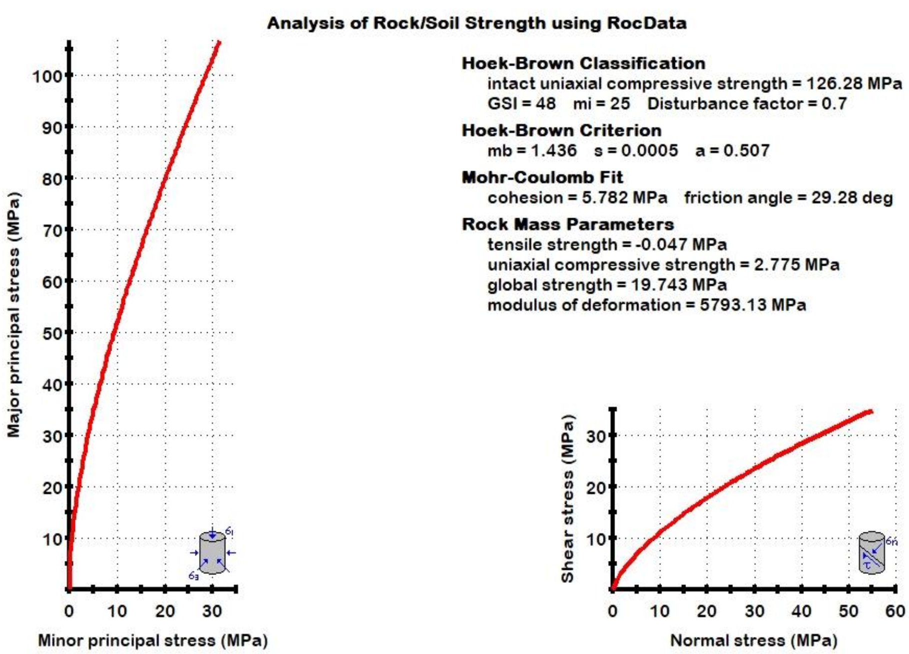

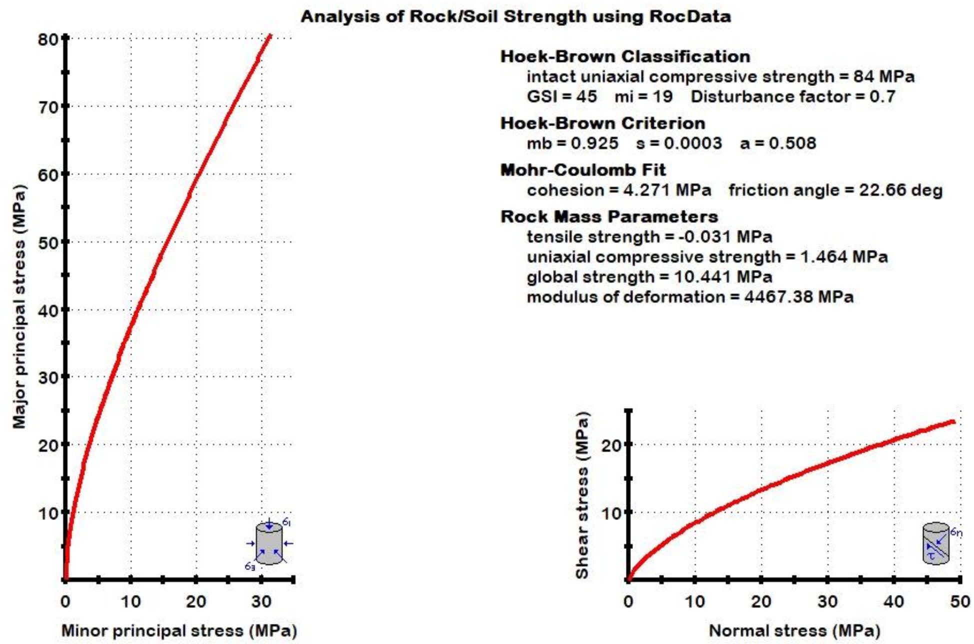
Analysis of Rock/Soil Strength using RocData
Hoek-Brown Classification
intact uniaxial compressive strength = 84 MPa
GSI = 45 mi = 19 Disturbance factor = 0.7
Hoek-Brown Criterion
mb = 0.925 s = 0.0003 a = 0.508
Mohr-Coulomb Fit
cohesion = 4.271 MPa friction angle = 22.66 deg
Rock Mass Parameters
tensile strength = -0.031 MPa
uniaxial compressive strength = 1.464 MPa
global strength = 10.441 MPa
modulus of deformation = 4467.38 MPa
Major principal stress (MPa)
Minor principal stress (MPa)
Shear stress (MPa)
Normal stress (MPa)

QSS_5

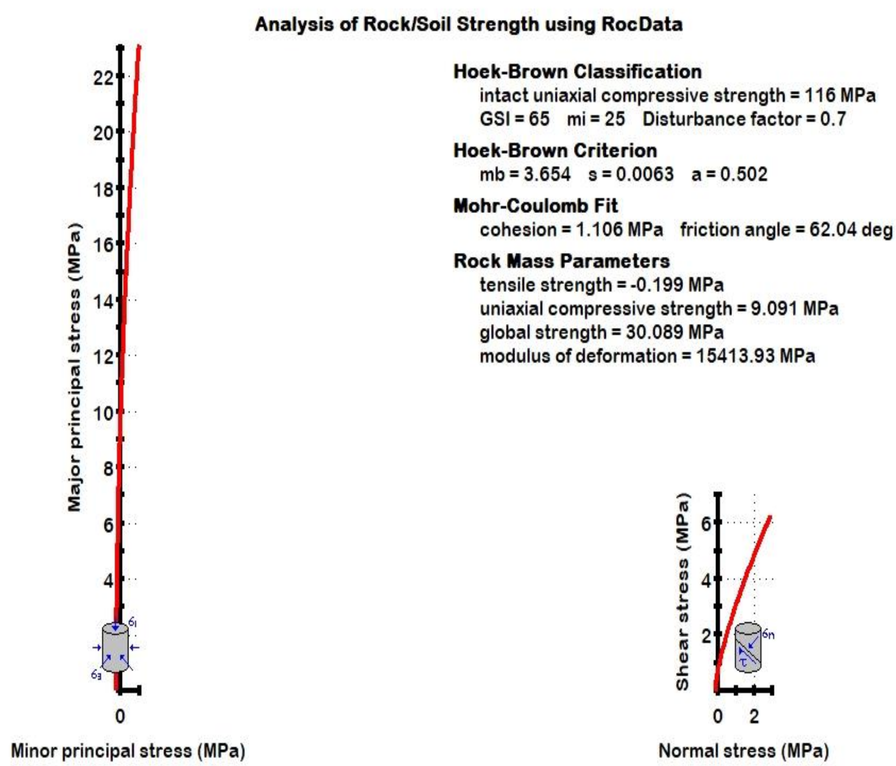
Analysis of Rock/Soil Strength using RocData
Hoek-Brown Classification
intact uniaxial compressive strength = 116 MPa
GSI = 65 mi = 25 Disturbance factor = 0.7
Hoek-Brown Criterion
mb = 3.654 s = 0.0063 a = 0.502
Mohr-Coulomb Fit
cohesion = 1.106 MPa friction angle = 62.04 deg
Rock Mass Parameters
tensile strength = -0.199 MPa
uniaxial compressive strength = 9.091 MPa
global strength = 30.089 MPa
modulus of deformation = 15413.93 MPa
Major principal stress (MPa)
Minor principal stress (MPa)
Shear stress (MPa)
Normal stress (MPa)